

COASTAL ENGINEERING
IN JAPAN

VOL. III

COASTAL ENGINEERING IN JAPAN

VOL. III

Edited by

MASASHI HOM-MA, DR. ENGG.

Professor of Hydraulic Engineering
Department of Civil Engineering
University of Tokyo

Published by

COMMITTEE ON COASTAL ENGINEERING
JAPAN SOCIETY OF CIVIL ENGINEERS
TOKYO JAPAN

1960

PUBLICATIONS OF THE COMMITTEE ON COASTAL ENGINEERING, JAPAN

English edition

- Coastal Engineering in Japan, vol. 1, 1958 (U.S. \$1.50)
- Coastal Engineering in Japan, vol. 2, 1959 (U.S. \$1.50)
- Coastal Engineering in Japan, vol. 3, 1960 (U.S. \$2.50)

Japanese edition

- Proceedings, 1st Conf. on Coastal Engineering, 1954 (out of print)
- Proceedings, 2nd Conf. on Coastal Engineering, 1955
- Proceedings, 3rd Conf. on Coastal Engineering, 1956 (out of print)
- Proceedings, 4th Conf. on Coastal Engineering, 1957
- Proceedings, 5th Conf. on Coastal Engineering, 1958
- Proceedings, 6th Conf. on Coastal Engineering, 1959
- Proceedings, 7th Conf. on Coastal Engineering, 1960
- Design Manual of Coastal Protection Works, 1957



Katase beach (Geological Survey, Ministry of Public Works)



Kamakura beach (Geological Survey, Ministry of Public Works)



Digitized by the Internet Archive
in 2023 with funding from
Kahle/Austin Foundation

PREFACE

The last two years were really an eventful period to the Japanese coastal engineers owing to the tremendous disasters caused by storm surges and also by a tsunami. In 1959 the Ise-Bay Typhoon marked the record-setting storm surge in the Ise-Bay area taking heavy toll of human lives and properties and causing heavy destruction of coastal structures. In 1960 the earthquake in Chile sent a series of big tsunami waves which crossed the Pacific Ocean in only a day and hit the Pacific Coast of Japan. Unpredicted damages were inflicted on Hokkaido and Sanriku (northeastern coast).

On the other hand the Seventh International Conference on Coastal Engineering was held in the Netherlands in August, 1960. Through this conference the exchange of our knowledge on coastal engineering has been promoted in the worldwide scale. It is our great pleasure to see that the coastal engineering practices in Japan have taken a large stride in the mean time, and that publication of the "Coastal Engineering in Japan" has also contributed to this end.

The present issue, Vol. 3, contains the papers published between 1958 and 1960 in Japan.

December, 1960

Masashi Hom-ma
Chairman
Committee on Coastal Engineering
Japan Society of Civil Engineers
Tokyo, Japan

CONTENTS

	page
Preface	M. Hom-ma
Studies on Meteorological Tides at the Mouth of the Tone River	T. Kishi M. Tominaga..... 1 I. Oeda
On the Similitude of Hydraulic Models Involving Tidal Motion	S. Hayami H. Higuchi 9 K.H. Yoshida
On the Density Currents in the Estuary	T. Ito S. Sato T. Kishi 21 M. Tominaga
Tsunami Caused by Chile Earthquake in May, 1960 and Outline of Disasters in Northeastern Coasts of Japan	T. Iwasaki K. Horikawa 33
Some Additional Remarks on the Chilean-Earthquake Tsunami	K. Horikawa..... 49
Wave Overtopping on Seawalls	T. Ishihara I. Iwagaki 53 H. Mitsui
A Study on the Volume of Littoral Drift	Y. Mashima 63
The Effect and Damage of Submerged Breakwater in Niigata Coast	N. Shiraishi A. Numata 89 N. Hase
A Study on Beach Erosion at the Sheltered Beaches of Katase and Kamakura, Japan	M. Hom-ma K. Horikawa..... 101 C. Sonu

STUDIES ON METEOROLOGICAL TIDES AT THE MOUTH OF THE TONE RIVER

*Tsutomu Kishi**, Dr.
*Masateru Tominaga***
*Ichiro Oeda****

I. INTRODUCTION

In determining the level of a design high water along a river course, it is generally required to give a boundary value at the mouth. While we often find the lack of record of the water level at the mouth of the river for such a long period of time as to be sufficient to carry out the frequency analysis. On the contrary, the meteorological data observed for a comparatively long period are usually available in this country.

In this paper, the authors investigate the relations of meteorological tides together with wind velocity and depression of atmospheric pressure at the mouth of the TONE RIVER. The results show that the possibility of occurrence of abnormally high meteorological tides may be estimated from the weather data. As the result, the authors present the figure showing the relation between the magnitude of meteorological tide and its return period.

II. EFFECTS OF WIND VELOCITY ON METEOROLOGICAL TIDE

At the mouth of the TONE RIVER a long sandy beach runs from NW to SE, and the NE component of wind would make an important role to cause a meteorological tide. In Fig. 1

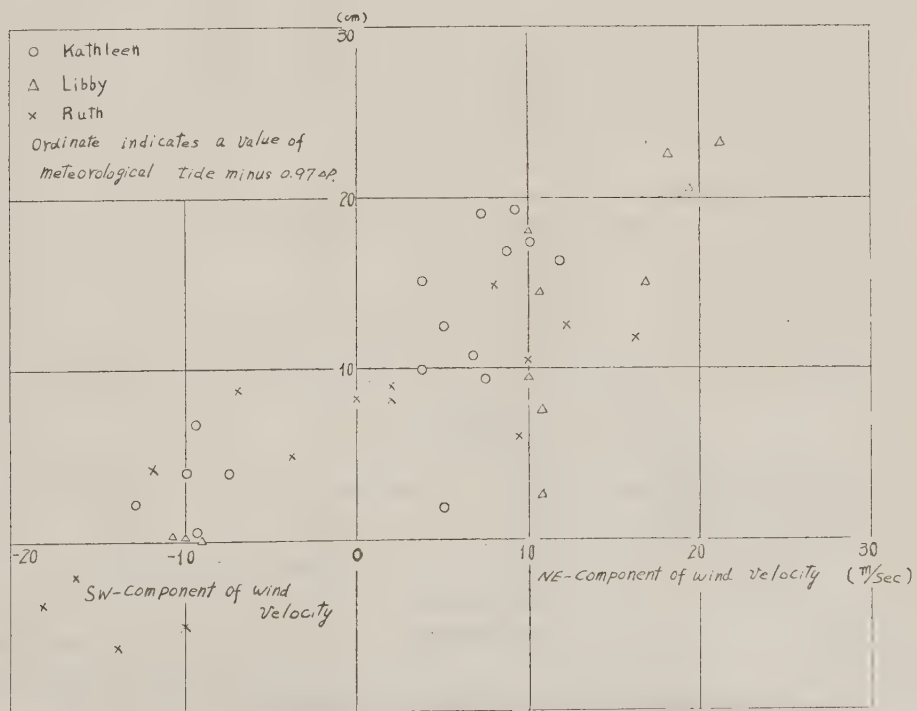


Fig. 1

* Dr. Eng., Assistant professor of Hydraulics, Hokkaido University

** Research Member, Public Works Research Institute, Ministry of Construction.

*** Technical Officer, Construction Bureau of Kanto District, Ministry of Construction.

the correlations between meteorological tide (actual tide — estimated astoronomical tide) and NE component of wind velocity are shown for the periods of several examples of typhoon. In the above figure, ordinate indicates a value of meteorological tide minus $0.97 \Delta p$. The value of $0.97 \Delta p$ means the meteorological tide caused by the static depression of atmospheric pressure of Δp mb. It may be seen from the figure that NE component of wind directly relates with the meteorological tide.

III. EMPIRICAL EXPRESSION OF METEOROLOGICAL TIDE BY WIND VELOCITY AND DEPRESSION OF ATMOSPHERIC PRESSURE

As stated in the preceding article, the meteorological tide at the mouth of the TONE RIVER is considered to relate both wind velocity and atmospheric pressure. By using the records of meteorological tides measured for six typhoons during 1947~1952, the relation of meteorological tide with wind velocity and depression of atmospheric pressure is examined, and the results are shown in Fig. 2. In this figure the curves showing equal meteorological tide are drawn. In spite of the fact that an instantaneous value of meteorological tide is substantially an unsteady process, an approximate evaluation of instantaneous value of tide seems to be possible by using the curves drawn in Fig. 2.

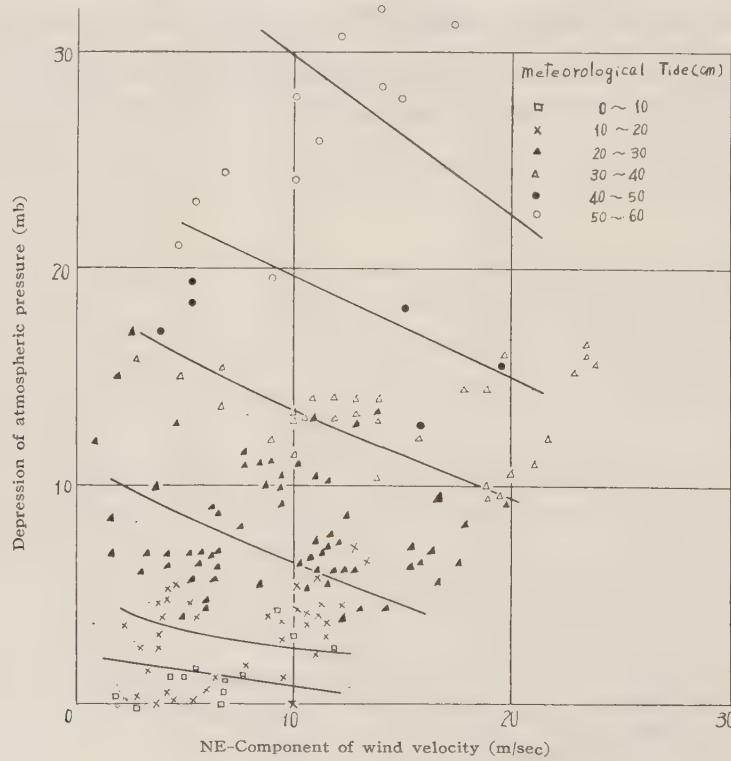


Fig. 2

IV. WIND VELOCITY DURING A PERIOD OF TYPHOON

As being shown in Fig. 2, a meteorological tide relates with wind velocity and depression of atmospheric pressure. The authors intend to study a method of computation of the probability of occurrence of abnormally high meteorological tides from the weather data. In

such procedure it is very troublesome to prepare a complete data of wind velocity and atmospheric pressure for a long period of time. When a correlation is found between wind velocity and depression of pressure such a trouble would be considerably reduced. Thus, the authors compared the recorded wind velocity with the geostrophic wind velocity.

Geostrophic wind velocity is given by the following expression,

$$V_g = \left[\frac{R}{\rho} \frac{\partial p}{\partial r} + (\omega R \sin \varphi)^2 \right]^{1/2} - \omega R \sin \varphi, \quad \dots \dots \dots (1)$$

where V_g = geostrophic wind velocity

R = radius of curvature of stream line of wind

ρ = density of air

$\partial p/\partial r$ = gradient of atmospheric pressure

ω = angle velocity of rotation of the earth

φ = latitude of the place under consideration

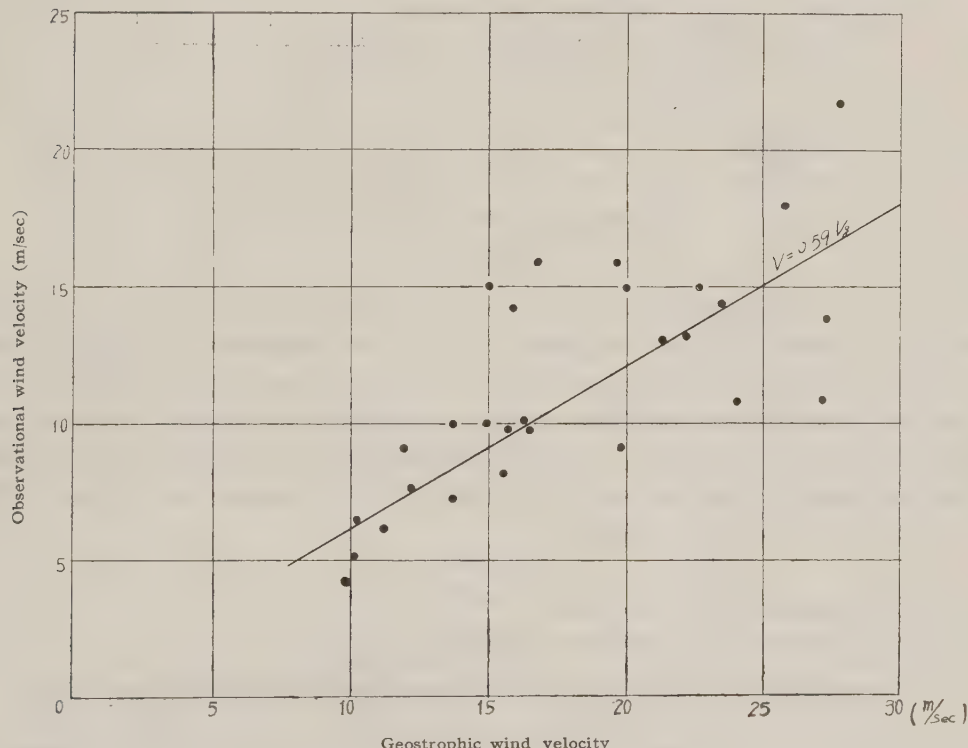


Fig. 3

The figure 3 shows the relation between observed wind velocity and the calculated values of V_g .

From this figure, recorded wind velocity on the average is found to be expressed by a simple relation of $V \approx 0.59 V_g$.

As the next step, the authors investigated the correlation between wind velocity and atmospheric pressure. The results are shown in Fig. 4. The curves which give the relations between them build up different loop for each typhoon. This fact shows that the wind velocity in a typhoon is hardly described only by the depression of pressure. The course of typhoon and the distance from the center of typhoon have to be considered as the controlling factors. The authors gave three representative curves for the relations between wind ve-

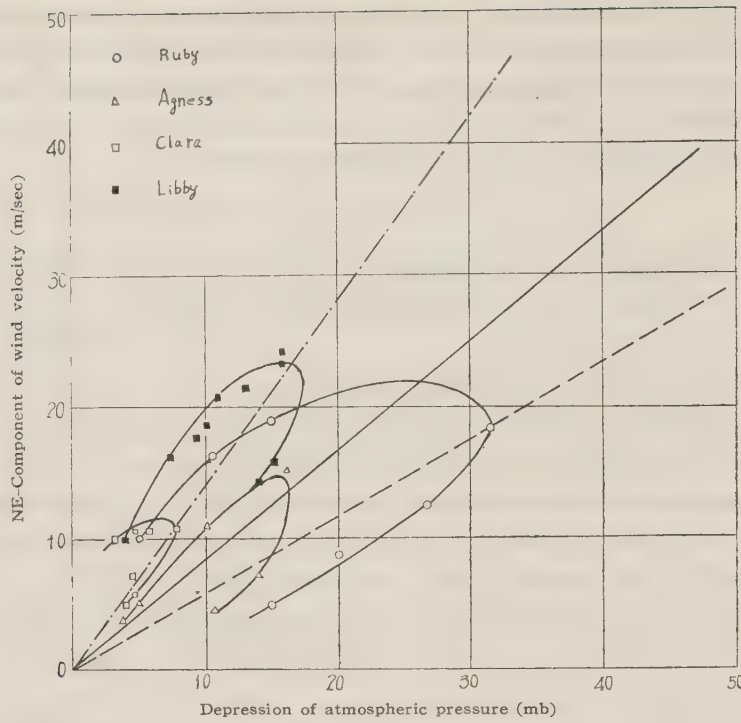


Fig. 4

lacity and depression of pressure. They are shown in Fig. 4 by chain line, full line and broken line. Introducing these three curves in to Fig. 2, one obtains the curves which express the meteorological tide only by the depression of pressure as shown in Fig. 5. The data obtained at Kathleen typhoon and Ruby typhoon are plotted in the figure. Although these approximate relations are considered to give a little larger value of meteorological tide near the peak, they seem to agree as a whole fairly well with the measured tidal records. The full line in Fig. 5 expresses the equation

$$H = 0.051 P^{0.74}, \dots \dots \dots \quad (2)$$

where H = meteorological tide in meter

P = depression of atmospheric pressure in mb.

V. STATISTICAL CONSIDERATION OF METEOROLOGICAL TIDE

As is stated above, the meteorological tide at the mouth of the TONE RIVER caused by typhoon can be expressed only by the depression of atmospheric pressure. Therefore the statistical treatment of pressure data gives us the knowledge about the statistical frequency of meteorological tide.

Almost all of the typhoons which had landed on or passed near this country changed their route from North-west to North-east at about N.L. 30° and thereafter they scarcely developed. The lowest pressure of any typhoon, therefore, is observed on the ocean. Some examples are shown in Table 1. As the mouth of the TONE RIVER is situated in N.L. 35° , pressures observed at the mouth are somewhat higher than the lowest pressure observed on the ocean.

The frequency of occurrence of respective value of atmospheric pressure was investigated on the line of N.L. 35° by the records of 335 typhoons observed during 1868~1951 and the

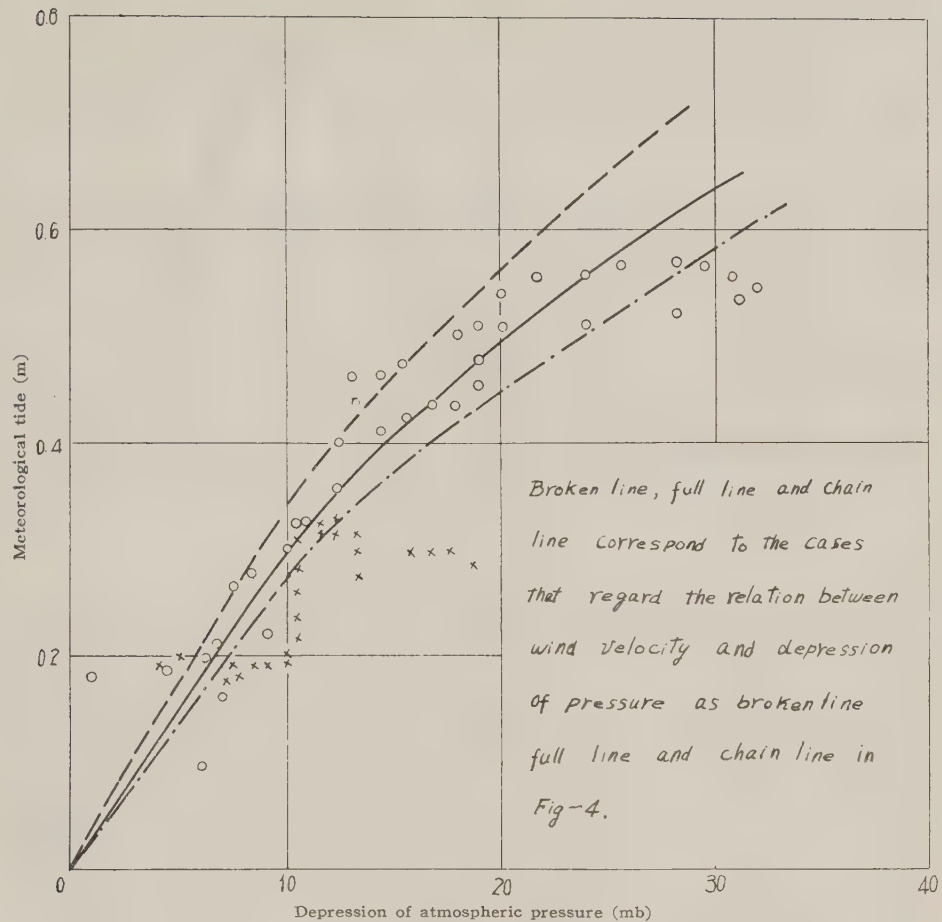


Fig. 5

Table-1

Date	Lowest pressure	Date	Lowest pressure
Mar. 19~23, 1934	939 (mb)	Nov. 1~12, 1940	953
Sept. 13~22, 1934	907 muroto	Aug. 21~29, 1942	933
Aug. 21~Sept. 2, 1935	957	Sept. 19~23, 1942	947
Sept. 1~12, 1935	957	Sept. 26~Oct. 5, 1943	947
Sept. 16~27, 1935	953	Jul. 28~Aug. 6, 1944	947
Sept. 24~Oct 6, 1936	933	Oct. 4~10, 1944	907
Sept. 2~12, 1937	947	Sept. 11~18, 1945	907 Makurazaki
Aug. 4~9, 1939	957	Aug. 10~21. 1946	950
Aug. 20~Sept. 3, 1939	933	Sept. 16, 1948	945
Jul. 3~16, 1940	931	Aug. 31, 1949	957
Aug. 26~27, 1940	947		

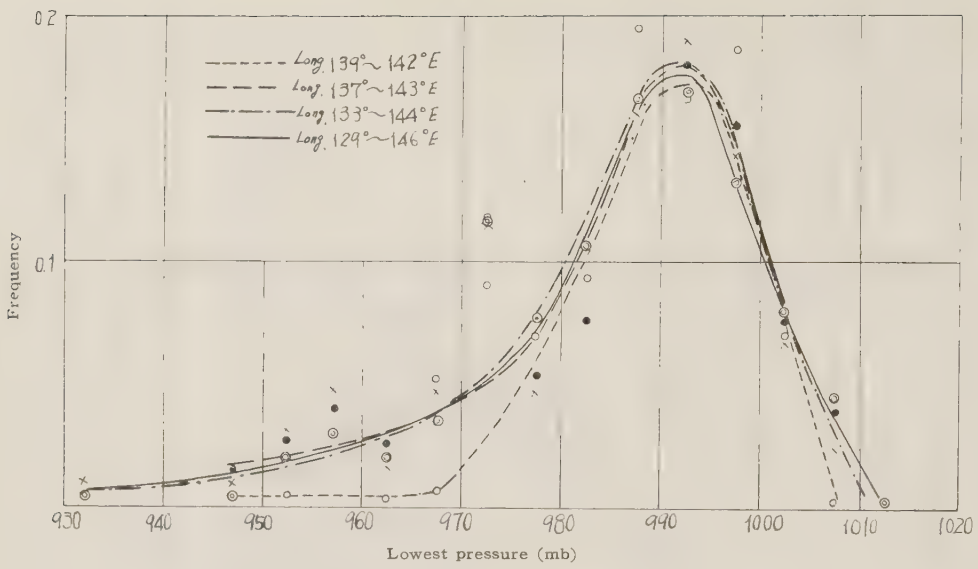


Fig. 6

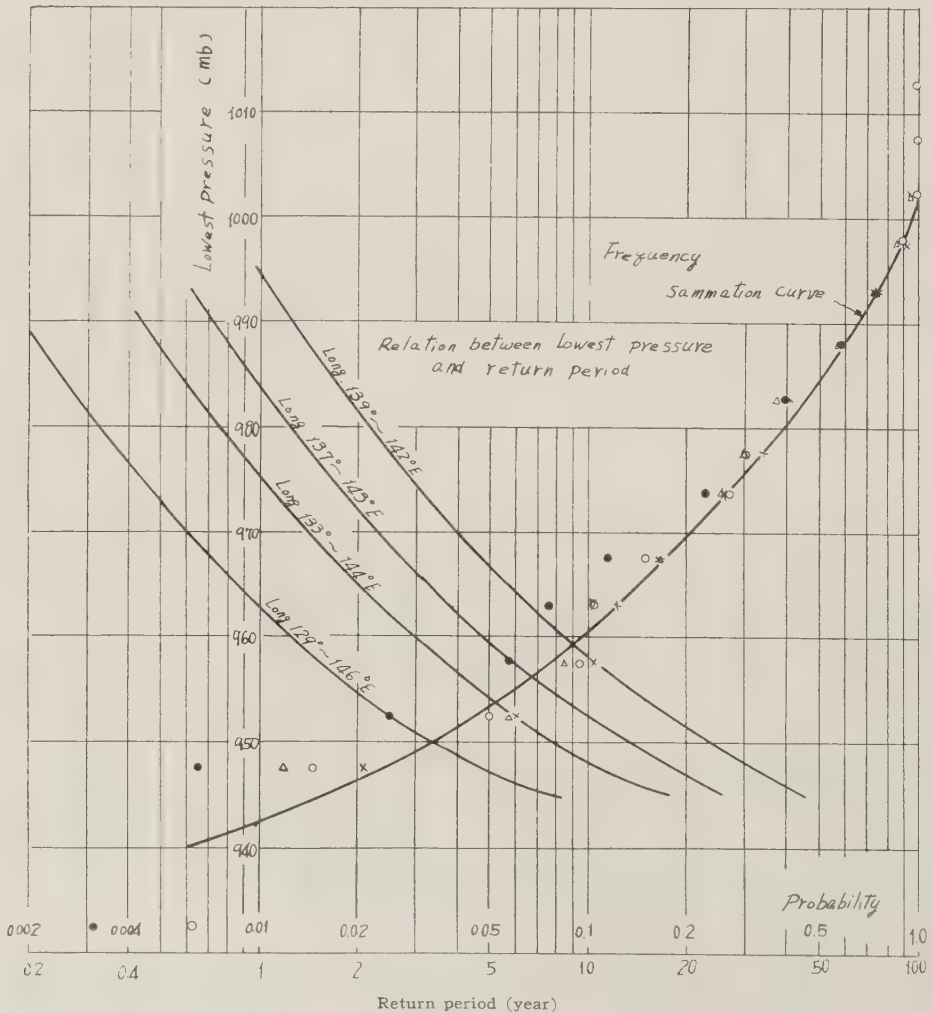


Fig. 7

results are shown in Fig. 6. As the range of observation extends from Long. 129°E to Long. 146° E, curves showing the frequency distribution for four ranges of longitudes are included. According to the figure, the frequency distribution curves of pressure seems to be identical. Pearson's distribution function type-III would fit these frequency distribution. Mode of the distribution is 990 mb. The distribution function calculated from the curve in Fig. 6 is given in Fig. 7.

When the distribution function and the average number of typhoons pass through the part under consideration in a year are given, one can calculate the return periods for any atmospheric pressure. The curves showing the relation of atmospheric pressure to its return period are included in Fig. 7. For example, when the whole range of longitude is considered, the return period of the pressure of 950 mb. is 3.6 years. While the return period of the same value of pressure is 24.5 years when the narrow range of longitude — from Long. 139°E to Long. 142°E — is considered. Return period may be calculated by the relation

$$T = \frac{1}{(\text{Probability})} \times (\text{Average number of typhoons pass through the part, under consideration, in a year}) \quad \left. \right\} \dots \dots \dots \quad (3)$$

Such a calculation is not adequate when the average number of typhoons shows a considerable variance or have a periodic character. The average number of typhoons pass through the line of N.L. 35° in a year is given in Fig. 8.

The relation between the pressure and its return periods calculated by the data observed at the mouth of the TONE RIVER is shown in Fig. 9. Comparing Fig. 7 with Fig. 9, one can easily find the interesting feature that the return period of any value of pressure varies with the range of longitude under consideration.

Combining the relations shown in Fig. 7 and Fig. 9 with the relations shown in Fig. 5 or

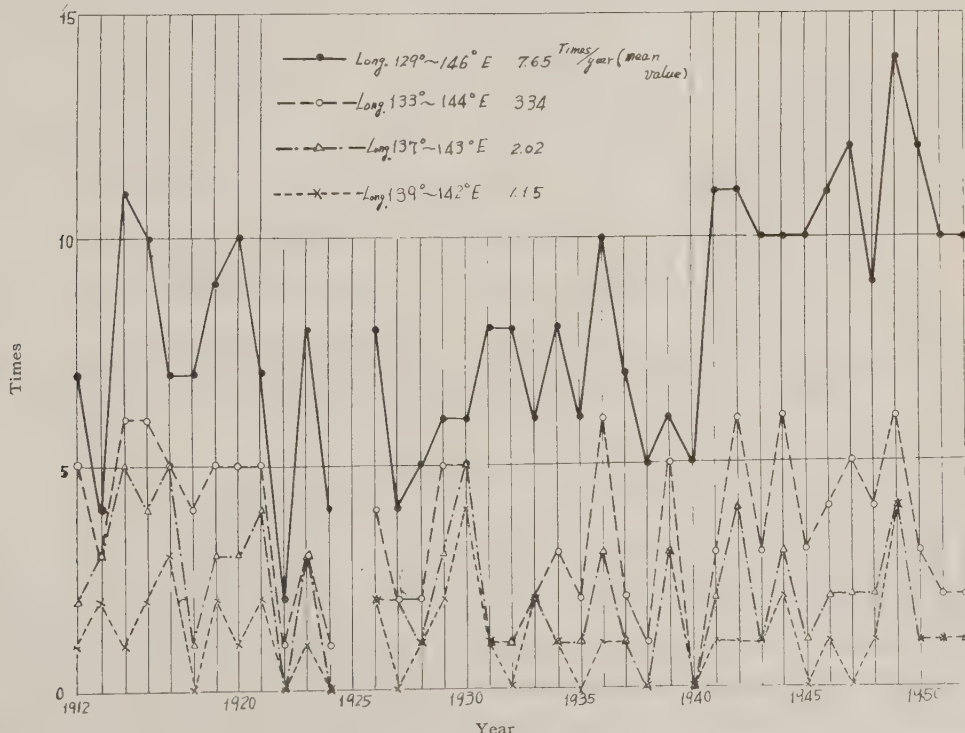


Fig. 8

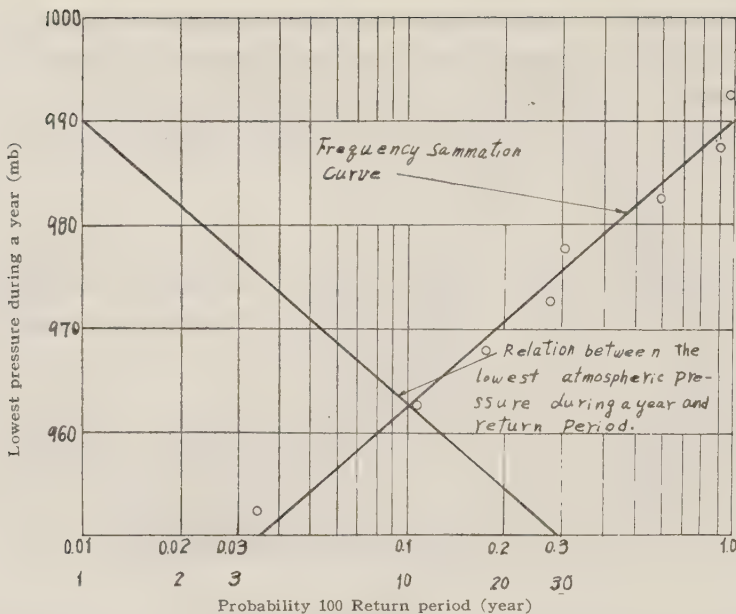


Fig. 9

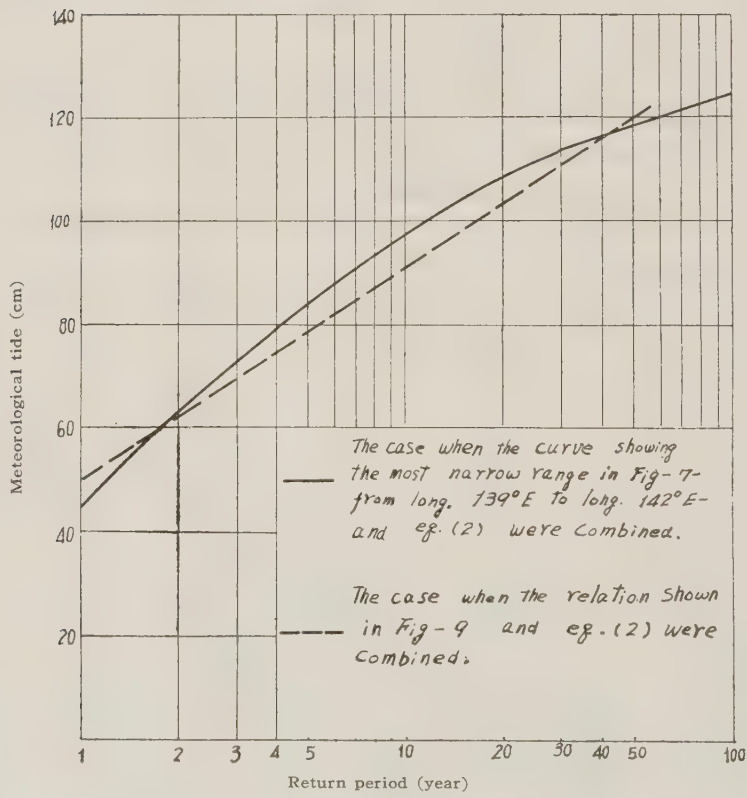


Fig. 10

equation (2), one obtains the relation of meteorological tides with its return periods. For example, the case when the relation shown in Fig. 9 and equation (2) were combined and the case when the curve showing the most narrow range in Fig. 7 — from Long. 139°E to Long. 142°E — and equation (2) were combined are shown in Fig. 10. The average pressure required in these calculation was assumed to be 1010 mb.

ON THE SIMILITUDE OF HYDRAULIC MODELS INVOLVING TIDAL MOTION

*Shōtirō Hayami**

*Haruo Higuchi***

*Kozo H. Yoshida****

SYNOPSIS

Conditions of dynamical similitude in the mean motion between a prototype which involves tidal motion and its model are given by

$$\text{drag coefficient ratio : } C_2/C_1 = \alpha/\beta$$

and

$$\text{Froude number condition : } r^2\beta/\alpha^2 = 1$$

where $1/\alpha$, $1/\beta$ and $1/r$ are horizontal, vertical and time scales, respectively, of the model with respect to its prototype, C is the drag coefficient, where subscripts 1 and 2 mean the prototype and the model, respectively. Since these conditions contain four unknowns C_2/C_1 , α , α/β , and r , at least one more condition is required to determine the scale values of the model which is dynamically similar to the prototype. In order to derive the required condition, a field observation of tidal current was made in Hiroshima Bay as a prototype while a series of hydraulic model experiments were carried out for this prototype for conditions with $\alpha=500$, $\alpha/\beta=8, 4$ and 2 , and r satisfying the Froude number condition. The comparison and analysis of the field observations and the model experiments show that (i) a very good similitude is observed for the case $\alpha/\beta=2$; (ii) Blasius' formula of drag coefficient is obtained for a tidal current in the model, if Reynolds number is constructed with the maximum tidal current velocity and tidal current velocity and tidal excursion; (iii) a relation between Reynolds number of the prototype (Re_1) and that of the model (Re_2) such as

$$Re_2 = Re_1 / (\alpha \sqrt{\beta})$$

which is theoretically derived for the dynamically similar prototype and model, is experimentally justified. Putting Re_2 given above into Blasius' formula for the model, the required condition is obtained as

$$C_2 = \frac{1.328}{\sqrt{Re_1}} \alpha^{1/2} \beta^{1/4}.$$

With this condition, the drag coefficient condition is reduced to

$$C_1 \sqrt{\alpha Re_1} / 1.328 = \beta^{5/4}$$

which enables us, with the Froude number condition, to determine the vertical scale $1/\beta$ and the time scale $1/r$ of the model for a given horizontal scale α of the model.

INTRODUCTION

The fishery population in Japan is about two millions, most of them engaged in shallow-sea fishery. Such shallow-sea fishery is carried out only near the coast in very small scale. The length of coast per head of fisher men in our country is only 12 m, while the total length of coast is about 2.5×10^4 km; therefore the higher standard of living is hopeless unless the productivity in shallow-water fishery is increased remarkably.

It is the current opinion of the world that the territory of a country covers the whole con-

* Geophysical Institute, Kyoto University.

** and *** Disaster Prevention Research Institute, Kyoto University.

tinental shelf and the shelf sea surrounding it. This opinion is based on a new point of view toward the territory such that the continental shelf is a part of continent and the shelf sea is under the influence of the land.

While the productivity is small in the deep-sea, it is very large in the shallow-sea as is well known. This is due mainly to the influence of land, and this influence is exerted upon coastal water beyond the coast. Hence, if we could place the sea near the coast under our control, we would also be able to control the productivity there.

Today, the development of a country is carried out as if the land is a principal theater, and the shallow-sea used to be treated as another world. However both worlds constitute essentially a single system, so that the development must be carried out synthetically. In order to realize this ideal we must understand what a change will take place in the shallow-sea by controlling the coast.

The concentration of physical quantities in the sea is governed by the parabolic differential equation derived from the law of conservation. To solve such a equation, the boundary conditions are required, which consist of the conditions at the coast, the surface, and the bottom. The condition which is controlled by the coastal construction is chiefly one at the coast.

The most important physical quantities related with the productivity are the materials contained in the sea water and the momentum of water. Some part of the materials, which is supplied from the land and the sea near the coast, are used to make living bodies and some part as the energy source for maintaining life. The momentum is important as the carrier of the materials in the water, and the most important one in the shallow-sea is tidal current. The current is directly influence by coastal construction, and the influence upon the distribution of materials takes place secondarily through the current. In this sense, the direct object of controlling the sea by coastal construction should be the current. Among others, the tidal current and the currents of various accompanying oscillations are most important as the carrier of the materials, and their effects are considered to consist in a sort of diffusion of large scale. However, it is not easy to imagine how these currents will be changed by coastal constructions. There are two ways to investigate the change of a tidal current by coastal constructions; the one is numerical integration of the differential equation, the other is a hydraulic model experiment. This very latter is the subject of the present study.

I. THEORETICAL CONSIDERATION ON SIMILITUDE

The most important problem in hydraulic models is of dynamical similitude. Since it is theoretically impossible to simulate prototype and model in every detail, we use the term "similitude" in the sense that some particular relationships hold between prototype and model. Only in such case a hydralic model experiment has meaning. In the present study where the change of tidal current by coastal construction is the main concern, we assume similitude in vertically mean motion as follows.

As the tidal current is dominant in the horizontal direction the vertical velocity may be neglected. Hence, if the mean velocities in horizontal directions are shown by U_j ($j=1, 2$), the equation of U_j is given by

$$\frac{\partial U_j}{\partial t} + \Sigma s U_i \frac{\partial U_j}{\partial x_i} = -\frac{C}{2H} U_j^2 - g \frac{\partial \zeta}{\partial x_i}, \dots \quad (1)$$

where t and x_i ($i=1, 2$) are coordinates for time and space respectively, and the subscripts 1 and 2 refer to horizontal direction, and subscript 3 vertical, ζ is the displacement of water

surface in the vertical direction, g is the acceleration of gravity, H is water depth, and S is the coefficient nearly equal to unity, decided by vertical distribution of velocity. In shallow water where the tidal current is dominant, we can neglect the force due to density distribution because it will be smaller than any other term of equation (1). Coriolis' force and wind stress are also neglected.

If the magnitudes for prototype and model are shown by subscripts 1 and 2 respectively, and the relationship between prototype and model by

where α , β , and r are scale constants, we obtain by substituting from (2) into (1)

$$\frac{\partial(U_j)_z}{\partial t_2} + \Sigma s(U_i)_z \frac{\partial(U_j)_z}{\partial(x_i)_z} = -C \frac{\alpha}{\beta H_z} (U_j)_z^2 - \frac{g r^2 \beta}{\sigma^2} \frac{\partial \zeta_z}{\partial(x_i)_z}. \quad \dots \dots \dots (3)$$

Assuming $s_1 \approx s_2$, we get from (1) and (3) the conditions of dynamical similitude as follows.

Equation (5) provides the relation between the time and space scales. It is nothing but the Froude number condition. Equation (4) provides the drag coefficient condition. The equation of continuity is not influenced because of uniformity of density.

If the ratio of C_1 to C_2 is known, and one of α , β and γ is given, the others are determined by equations (4) and (5). Supposing, while C_1 corresponds to the drag coefficient for a turbulent flow, C_2 corresponds usually to that for laminar, we may infer $C_2/C_1 = 2 \sim 3$. However, we do not know the actual value of this ratio for the case of tidal current. When the ratio is not given, α , β and γ are not determined by equations (4) and (5). In order to obtain the value of this ratio, a series of experiments have been carried out. Since γ is given by equation (5) for given α and α/β , we have tried to find out the best value of α/β by comparing the results of model experiments with prototype for various values of α/β for given α .

The assumption mentioned above is that, when equations (4) and (5) are satisfied, the similitude between prototype and model holds with respect to vertical velocity. It will be interesting and also important to know how far this assumption is satisfied.

II. MODEL EXPERIMENT AND FIELD OBSERVATION

The hydraulic model experiments were carried out by using the experimental facility designed for an estuarine model experiment at Hydraulics Laboratory of Disaster Prevention Research Institute, Kyoto University. As shown in Fig. 1, the equipment consists of a water basin, a river channel, a pneumatic tide generator, and a control room. The basin is built of concrete and is 20 m in width along the coast, 15 m to the offing and 0.5 m in depth. The pneumatic tide generator which is also made of concrete, is 20 m in length, 2 m in width, and 2 m in height, and the water communicates through the gap beneath the front wall. When the pressure in the air chamber is decreased by sucking the air with a blower in the control room, the water level in the chamber rises, while, when the air flows into the chamber, the level falls, and the water in the chamber flows out into the basin. Controlling the volume of air flowing into the chamber by automatic controller, and desired range of tide can be generated. The bottom topography of sea and estuary was formed by sand. The ve-

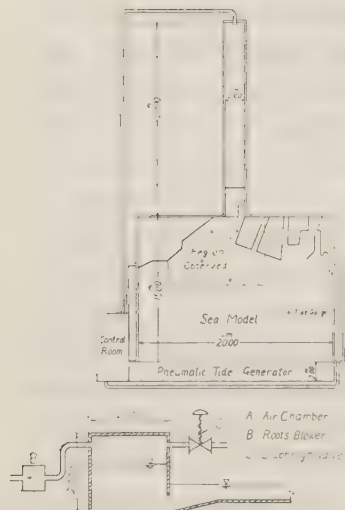


Fig. 1 Experimental facilities

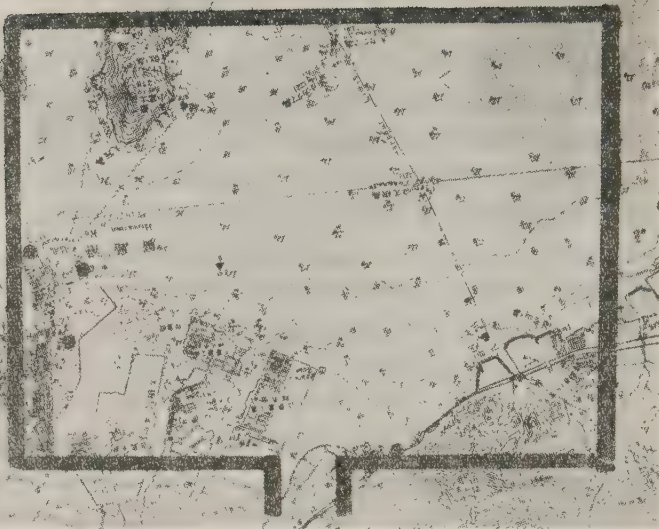


Fig. 2 Prototype

locity of flow in the model was within the laminar region, and the bottom material did not move at all.

A part of Hiroshima Bay was chosen as prototype. The region involved in the model is rather large as shown in Fig. 2. The reason why this region was chosen is that since Inland Sea Fisheries Research Institute had previously investigated this region in detail, it was thought convenient to obtain the data for prototype. Moreover a training jetty of 1.5 km long was being planned at the right bank of Fukushima River which empties into this sea region so also was interesting to see what change of state of sea may take place in future by this construction. As to the prototype a field observation was carried out. Many observing stations were set there and the flow velocities at the depth of 50 cm below the sea surface were measured. The measurements were executed during the most intense currents both at flood and ebb. The flow velocities were measured by float because the velocity is small changing rapidly in both magnitude and direction. The velocity was read by the length of a thread connected with the float and the direction by the compass.

The model was built according to this prototype. The horizontal scale is 1/500, i.e. $\alpha = 500$. The width of the basin is 20 m so that it contains the coast of 10 km. Over the model many white threads were rigged to form reference coordinates and a net work of a



Fig. 3 Floats used for the current measurements in the model.

number of 1 square m covered the whole surface. The velocity and line of flow at each point were measured by photographing every minute many floats, whose specific gravity was about 1, from the top of a tower 3 m high. (Fig. 3). The water levels at 5 points shown in Fig. 1 were recorded by an oscillograph ink-recorder attached to a resistance type wave meter. The direction of progression of tidal wave was decided by referring to the prototype. The rate of flow in Fukushima River was neglected because the rate of flow in actual river which was under improving work during field observation was very small.

III. RESULTS OF OBSERVATION AND EXPERIMENT

The field observations of tidal current were done when the velocity attained maximum value both in flood and ebb tides from May 14 to 16, 1957. A tidal curve during those days is shown in Fig. 4, where the times of observation are shown in broken line (at flood; 7 : 20~9 : 10, at ebb 12 : 50~14 : 40). Because of the effect of wind the observation did not give the same result. Figs. 5 and 6 show the result on May 16 when it was comparatively calm. The wind observed at Hiroshima Weather Bureau on that day is given in Table 1.

Although several boats were engaged in this work, it took nearly two hours everytime to complete observations at all stations. Accordingly this figure does not precisely show the tidal currents at the same time. As shown in this figure, current velocity is generally small and seldom exceeds 20 cm/sec. Especially it is remarkable that near the contourline of 5 m the velocities are very small both at flood and ebb. Inside the 5 m contour the

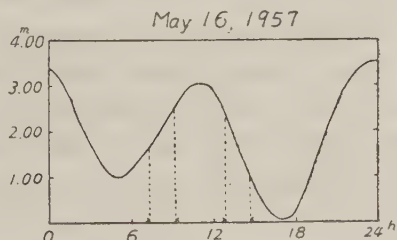


Fig. 4 Tidal curve. Periods of current observations are indicated by dotted lines.

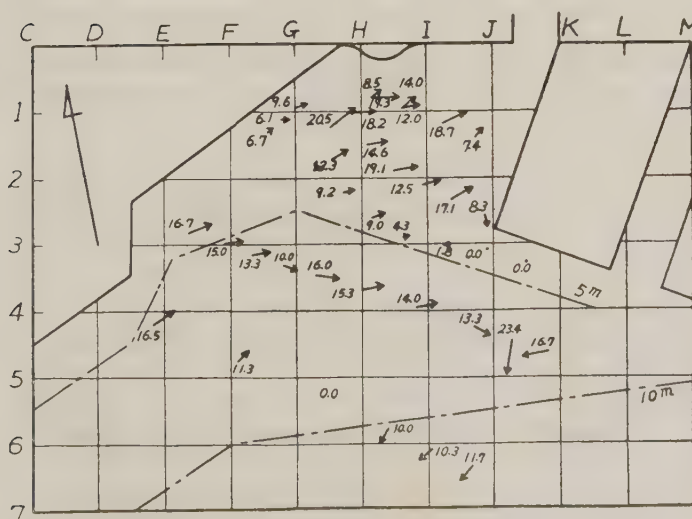


Fig. 5 Pattern of the maximum rising current. Prototype, May 16, 1957.

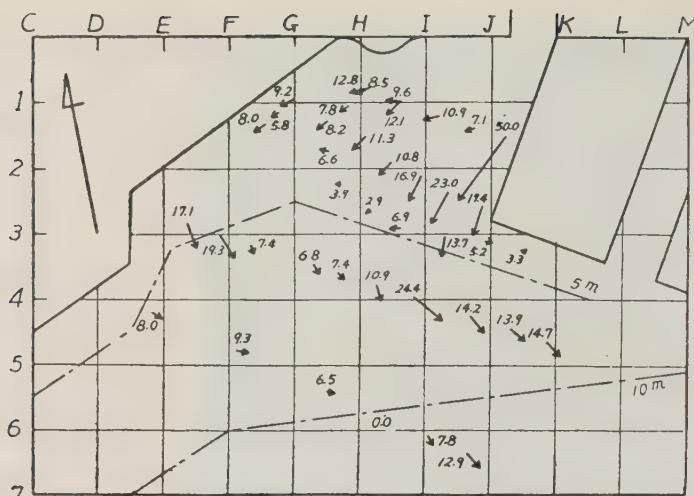


Fig. 6 Pattern of the maximum falling current. Prototype. May 16, 1957.

Table 1

May 16, 1957		1	2	3	4	5	6	7	8	9	10	11	12	13	14	15	16	17	18	19	20	21	22	23	24
Time																									
Wind	Direction	NNE	"	"	"	"	"	"	"	"	"	S	SSW	SW	"	"	SSW	SW	"	"	"	NNE	"	"	"
Wind Speed	(m/sec)	5.5	6.1	6.5	7.6	5.7	5.7	5.4	3.6	2.4	2.8	4.6	1.3	4.2	1.3	4.2	3.8	3.6	1.3	4.8	0.2	2.6	4.6	3.8	4.0

water depth decreases rapidly to 2 m or less while in the outer part of this contour it increases rapidly to more than 10 m. That is, there is a step on the bottom of the sea along this contourline marking the front of the delta of Fukushima River. The bottom materials consist of sand or mud in the inner and outer part of this line respectively.

As the model experiment for this prototype, experiments were carried out for three cases of $\alpha/\beta=8$, 4 and 2. In each case the horizontal scale was 1/500, i.e. $\alpha=500$. The values of γ for those sets of α and β are calculated from equation (5), giving $\gamma=63$, 45, and 32 respectively. Since the observed current may be regarded as semi-diurnal, the corresponding periods of tide in the model were taken as 11.5, 16 and 22.5 min. respectively. The standard tidal range in prototype was assumed as 2.5 m, so that they were reduced in accordance with the values of β in the model. Examples of tidal curves in the model are shown in Fig. 7, which were measured at the station nearest to the wave generator shown in Fig. 1.

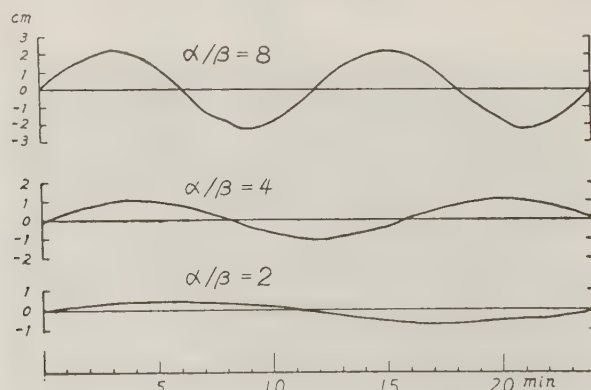


Fig. 7 Tidal curve in the model.



Fig. 8 Wind protection cover of the model.

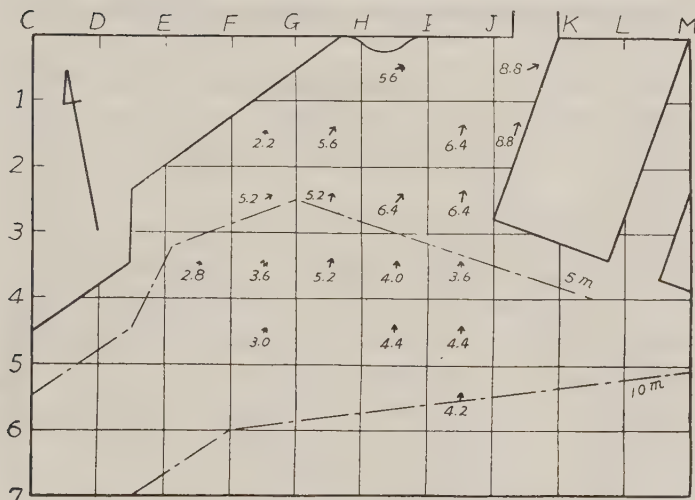


Fig. 9 Pattern of the maximum current. Model, $\alpha/\beta=8$.

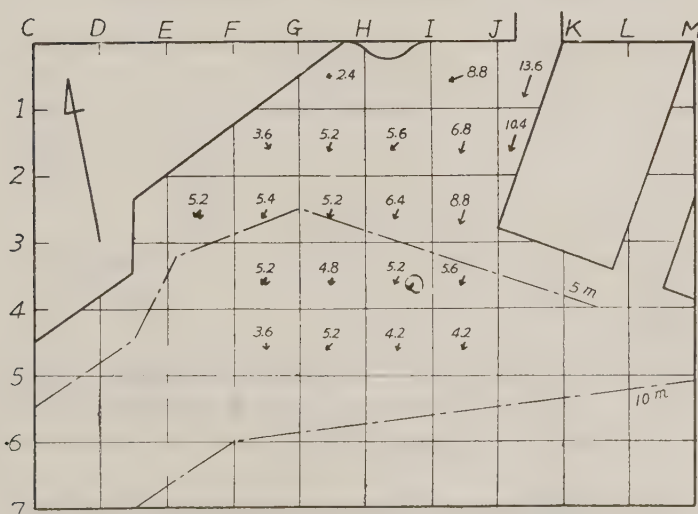


Fig. 10 Pattern of the maximum falling current. Model, $\alpha/\beta=8$.

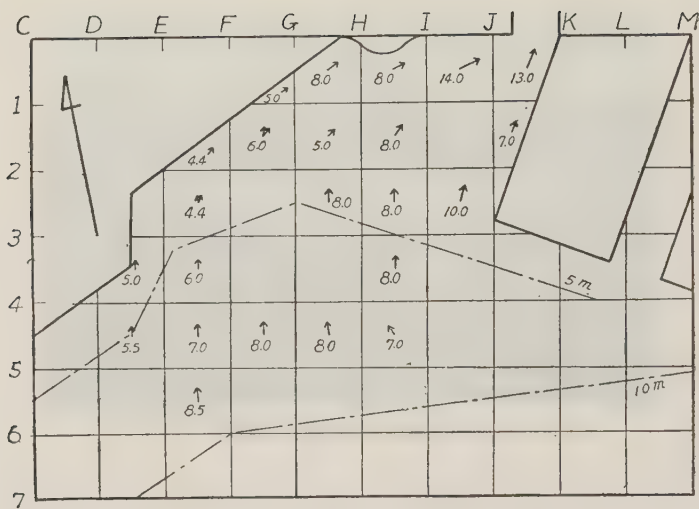


Fig. 11 Pattern of the maximum rising current. Model, $\alpha/\beta=4$.

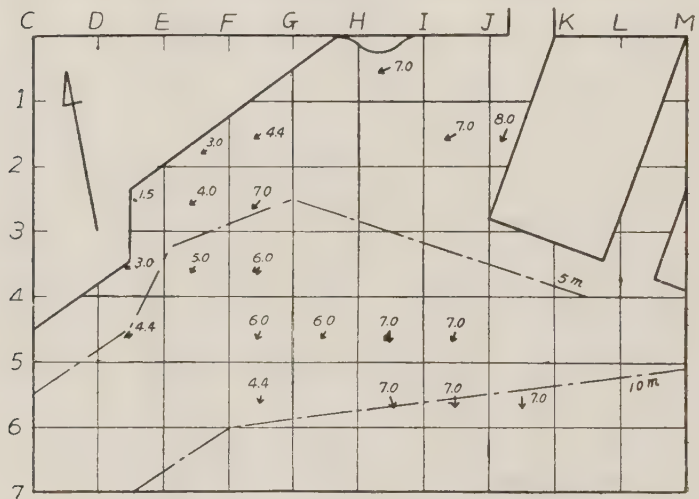


Fig. 12. Pattern of the maximum falling current. Model, $\alpha/\beta=4$.

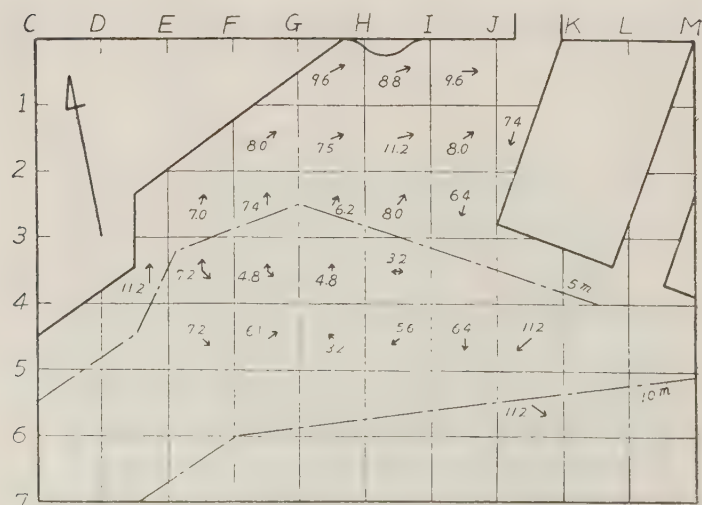


Fig. 13 Pattern of the maximum rising current. Model, $\alpha/\beta=2$.

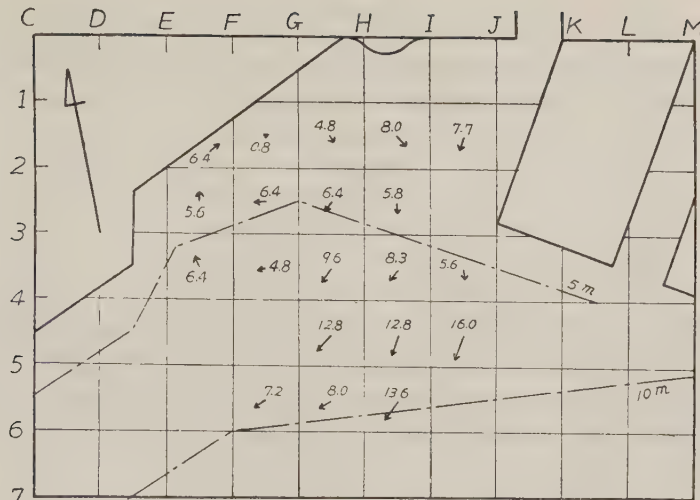


Fig. 14 Pattern of the maximum falling current. Model, $\alpha/\beta=2$.

During the preliminary experiment it was found that the effect of wind was very large, and hence the equipment was covered temporarily with polyethylene sheets (Fig. 8). However, as it was impossible to protect it completely from wind, the experiments were carried out only on calm days.

The results of experiments are shown in Figs. 9~14. In order to compare with Figs. 5 and 6, the tidal currents only near the maximum velocity are shown in these figures. General results of all experiments will be reported on another occasion. Fig. 9 and 10 show the result for the case of $\alpha/\beta=8$, Figs. 11 and 12 for $\alpha/\beta=4$, and Figs. 13 and 14 for $\alpha/\beta=2$. The values of velocity in these figures were calculated from $(U_j)_1 = (\alpha/\tau)(U_j)_2$ —the relation derived from scale values. In these figures it is found that in the case of $\alpha/\beta=8$ the velocity is smaller than in the prototype and it increases from offing toward the mouth of river. In the case of $\alpha/\beta=4$ the velocity is also smaller than in the prototype and almost uniform everywhere. However, in the case of $\alpha/\beta=2$ the velocity agrees well with the prototype and the decrease of velocity is noticed near the 5 m contour. Furthermore near the left bank of Fukushima River a counter-current is found in the prototype at flood tide, and near Iguchi an eddy motion at falling tide. So, in this case it may be said that the tidal current in the model is similar to that in the prototype not only qualitatively but also quantitatively. Considering the error of observation and experiment, the similarity between prototype and model is quite well.

IV. CONSIDERATIONS

From the results obtained above the ratio of drag coefficients may be decided as follows

$$\frac{C_2}{C_1} = 2 \quad \dots \dots \dots (6)$$

The drag coefficient is generally a function of Reynolds' number, i.e. for laminar flow this functional relation is sufficiently expressed by Blasius' formula,

$$C = \frac{1.328}{\sqrt{Re}}, \quad Re < 10^5 \quad \dots \dots \dots (7)$$

Although this formula holds good in the case of a stationary motion, it is tentatively assumed that it holds also good for vertically mean velocity of tidal current when the Reynolds'

Table 2

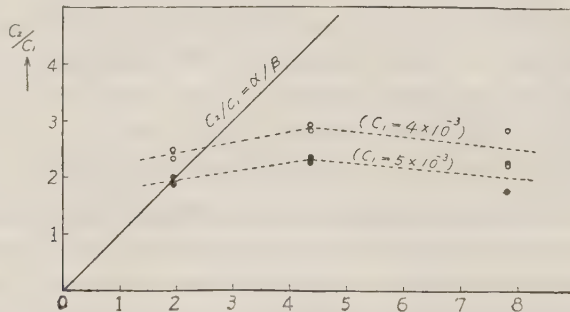
α/β	8	4	2
Re	1.38×10^4	1.28×10^4	1.79×10^4

Table 3

α/β	8	4	2
C_2 (c.g.s.)	1.13×10^{-2}	1.17×10^{-2}	0.99×10^{-2}

number is expressed by maximum velocity of tidal current (U), and the distance of maximum tidal excursion (L) because the tidal current in the model changes very slowly. Such Reynolds' numbers calculated from the results of experiments are shown in Table 2, each of them being in the region of laminar flow. Therefore, equation (7) may be applied to this case and the calculated values of C_2 are given in Table 3.

Although there is no precise information about drag coefficient of prototype C_1 , it has been usually said that it takes the value of $4 \times 10^{-3} \sim 5 \times 10^{-3}$ (c.g.s.) from the result of many observations on the wind and water flow over solid rough surface. Now assuming $C_1 = 4 \times 10^{-3}$ (c.g.s.) and $C_1 = 5 \times 10^{-3}$ for C_1 and the values in Table 3 for C_2 , the relation between C_2/C_1 and α/β is shown as Fig. 15. In this figure a straight line indicates the relation $C_2/C_1 = \alpha/\beta$. Any point on this line satisfies the theoretically required condition. From our result it may be admitted that $C_1 = 5 \times 10^{-3}$, $\alpha/\beta = 2$ and formula (7) are obtained for tidal motion in the model.

Fig. 15 Relation between C_2/C_1 and α/β (observed and theoretical)

When the similitude between the prototype and model holds good, the relation of velocity $(U_j)_1 = (\alpha/r)(U_j)_2$ must be established and further, equation (5) is substantial. Substituting these relations into Reynolds' number of prototype $Re_1\{(U_j)_1 L_1 / \nu\}$, we obtain the next equation.

$$Re_2 = \frac{Re_1}{\alpha \sqrt{\beta}} \quad \dots \dots \dots (8)$$

This equation shows that the relation is satisfied by both Reynolds' numbers in prototype and its model. The mean value of Re_1 , calculated from the results of observation in the prototype is $Re_1 = 1.4 \times 10^8$ ($U = 9.7$ cm/sec, $L = 1.4 \times 10^5$ cm). The values of Re_2 for various

Table 4

α/β	8	4	2
Re_2 (8) による	3.4×10^4	2.5×10^4	1.7×10^4

values of α/β are calculated from equation (8) and shown in Table 4, where $\alpha = 500$.

In this table the calculated value coincides with experimental value for $\alpha/\beta=2$, implying that when the similitude holds good the equation (8) is substantial. If we substitute Re_2 of equation (8) into equation (7), C_2 is expressed by Re_1 . Substituting this C_2 into equation (4) we get the following relation.

$$\frac{C_1 \sqrt{\alpha Re_1}}{1.328} = \beta^{5/4} \quad \dots \dots \dots \quad (9)$$

This formula provides a general relation between horizontal scale and vertical scale of the model which is dynamically similar to the prototype. According to this formula, realization of similarity in the case of $\alpha/\beta=2$ is due to the adopted value of horizontal scale, i.e. $\alpha=500$. A different value of α gives a different value of β , for example, $\beta=190$ for $\alpha=250$. A larger β corresponds with a larger α , then the water depth of the model becomes very small to render the experiment difficult to carry out. On the contrary, a smaller β corresponds with a smaller α , then the model becomes large and a fear arises that the tidal current in the model surpasses the laminar region, and further it becomes difficult to protect the model from wind effect. It is important to consider these points before the model experiment is carried out.

V. EFFECT OF TRAINING JETTY

As mentioned above there is a plan under way to construct a training jetty of 1.5 km in length in the estuary as the continuation of right bank of Fukushima River. It is interesting how the tidal current in this neighborhood will be changed after realization of this plan. Since the similitude was verified, the model experiment on the tidal current of this region after the construction of this training jetty has been carried out by the same method and procedure under the same conditions. The result of experiment is shown in Figs. 16 and 17. According to this result the velocity in western region of the training jetty is reduced to less than half of the previous one since the communication of water between sea and Fukushima River is shut off except through the river mouth. Especially near the jetty the reduction of velocity is extreme. The influenced region seems to be of a square area formed by the length of jetty.

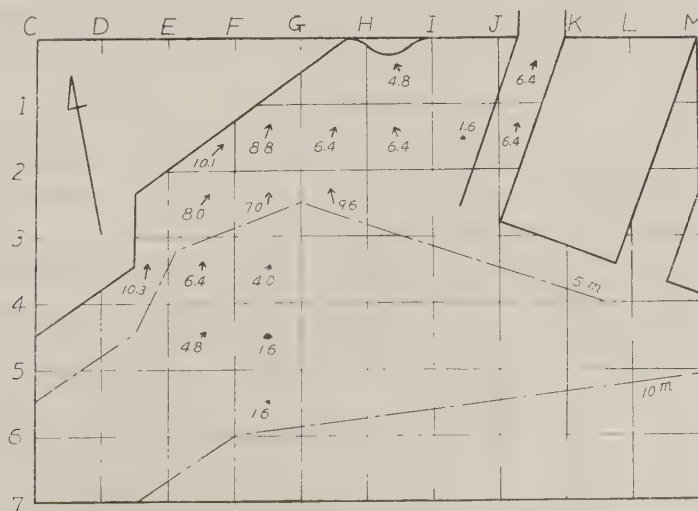


Fig. 16 Effect of the training dyke in the estuary of the Fukushima River now under planning. Pattern of the maximum rising current. $\alpha/\beta=2$.

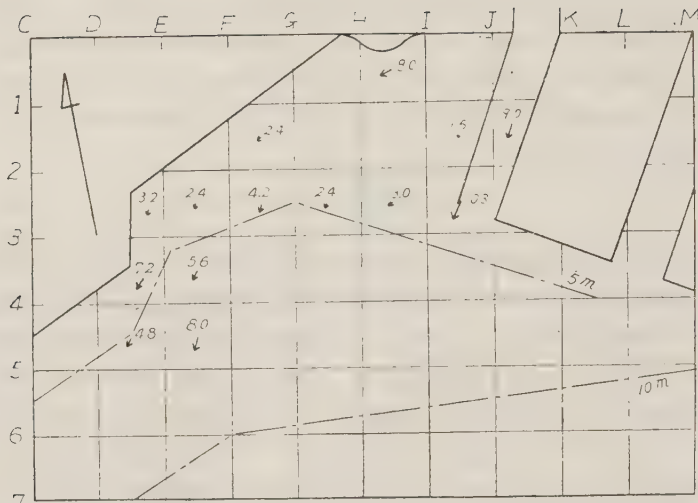


Fig. 17 Effect of the training dyke in the estuary of the Fukushima River now under planning. Pattern of the maximum falling current. $\alpha/\beta=2$.

Mixing of sea water through a tidal current is regarded microscopically as diffusion, and the coefficient of diffusion is given by AUL. Since A is a constant, it is proportional to the square of velocity. Accordingly, when the velocity is reduced to half, the coefficient in the influenced region becomes 1/4.

Since the supply of nourishing material, the exclusion of excremental material and the mixing of water are effected by the tidal diffusion, the influence of jetty over marine lives may be effected to a large extent through this reduction of the coefficient of diffusion.

ACKNOWLEDGEMENT

The field observation in the prototype Hiroshima Bay was executed in cooperation with Inland Sea Fisheries Research Institute and Geophysical Institute, Kyoto University. We are very grateful to Dr. Hanaoka, Chief of ISFRI, and the members of his staff for their kind co-operation.

Mr. Shohei Adachi and Mr. Hideaki Kunishi offered us many imformations regarding the model experiment. This study was made with grants of the Bureau of Fishery and the Ministry of Education.

REFERENCES

- 1) Hayami, S. (1956). Study on the Improvement of Productivity of the Coastal Waters by Coastal Constructions (I). Disaster Prevention Research Institute, Kyoto University. (In Japanese).
- 2) _____ (1957). Ditto (II).
- 3) Hayami, S., Y, Fukuo, D, Yoda. (1958). On the Exchange of Water and the Productivity of a Bay (I). Rec. Oceanograph. Work in Japan, Sp. No. 2.
- 4) Hayami, S. and Y, Fukuo. (1959). Ditto (II). Rec. Oceanograph. Work in Japan, No. 3.

ON THE DENSITY CURRENTS IN THE ESTUARY

*Takeshi Ito
Sei-ichi Sato
Tsutomu Kishi
Masateru Tominaga**

SUMMARY

On the Pacific coast of Japan most of the rivers are of the moderate mixing type having a density gradient both in the vertical and horizontal directions. From the field observations made on the Tone and Gokase rivers both of which empty themselves to the Pacific it was found that these rivers were both of the moderate mixing type and the salt water intrusion had a wedge-like shape. It was further observed that on the Tone river exchange flow was maintained for a long time, while on the Gokase river it was very short lived and salt water intruded the river so that the river was dammed up by a salt water wedge. On the other hand a detailed analysis of salinity distributions revealed that the duration of exchange flow was longer in case the upper and lower layers had different density gradients, while the duration was shorter when the gradients were nearly uniform.

In general it is not easy to treat theoretically the salinity distributions in the rivers of the moderate mixing type. Nevertheless a method is proposed from the engineering point of view for locating the upper limit of salt intrusion. The method is applicable to those rivers such as the Gokase river where salt water intrudes the river in a wedge-like shape and dams fresh water. The results obtained by this method on the Gokase river was found sufficiently well in agreement with the observational data.

I. INTRODUCTION

At the estuary fresh and salt waters come in contact with each other and a large-scale density current takes place as a result of the difference in their respective densities. According to the classification proposed by H. Stommel¹⁾ (1953) on the basis of the degree of mixing, there are as shown in Fig. 1 three types of mixing, namely, negligible, moderate and intense mixings. The distribution of salinity along the current is shown in the figure with respect to each of these types, where the thickness of the green shading is proportional to salinity.

Fig. 1 (a) gives an example of the type of negligible mixing, where fresh and salt waters are not mixed and respectively form separate layers. Since there takes place only a little mixing, the density gradient in the horizontal direction is practically negligible. Such a type of mixing is frequently observed at the estuary with a small tidal range.

Fig. 1 (c) on the other hand renders an example of the type of intense mixing, which takes place as a result

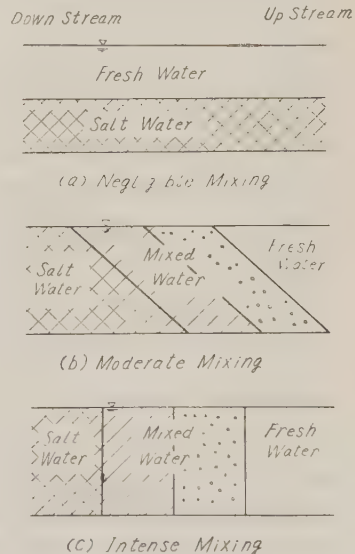


Fig. 1 Type of salt water intrusion

of an intense mixing between fresh and salt water layers. In this case no density difference is seen in the vertical direction, but the density gradient is obviously in existence in the horizontal direction with vertical iso-chrolines. While Fig. 1 (b) gives us an idea of moderate mixing. In this type of mixing the density gradient does not vanish both in vertical and horizontal directions.

At the estuary with a large tidal range, the periodical alternation of flood and ebb tides gives rise to the formation of turbulence from the river bottom so that surf surface and bottom layers are mixed up with each other. In such cases the type (a) occurs very rarely and usually the type (b) or (c) takes place. Of course some of the type (b) are nearer the type (a) with a smaller degree of mixing, while some others are more or less closer to the type (c).

The tidal range varies in the range of 1-2 m on the Pacific coast of Japan, where most of the rivers are of the type of moderate mixing as exemplified by the Tone and Gokase rivers, which will be discussed in the sequel. On the other hand, the tidal range is very small on the Japan Sea coast. Most of the river on the coast therefore seem to be of the type of negligible mixing or of similar types. In Fig. 2 there is shown the salinity distribution of the Chikugo river, which empties itself to the Sea of Ariake. The distribution is obviously of the type of intense mixing. This is because the tidal range is very large in the Sea of Ariake being as large as some four meters.

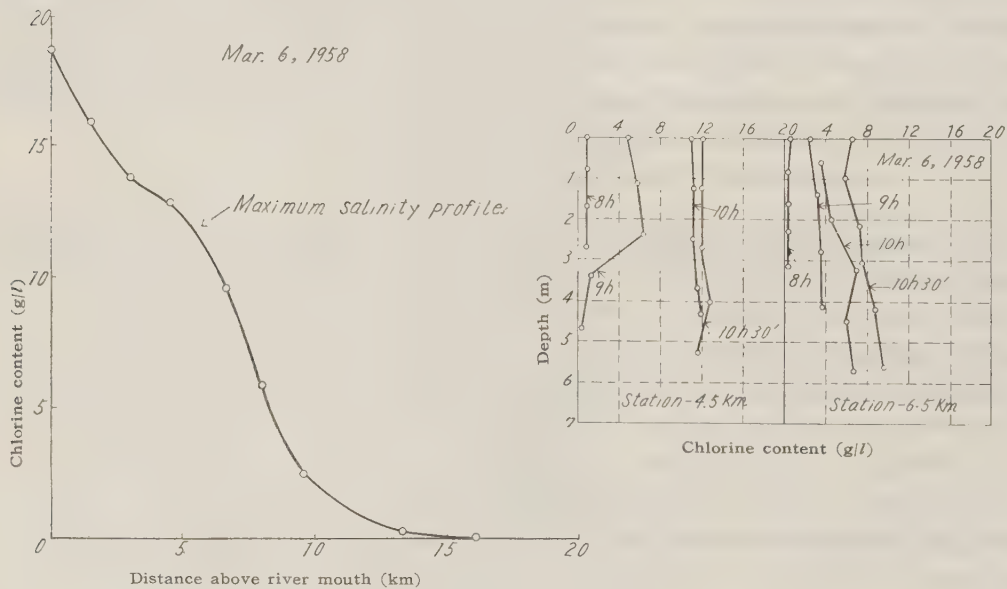


Fig. 2

As for the mechanism of density currents, some theoretical treatments have been attempted in relatively simple cases. In more complicated ones such as those of the type of mode rate mixing, very little has been explored so far. In what follows the salt water intrusion of the moderate mixing type will be observed on the basis of the data obtained on the Tone and Gokase rivers. Further a method will be proposed to find the range of the salt water intrusion (which will be in the sequel abbreviated as upper limit).

II. THE SALT WATER INTRUSION OF THE MODERATE MIXING TYPE

2.1. Examples of the salinity distribution of the moderate mixing type

In Japan the rivers which discharge themselves into the Pacific are affected by a fairly large tidal range. The intrusion of salt water is therefore of the type of moderate mixing. Fig. 3 gives the results of the observations made on the Tone river on August 13 and 14, 1954. On the basis of the data obtained at the Fukawa Observatory during the years 1941-1950, the discharge for normal times at the downstream of the Tone river is given in Table 1.

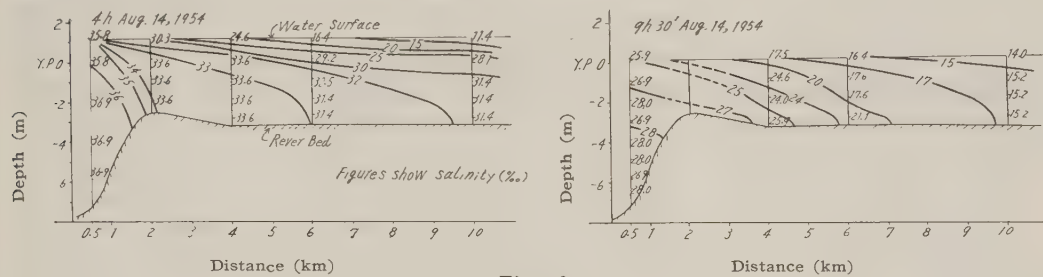


Fig. 3

Table-1 Normal Discharge at Fukawa

High Water Discharge	Mean Discharge	Low Water Discharge	Minimum Discharge
323. m³/sec	175.4	100.5	46.5

On the other hand the discharge at the time of the above observations was 60 m³/sec (at Toride) the amount being about the same as the minimum discharge, while the tidal range was 1.10 m. Fig. 3 (a) and (b) respectively give the salinity distributions at the time of flood and ebb tides. Fig. 3 (a) shows that the salt water with the salinity of more than 30‰ intrudes the river upwards as far as some 10 km from the river mouth and the iso-chlorine curves take a wedge-like shape.

Fig. 4 is the results of the observations made on the Tone river on October 15, 1954. The tidal range was about the same as in the preceding observations being 1.25 m, but the discharge amounted to 183.3 m³/sec (at Toride) being three times as much. Fig. 4 (a) and (b) respectively give the salinity distributions at the time of flood and ebb tides. Since the discharge is large, salt water intrudes the river only little and as shown in Fig. 4 (a) the salinity of more than 30‰ is found only within the distance of 2 km from the river mouth and even such strong salinity is located only near the bottom. On the other hand, as is clear from Fig. 4 (b) the salt in the river channel is almost completely discharged at the time of ebb tide.

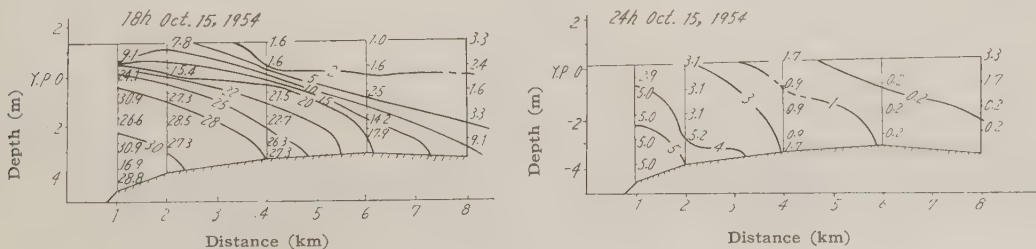


Fig. 4

Fsg. 5 gives the salinity distributions at the Gokase river as observed in April, 1945. In Fig. 5 is shown the results of the observation on April 4, when the tidal range and discharge were respectively 1.95 m and 15 m³/sec. In these figures the salinity distribution is given in terms of the chroline content. Between the chroline content Cl and salinity s there holds the equation

$$s = 0.030 + 1.8050 \text{ Cl}.$$

For instance we have $s = 34.33\%$ for $\text{Cl} = 19000 \text{ ppm}$.

On the Gokase river the intrusion of salt water again takes the type of moderate mixing. However the iso-chlorines have a steeper gradient, which characterizes the river as coming near the intense mixing type. For instance Fig. 5 (b) gives the iso-chlorines at the time of flood tide, which were obtained during the observation in April. Here the curve corresponding to 5,000 ppm has a gradient of 11×10^{-4} , while in the Tone river that corresponding to salinity 9% i.e. 5,000 ppm, has a gradient of 6.2×10^{-4} being about a half of the gradient of the former.

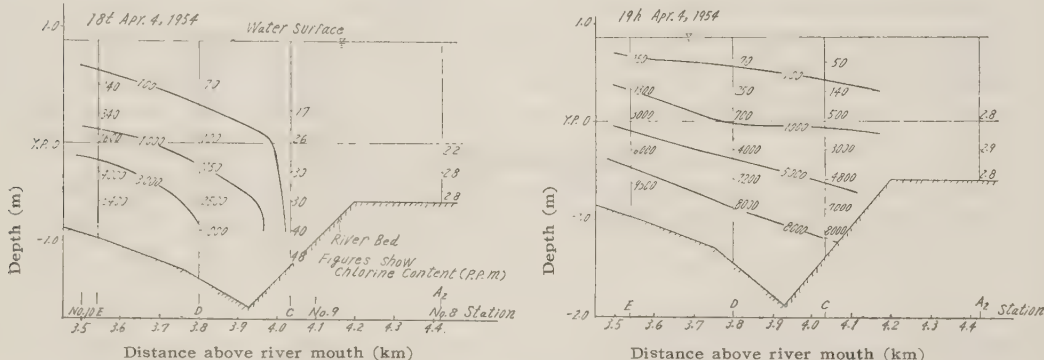


Fig. 5

2.2 Velocity distribution of the type of moderate mixing

Fig. 6 gives the velocity distribution of the Tone river obtained during the above-mentioned observations. Here the velocity distributions at the time of normal and reverse flows take peculiar forms as a result of the existence of a horizontal density gradient.

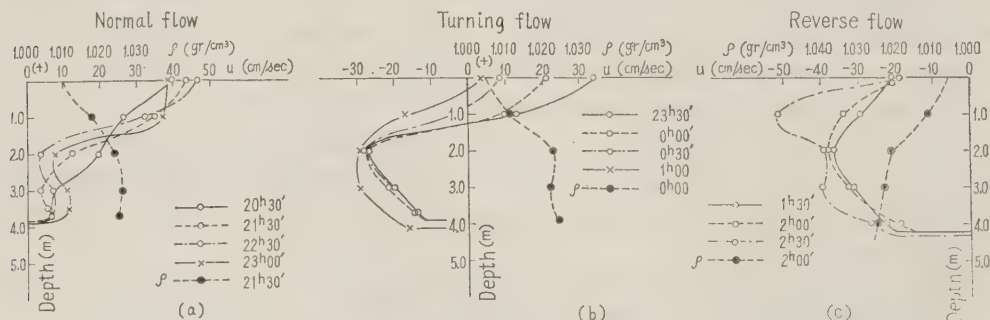


Fig. 6

At the stage of normal flow the horizontal density gradient has the sign converse to the surface gradient with the effect to reduce the velocity. Accordingly the velocity in the lower layers with stronger density currents is clearly distinguishable from that in the upper ones with stronger gradients currents. This is clear by seen from Fig. 6 (a).

At the time of reverse flow the horizontal density gradient has the same sign as the

surface gradient with the effect to accelerate the flow. Since the density gradient is larger in the lower layers, the velocity takes its maximum value at a certain depth from the surface and the velocity distribution takes a form similar to that in a pipe.

Since the surface gradient almost vanishes when the normal flow changes into the reverse one, the density gradient is larger than the surface gradient in the lower layers. Thus the normal flow prevails in the surface layers, while the reverse flow is dominant in the lower layers. This gives rise to the so-called state of exchange flow.

On the Tone river the velocity was observed several times during the years from 1954 to 1956 and the relation between the duration of exchange flow, the discharge and the tidal range was obtained as tabulated in Table 2.

Table-2 Duration of Exchange Flow

Date	Discharge m ³ /sec	Tidal Range m	Station			
			0 km	1 km	2 km	4 km
Jul. 28 1954	121.6	1.0	60 min			
Aug. 13 1954	60.0	0.45		60	75	
Oct. 15 1954	183.3	0.55	40	55	70	
Aug. 22 1956	15.0	1.0	30			80

From Table 2 we cannot see any definite relation which might hold between the duration on the one hand and the discharge and tidal range on the other, the exception being the short duration observed on August 22, 1956, when the river was in the state of minimum discharge. There is seen on the other hand a tendency that the duration increases as we go upwards from the river mouth. As the surface gradient is small near the mouth of the Tone river, a reverse flow is formed unless the river is flooded to a certain extent. At the time when the flow turns, an exchange flow is therefore formed if there is in existence a horizontal density gradient in the bottom layers and its duration is determined by the interrelation between the surface and density gradients. At the time of 1956 observation the discharge was very small and as a result the density gradients differed only a little from each other in the surface and bottom layers. It seems that this was mainly responsible for a short duration which took place at that time. On the other hand, the duration tends to

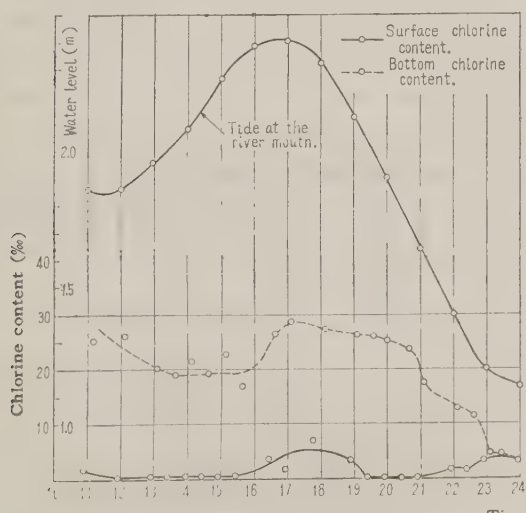


Fig. 7 (a)

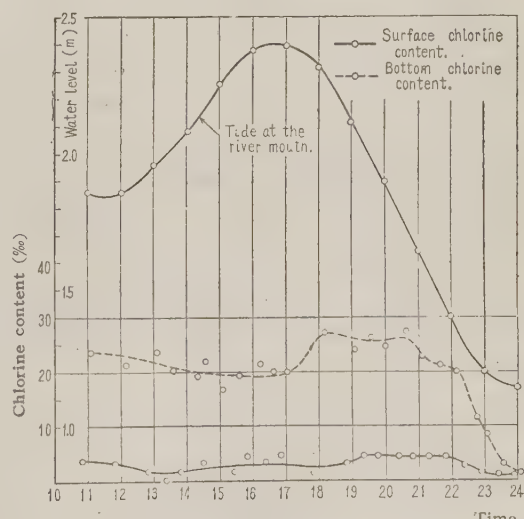


Fig. 7 (b)

become longer as we go up the river. This is presumably due to the fact that the difference of the density gradients in surface and bottom layers tends to become larger in the upstream. For instance Fig. 7 shows on the basis of the observation made on October 15, 1954, the temporal variations of the salinities in surface and bottom layers respectively

2 km, 4 km and 6 km from the river mouth. At the surface the variation remains the same throughout these places and the horizontal density gradient almost vanishes. At the bottom only a small difference is seen in salinity at the places respectively 2 km and 4 km from the river mouth. However a fairly large difference is noticed at the places respectively 4 km and 6 km from the mouth. This is the evidence that the horizontal density gradient is concentrated upon the bottom layers.

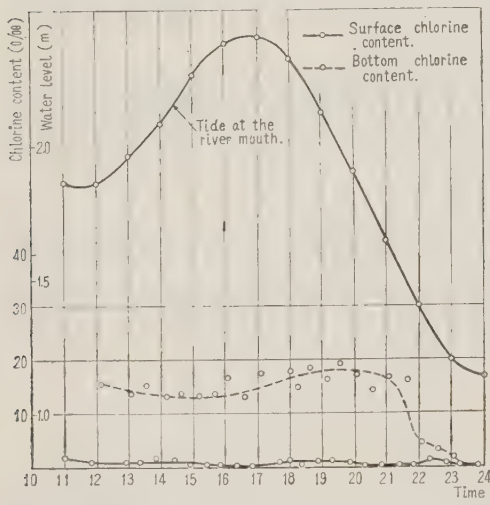
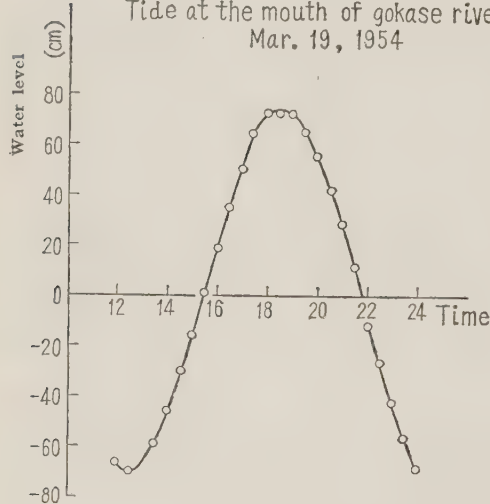


Fig. 7 (c)

Tide at the mouth of gokase river
Mar. 19, 1954

Station-No.9' Mar. 19, 1954

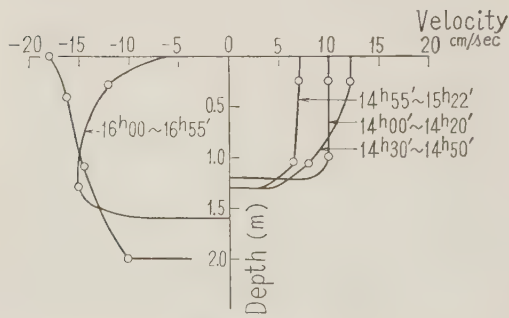
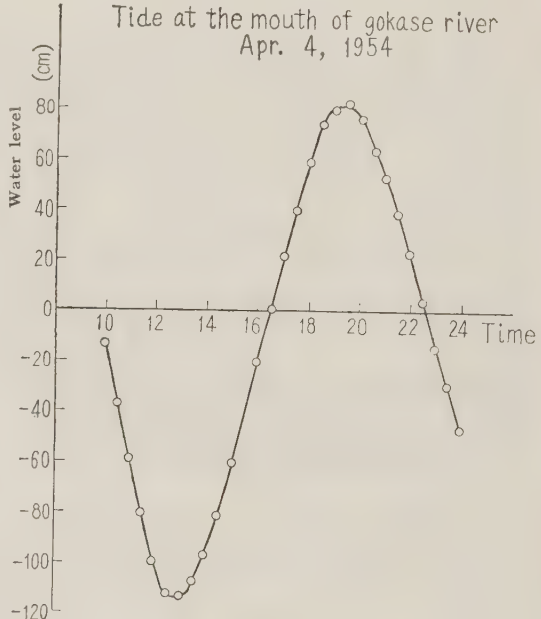


Fig. 8 (a)

Tide at the mouth of gokase river
Apr. 4, 1954

Station-No.11' Apr. 4, 1954

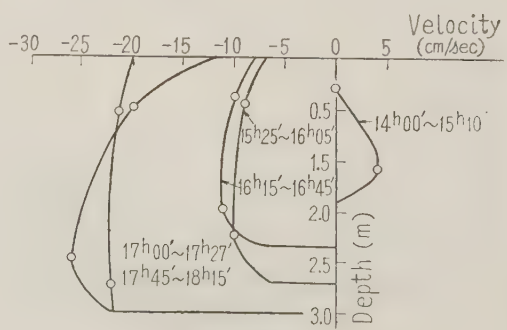


Fig. 8 (b)

Now we shall proceed to the velocity distribution in the Gokase river. As aforementioned, the chlorinity distribution takes a form closer to the type of intense mixing than the distribution in the Tone river. We shall next be concerned with the problem in what may such characteristics are represented in the velocity distribution. Fig. 8 gives the velocity distribution of the Gokase river as observed in 1954. If we compare Fig. 8 with Fig. 6, it is easily seen that exchange flow does not take place on the Gokase river. Further, even at the time of normal and reverse flows there does not appear so distinctly the pattern of the velocity distribution characteristic to the Tone river. This is because the chlorinity distribution of the Gokase river is almost of the type of intense mixing with the small difference in the horizontal density gradients in surface and bottom layers. In Fig. 9 we have, on the basis of the observation made in April, 1954, the temporal variations of the surface and bottom chlorinity at the station E (See Fig. 5.) and another one located 500 m up. Here the horizontal density gradient is almost uniform from the surface down to the bottom.

From Table 2 it is seen that, in the Tone river, exchange flow is maintained for some time irrespective of the amount of the discharge and tidal range, whereas no exchange flow is observed on the Gokase river. As above mentioned the former is the case that the surface and bottom layers have different horizontal density gradients, while the latter is seen in case the value of the gradients is nearly uniform in the surface as well as in the bottom layers. In a word the problem which case really happens is reduced to the degree of turbulent mixing which might take place between the surface and bottom layers. The degree is more specifically represented as the coefficient of roughness of the river. Thus there is a possibility to connect the duration to the coefficient of roughness.

III. UPPER LIMIT OF SALT WATER INTRUSION OF THE MODERATE MIXING TYPE

3.1. Summary

As above mentioned there is no general principle which takes account of the mechanism of salt water intrusion of the moderate mixing type. In other words it is highly difficult to obtain the velocity and salinity distribution and other informations from a fundamental equation which takes into consideration the effect of the density current. Nevertheless, in

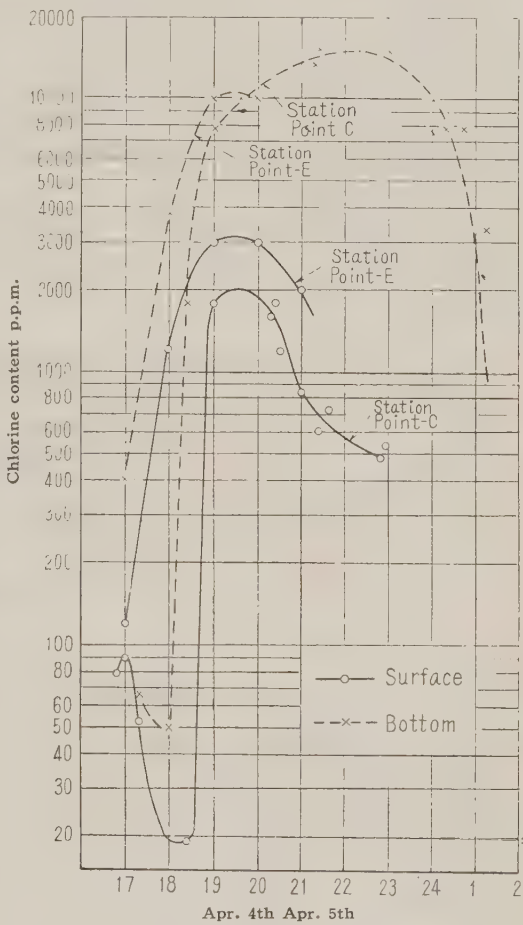


Fig. 9

many cases we only interested in locating the upper limit of salt water intrusion from the engineering point of view. Thus we shall give a procedure which will enable us to fix the upper limit from the practical point of view.

3.2. Principles and procedure

In the case of the moderate mixing type the iso-chlorine take a wedge-like shape and salt water gradually fades out into fresh water. For practical purposes it is however sufficient to locate any fixed one of these iso-chlorines. With this in view the iso-chlorine thus fixed will be considered to be a front of the salt water wedge and we suppose that the upstream and downstream sides of the front respectively consist of fresh and salt waters. It is therefore our task to locate the front.

In case no exchange flow takes place at the time of turning flow and the river is supposedly dammed up by a salt water wedge, we can locate the wedge at a certain time in the following way.

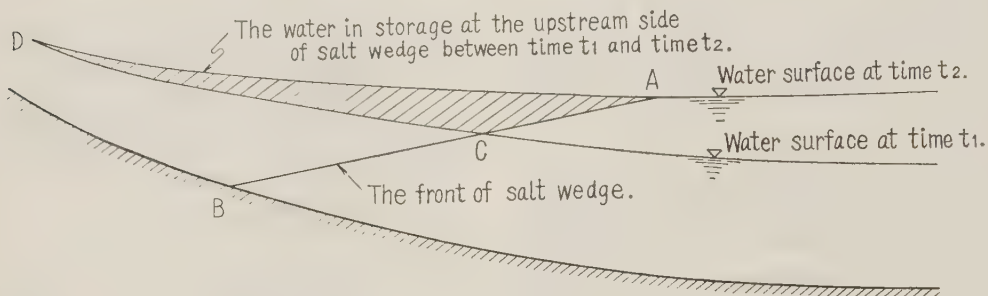


Fig. 10

In Fig. 10 the domain which lies between the water surface at the time t_1 and that at the time t_2 constitutes the amount of intruding salt water and the water in storage at the upstream side of the wedge. As it is supposed that fresh and salt waters practically do not mix with each other and the former is stored at the upstream side of the latter, the curve, if properly drawn with the same gradient as the salt water wedge, will divide the said domain into two parts, the one at the upstream side corresponding to the water in storage. Thus the whole problem is solved if we can obtain the frontal gradient of the salt wedge, which is approximately calculated as follows :

In terms of the notations in Fig. 11 we have as the equation of motion of the fluids in upper and lower layers²⁾

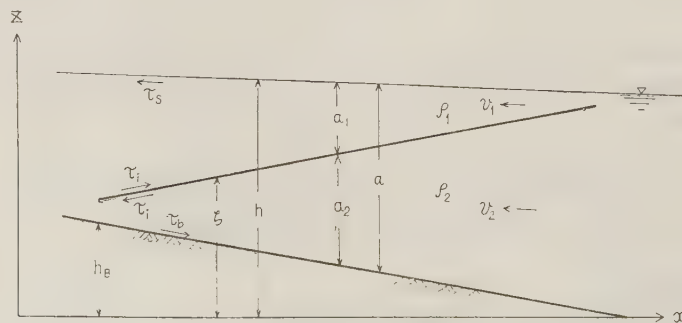


Fig. 11

$$\frac{\partial v_1}{\partial t} + g \frac{\partial a_1}{\partial x} - g \frac{\partial a_2}{\partial x} + v_1 \frac{\partial v_1}{\partial x} - g(i_1 - i_b) = 0 \quad \dots \dots \dots (1)$$

where

$$i_1 = \frac{\tau_i - \tau_s}{\rho g a_1}, \quad i_2 = \frac{\tau_b - \tau_i}{\rho_2 g a_2},$$

and

τ_s : the shearing force of the surface,

τ_i : the shearing force of th boundary,

τ_b : the shearing force of the bottom,

i_b : the bottom gradient $= -\frac{dh_B}{dx}$

$$\varepsilon = \frac{\rho_2 - \rho_1}{\rho_2}$$

ρ : density,

Assuming $\tau_s = 0$ in the equations (1) and (2), we obtain in general

Assuming $i_1 \neq 0$ in eq. (1), we have

$$\frac{\partial v_1}{\partial t} + g \frac{\partial h}{\partial x} + v_1 \frac{\partial v_1}{\partial x} = 0.$$

from which we obtain

Rearranging (2) and substituting it to (6), we obtain the following equation under the condition $v_1 \neq v_2$,

$$\frac{1}{g} \left(1 - \frac{\rho_1}{\rho_2} \right) \left(\frac{\partial v_2}{\partial t} + v_2 \frac{\partial v_2}{\partial x} \right) + \left(1 - \frac{\rho_1}{\rho_2} \right) \frac{\partial \rho}{\partial x} + \frac{\rho}{\rho_2} \frac{|v_2| |v_2|}{a_2 c b^2} = 0. \quad \dots \dots \dots (7)$$

Since $\frac{1}{g} \left(\frac{\partial v_z}{\partial t} + v_z \frac{\partial v_z}{\partial x} \right)$ is the same order as the surface gradient, it is supposed to be small compared with $\frac{\partial \zeta}{\partial x}$ in the case of the moderate mixing type. We can therefore neglect the second and third terms of (7) and obtain

$$\left(1 - \frac{\rho_1}{\rho_2}\right) \frac{\partial \rho}{\partial x} + \frac{\rho_1}{\rho_2} \frac{v_2 |v_2|}{a_2 c_b^2} = 0. \quad \dots \dots \dots \quad (8)$$

In the above formula the resistance coefficient c_b is determined by the field observation, while other quantities are all obtained by computation. Thus we are able to get the gradient therefrom. On the other hand it is sufficient to let α_2 be about 1/2 of the average depth of the region where the wedge is located.

Summing up the procedure to locate the salt water wedge,

(1) Surface profiles are determined either by calculation or by measurement at a time of flood ebb t_1 and at another time t_2 , the location of the wedge at which we are looking for.

(2) Next we compute the discharge stored in the domain lying between the two profiles during the course of time from t_1 to t_2 .

(3) From (8) the gradient of the salt water wedge is obtained.

(4) Lastly we determine the location of the wedge so that the domain surrounded by the two surface profiles and the wedge front with the gradient (determined in (3)) may be equal to the discharge as obtained in (2).

3.3. Applications

With a view to obtaining information on the salt water intrusion on the Gokase river, a comprehensive survey was carried out in 1954 about the level, velocity, chlorinity and other items.

On the Gokase river exchange flow is almost negligible. We can therefore suppose that salt water intrudes the river and dams fresh water. As seen from the pattern of salt water in Fig. 5, iso-chlorine are almost parallel to each other and $\partial\rho/\partial z$ distinctively changes when we pass 1,000 ppm curve. We can therefore consider 1,000 ppm curve to be the front of the salt wedge, which separates the fresh water located above the curve from the salt water with the chlorinity from 5,000 to 6,000 ppm.

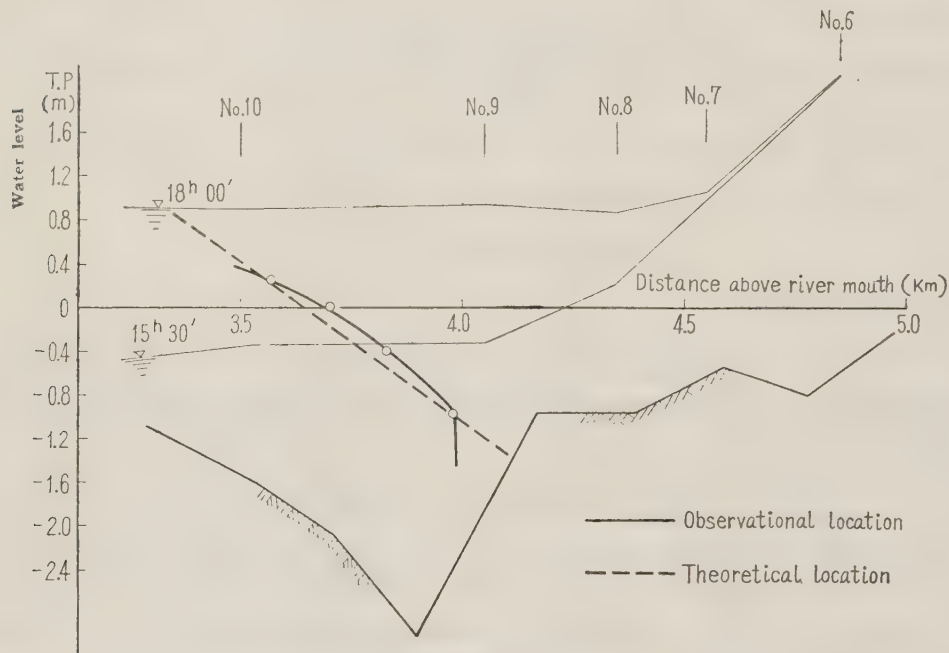


Fig. 12

In Fig. 12 there are given the theoretical value¹¹⁾ of the location of the salt water wedge as at 18 : 00 hr April 4, 1954, obtained during the afore-mentioned survey and the one obtained by the actual measurement³⁾. In theoretical computation as well as in the actual measurement, 1,000 ppm curve in Fig. 5 (a) is supposed to constitute the boundary between salt and fresh waters. As is clear from Fig. 12, the theoretical value fairly well coincides with the observational one. This is one of the evidences that the proposed method is satisfactory from the practical point of view.

It should however be noticed that there will remain some mixed layers even if the salt wedge is located by this method. It is therefore necessary to evaluate the thickness of these layers by field observations, if we want to find the upper limit of salt intrusion.

IV. CONCLUSION

The intrusion of salt water into the river was classified into three types, i.e. intense,

moderate and negligible mixings and a method was proposed for locating the upper limit of salt intrusion of the moderate mixing type. This method is applicable when the salt water has the following characteristics :

(1) The salt water intrusion takes a wedge-like shape,
and

(2) No exchange flow is formed and faesh water is dammed by water.

Since the Gokase river was found satisfying these conditions by the survery, the location of the salt wedge was obtained by computation well in agreement with tha observational value. It is however very difficult to evaluate the upper limit of salt intrusion if we should take into consideration plannings of improvement and other particulars which might change the river and we have not been successful in finding any reliable general method to locate the upper limit. Nevertheless the following method is available even in such cases :

- (1) The tidal level curve and discharge data are first obtained,
- (2) Neglecting the density difference, hydrographical computation is made by means of the method of characteristics. The necessary data are furnished by field observations,
- (3) The water surface profile is drawn at the time of ebb tide,
- (4) A fixed time between the flood tide and the instant when the upper limit of tidal reach begins to flow reversely is selected and the water surface profile thereof is drawn.
- (5) The discharge stored in the domain lying between these two profiles is computed,
- (6) The salts wedge is roughly located using the information obtained in (5) and if the time of turning flow at this location does not coincide with that previously selected, then the same process is repeated until the coincidence is attained,
- (7) When the coincidence is attained, the gradient of the salt wedge is calculated, wherein we employ as velocity the average velocity at the location obtained in (6), while the coefficient of roughness is determined by field observations.
- (8) The exact location of the salt wedge is then obtained from the discharge in storage and the gradients respectively obtained in (5) and (7).
- (9) The thickness of the mixing layers is evaluated on the basis of field observations and the upper limit of salt water intrusion is finally determined therefrom.

This method is of course based upon the one proposed above. Into it there is further incorporated an idea that the chlorinity at a certain place increases as far as the flow is reverse at the place and decreases when the flow turns. The steps (5) and (6) in the above method is based upon such an idea.

REFERENCES

- 1) Stommel, H. : The role of density current in estuaries; Proc. Minnesota Int. Hyd. Convention, I.A.H.R. Sept. 1953
- 2) Schijf, J.B. and J.C. Schönfeld, : Theoretical considerations on the motion of salt and fresh water; Proc. Minnesota Int. Hyd. Convention, I.A.H.R. Sept. 1953
- 3) Ito, T. S. Sato, T. Kishi and M. Tominaga : On the salt wedge in estuaries; Jour. of the Public Works Research Institute, Vol. 101

TSUNAMI CAUSED BY CHILE EARTHQUAKE IN MAY, 1960 AND OUTLINE OF DISASTERS IN NORTHEASTERN COASTS OF JAPAN*

*Toshio Iwasaki***

*Kiyoshi Horikawa****

I. GENERAL REVIEW

At the dawn of May 24, 1960, the entire stretch of the Pacific coasts of Japan was overwhelmed by a surprise assault of a tsunami without any previous sign of warning due to tremors of an adjacent earthquake. The resulting disasters were tragic and farreaching. The fact that this tsunami was generated near Chile which is located at the diametrically opposite position of the globe to Japan, upset the conventional notion that "a tsunami accompanies an earthquake having the epicenter in the neighboring ocean bed of Japan." This and other peculiarities of this tsunami gave rise to numerous problems the kind of which was all but unprecedented.

The authors led a group of the investigation parties which were organized immediately after the disaster, making an investigation tour to the northeastern coasts**** of Japan where the disasters were believed to be most serious. The principal objectives of our investigation included primarily the civil engineering structures, together with gauge records and traces of the tsunami, and the effects exhibited by the existing counter-tsunami measures.

The project consisted of 2 separate operations each covering the periods from 26 to 31 May and from 5 to 12 June, and the investigation was carried out in such cities, towns, and their vicinities as :

Shiogama, Ishinomaki, southern coasts of the Ojika peninsula, Onagawa, Okachi, Shizukawa and Kesenuma, Miyagi Prefecture;

Rikuzen-takada, Ofunato, Kamaishi, Ryoishi, Ozuchi, Funakoshi, Yamada, Miyako, Taro and Kuji, Iwate Prefecture; and

Hachinoe, Aomori Prefecture.

We should like to express our grateful appreciation to the local authorities who willingly took trouble to provide us with whatever information and assistance available, although they were swamped with recovery and rescue activities of great urgency.

We fear that this report is incomplete as it is, since some of the data utilized here had to be presented without due theoretical treatments owing to pressing limitation of time. However, the authors shall feel deeply obliged if the readers could learn something of value from our account which meant to convey vivid scenes of disaster to the interested world as early as possible.

* Translated from the paper presented to Journ. Jap. Soc. Civil Engrs., Aug. 1960,

** Professor of civil engineering, Tohoku University, Japan.

*** Assistant Professor of civil engineering, University of Tokyo, Japan.

**** Commonly known as the Sanriku coasts in Japan.

II. CHARACTERISTICS UNIQUE TO THE TSUNAMI CAUSED BY THE CHILE EARTHQUAKE, 1960.

It was approximately 7:23 p.m. 21 May that the observation department of the Japan Meteorological Bureau caught the first wave of the Chile earthquake with the estimated magnitude $M=8$. The second wave was observed at 7:51 p.m. 22 May, the next day, and the 3rd and 4th waves respectively at 4:15 and 4:31 a.m. 23 May. The 4th wave is regarded as responsible for the tsunami which struck Japan across the Pacific. According to the hindcast made by the observatory at Matsushiro, Japan, this wave was of the magnitude 8 3/4 with the epicenter located offshore of the Concepcion city, Chile, at long. 73° W. and lat. 37° S. Later on, a Japanese correspondent covering the activities of the Japanese Investigation Delegation for Technical Cooperation with Chile on Earthquake Disasters, led by Professor Ryutaro Takahashi, University of Tokyo, as chief delegate, reported that a series of earthquakes dealt successive blows to the area ranging from Concepcion, north, to Puerto Monto, 780 km south, and I. de Chiloe, and that the earthquake which sent the disastrous tsunami to Japan occurred in the vicinity of Valdivia. The magnitude was estimated to be 8 1/2 to 8 1/4 by the C. & G.S., U.S.A., which gives a rough idea on the tremendous scale of this earthquake. The tsunami which followed this earthquake traveled westward and, striking the Hawaiian islands en route, reached Japan after 24 hours approximately of propagation across the Pacific. When calculated for the assumed average depth of the Pacific Ocean, i.e. 4282 m, the celerity of this tsunami is 216 m/s, which is in rough agreement with the relationship \sqrt{gh} , the propagation velocity of a long wave.

Professor Kozo Yoshida of the University of Tokyo constructed a refraction diagram which seems to offer a very interesting account of the movement of this tsunami. The diagram shows that, of the energy of the tsunami generated from the offshore water of Chile the portion confined to a 90° fan was steered to converge toward Japan due to bottom topographies of the Pacific Ocean, or particularly to shallow floors around the Hawaiian islands lying in midway. Naturally, other contingents of energy should also be considered, such as the portion of energy which must have been repelled due to reflection at the edge of the continental shelf, or that contributed from reflection at the Pacific coasts of north America. The complexity of the problem seems to require a further refined treatment by cooperating branches of geophysical science on the basis of the tidal records observed along the various coasts of the Pacific Ocean. However, a detailed discussion of these factors is beyond the scope of this paper.

In fact, there is a historical evidence that such unwarned tsunami without preceding tremors of a nearby earthquake as the 1960 tsunami has also taken place in the past. The Asahi called attention to the fact that the great earthquake of Chile in 1906 sent a tsunami wave as far as Japan.* It also reports that a tsunami generated by the Tokaido earthquake of Japan on November 4, 1854, arrived in San Francisco. After a laborious examination of the ancient chronological records of tsunami, Mr. Saburo Ninomiya, head of the Meteorological Observatory at Miyako, Japan, points out the coincidence between the tsunami which struck the Ozuchi district at 2:00 a.m., 26 May, 1751, and the entry in the Science Table edited by the Tokyo Astronomical Observatory which says: "On 2 May, 1751, a great

* One of the leading dailies in Japan.

earthquake followed by a tsunami struck Concepcion and Santiago of Chile necessitating re-siting of the former." Mr. Ninomiya further quotes the old record which describes the phenomena of this tsunami saying that the water was heaved in an overflowing manner causing no injuries on men and horses.

A tsunami which used to propagate a long fetch between the generating area and Japan is defined by Professor Jiro Suzuki of the Geophysical Department of the Tohoku University as a plane wave with the front lines aligned parallel to the direction of the Japan Islands. On the other hand, the Sanriku tsunami in 1933 had the generating center at the Tuscarora Deep, slightly over 200 km off the northeastern coast of Japan, and the waves which arrived on these coasts had the front lines shaped similar to the hyperbolic curves of a short focal length. Consequently, the maximum water level produced by the Sanriku tsunami was extremely high at some localities, but they tended to fall sharply as the distance grew. On the other hand the tsunami of 1960 gave the maximum levels almost uniform everywhere. Fig. 1 shows the distribution of the highest levels recorded by the 1960 tsunami and the time sequence of their occurrence along the coasts of Japan, summarized from the data published by the Meteorological Board and other authorities. It is noted that a wave of 3 to 5 m is predominant at the Tohoku and Hokkaido districts, while the height is reduced to 1 to 3 m to the west of the Kanto district. It appears that the tsunami arrived at north earlier; however, any definite remark should be avoided at present.

It appears almost certain that the tsunami of 1960 was of the period approximately 60 minutes at the ocean fringe off the Japan Islands. The periods of the past Sanriku tsunami



Fig. 1 Location map and distribution of tsunami levels. (unit : m)

were around 12 minutes.* The discrepancy in the periods of the tsunamis is largely responsible for the patterns of the heaving motion of water in the bay areas. In fact, it is said that, when the period of a tsunami exceeds that of the normal vibration of a bay, the wave height generally tends to attenuate as it advances toward the recess of the bay; while in the case of the period of the normal vibration greater than that of a tsunami, it gains in height as it advances. The levels over the standard datum of the Tokyo Post are shown from the authors' investigation of the traces and gauge records of the 1960 tsunami for the Kesenuma bay in Fig. 2, the Ofunato bay in Fig. 3, the Hirota bay in Fig. 4, and the Miyako bay in Fig. 5. As the figures show, the wave heights tend to increase towards the recesses of the bays except for Kesenuma. However, the Sanriku tsunami gave a contrary result at the bays of Ofunato and Miyako. The Shizukawa bay naturally tends to resonate against such a long period wave as the 1960 tsunami giving the highest wave at the deepest recess of the bay. A small inlet of Tsurugaura immediately adjoining the Kesenuma bay to the east was struck by an exceedingly high tsunami in 1933, but suffered almost no casualties by the 1960 tsunami. This fact is duly explained by Mr. Tadayasu Saijo of the Fishery High School at Kesenuma: The Kesenuma bay consists of 2 separate sectors east and west bordered by the Oshima island; the eastern sector is 6 km long and 27 m deep with 24-minute period of normal vibration, while the western sector, 10 km long

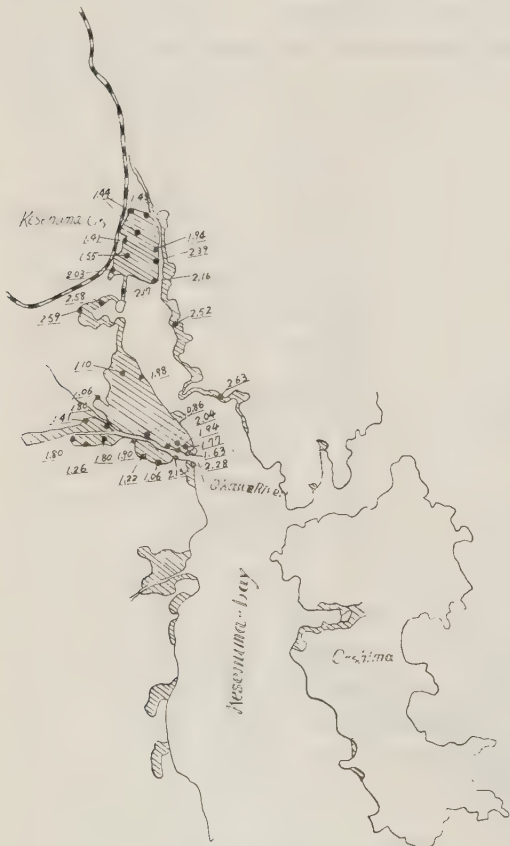


Fig. 2 Inundated area and highest level over T.P. (m)



Fig. 3 Inundated area and highest level over T.P. (m)

* Shinobu Sasaki : On Counter-tsunami Measures along the Sanriku Coasts, Proc. 6th Conf. Coastal Engg., Japan, November, 1959.



Fig. 4 Inundated area and highest level over T.P. (m)

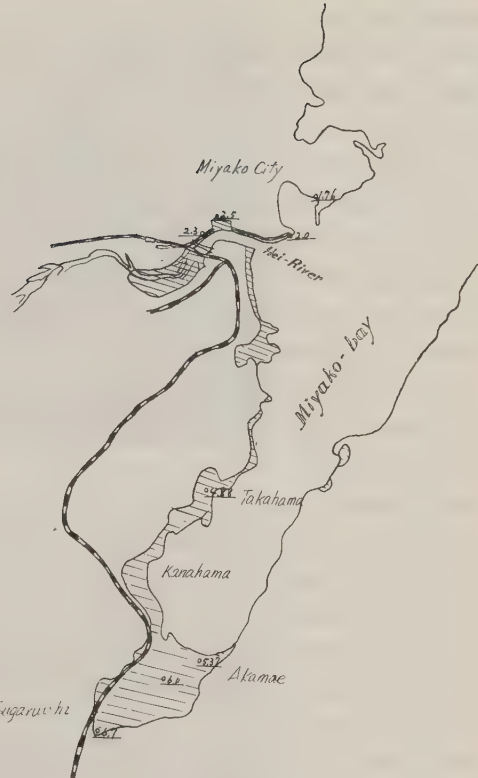


Fig. 5 Inundated area and highest level over T.P. (m)

and 10 m deep, has the normal period of 60 minutes.

The incident direction of a tsunami is unlikely to depend on the exposure of a bay, as seen from the phenomenon that the Onagawa and Ogihama ports, located respectively east and west of the Ojika peninsula with the exposing directions opposed by approximately 180° , showed the almost equal trace levels each T.P.+4.77 m and T.P.+4.50 m. This fact is easily understood by considering that the 1960 tsunami was a plane wave having a very large period.*

During our investigation we made an inquiry into the appearance and other related patterns of the tsunami wave through the local residents or photographic snaps. They all agreed to witness that the tsunami did not take a form of a bore or a spilling front, and that the sea gradually gained height over the entire surface of a bay. It will be of interest to quote here Dr. Akitsune Imamura who wrote in "Civil Engineering Records of Earthquake and Tsunami Disasters" published by the civil engineering department of Iwate Prefecture, 1936, that ".....a written account of an ancient who met with a tsunami compares it to a condition which might result from tilting the sea bed upward around a hinge resting at the shoreline," and that "this description truly depicts the situation."

On the other hand there are evidences showing a fairly large velocity of the water mass which accompanied the movement of the 1960 tsunami. According to Mr. Hajime Kanno, head of Port Development Office at Hachinoe, a dredger was ripped from the lightly

* In preparing this paragraph a reference was made to the Report No. 10 of the Department of Sciences which was addressed to the general seminar on the 1960 tsunami held at the Tohoku University on 28 June, 1960.

moored position and carried off at the velocity of approximately 10 knots by a stream which took place inside the harbor basin during reflux of the tsunami, finally resting on a reef outside the breakwater. There was a strong flow of water through the breakwater gap of the Miyako port during flux of the tsunami. The stream was so rapid that a fisherman barely succeeded in traversing it in a boat equipped with a 20 HP Yanmar diesel engine at the top speed of 8 knots. He vowed before the authors that the stream velocity was approximately 5 kots. We were also encountered with the witnesses at Miyako and Shizukawa stating that the drifting timbers fleeted at an amazing speed toward the length-wise direction, or that the stream was so violent that it looked as if a real river had suddenly appeared in the midst of the sea water.

There is a photographic evidence of a bore-shaped pattern of the tsunami circulated by the Kahoku Shimpo*, 2 June, which occurred at the river-mouth port of Ishinomaki as the tsunami advanced upstream pushing the boats along the wave front. We also heard a story repeatedly that the reflux was even more violent than the flux.

Much remain unsolved as to the effects of reflection and refraction of the tsunami occurring inside a basin as well as various phenomena quoted above.

Finally, we should like to invite the general attention to the efficiency of a tidal gauge. Of the 12 records which we obtained during the tour, none but 3 gives a correct recording of the maximum and minimum water levels. Some of them successfully traced the water level until scaling-out, or some of the apparently reasonable records had to be discarded later when it was found out that the underwater leading pipe had been clogged with mud. The officials of the Hachinoe Meteorological Observatory were wise enough to examine the leading pipe by taking advantage of a short duration of reflux and to discover that it had been bent. The pipe was quickly repaired and an almost perfect record of subsequent waves was obtained. We were also deeply impressed by some limited number of person, namely Mr. Koei Hashimoto of the Nissan Civil Engineering Co. at Ofunato and Mr. Michitoshi Ishizawa of the Furukune Construction Co. at Taro, who did not lose the presence of mind amid the general confusion to take a meticulous note of the movements of the tsunami. Nevertheless, we feel strongly the need to establish a sufficient number of tsunami stations each equipped with a tsunami recorder and appropriately distributed at every strategic locations in order to obtain the reliable data on which alone a really scientific analysis on the nature of a tsunami could be based.

III. CASE STUDY OF DISASTERS INFILCTED ON THE CIVIL ENGINEERING STRUCTURES

Of the disasters inflicted on civil engineering structures some salient examples are introduced below for each classified type of structures.

1) Bridges

The tsunami invading upstream of a river frequently washed wooden bridges clean of their posts such as a bridge at the Araita river of Shizukawa. Plate 1 shows the Naikai bridge spanning a branch stream of the Kitagami river and located inside the city of Ishinomaki, which had the railing destroyed by violent impacts of fishing boats rushed upstream by the tsunami. Plate 2 shows another example of disaster which fell upon the Mangoku

* One of the local papers at Sendai, Japan.

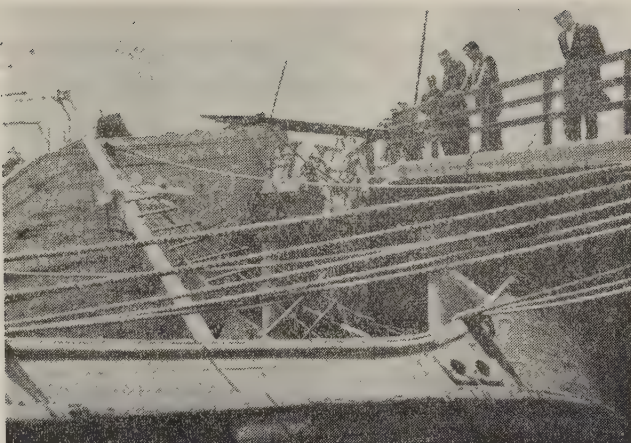


Plate 1 Naikai Bridge shown with destroyed railings and sunk boats.



Plate 2 Mangoku Bridge, The 2nd post slumped by 0.97 m.

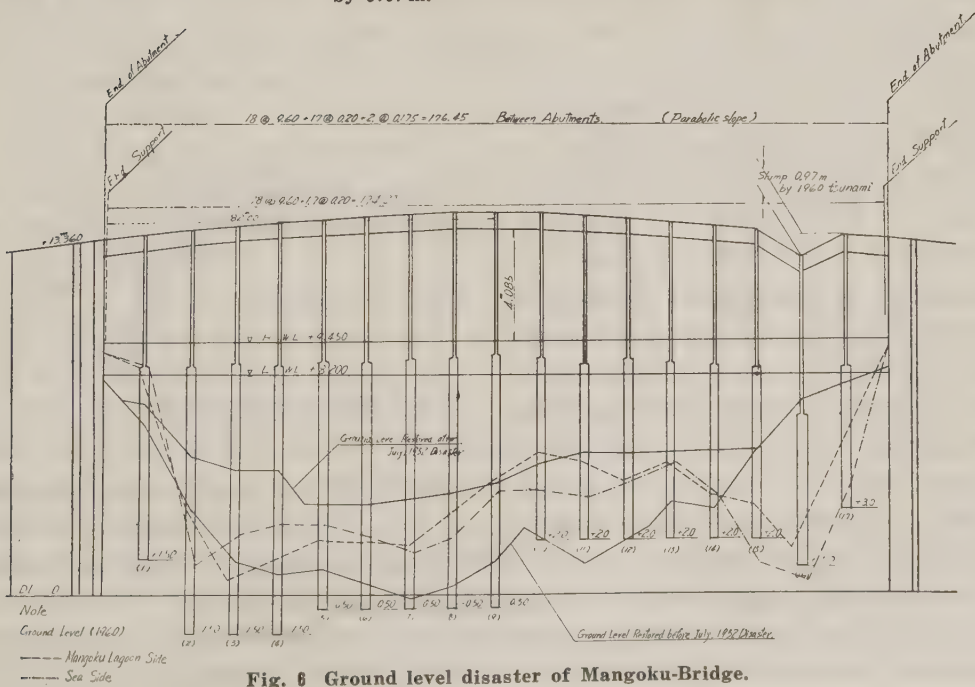


Fig. 6 Ground level disaster of Mangoku-Bridge.

bridge spanning a small tidal inlet connecting the Mangoku lagoon and the sea and located between Ishinomaki and the Ojika peninsula. In 1952 the tsunami caused by the Kamchatka earthquake scoured the foundation of the bridge posts, which were later reinforced with rubble mounds excepting the bed near the 2nd post from the right side. (See Fig. 6). During the tsunami of 1960 a boat capsized and sank here, and an increased velocity of water during flux started scouring on the bed. At 7:00 p.m., 24 May, the post gave way and began to subside amounting to 0.95 m of slump until 2:00 p.m. 25 May, the next day. This bridge also subsided at the 13th post during the tsunami of the Kamchatka earthquake. The subsidence of a bridge post took place also at a bridge of the Sekida river, Yamada, which occurred 2 days after the tsunami.



Plate 3 Highway revetment failed by receding water during reflux between Hadanya and Mitobe, Shizukawa.

2) Highway Revetment

Plate 3 shows failure of the highway revetment which is located between Hadanya and Mitobe, Shizukawa bay. The schematical diagram of this structures is shown in Fig. 7. Examination of the traces disclosed that the 1960 tsunami overtopped the wall at the maximum level of T.P.+4.36 m, i.e. 1.49 m higher over the crown of the parapet wall. 2 houses located at a hill foot behind the revetment were washed clean off the base stones. It was estimated that the failure of the revement occurred due primarily to scouring of the foundation by the receding water during reflux and secondly to subsequent increase of earth pressure against the revetment wall owing to loosening of the bond between the backfilling concrete and soils. During reflux the receding water seems to scour the base of a revetment so violently that the flow pattern takes on a water fall drilling a pool below. Such phenomenon is shown in a front-piece of the June issue, Journal of the Japan Society of Civil Engineers, giving the scene of the quay wall of Ofunato with the frontage depth of 4 m below the lowest low water level.

The similar pattern of failure was observed at the highway revetment in front of the observatory of earthquake, terrestrial magnetism and tsunami of the Tohoku University in

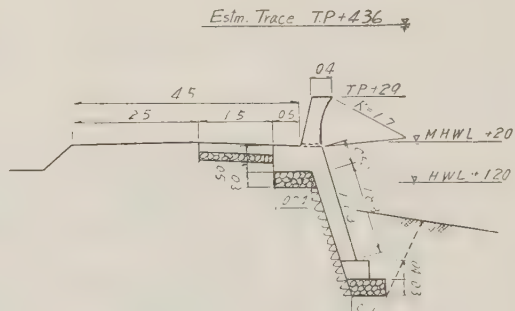


Fig. 7 Road revetment at Hadanya. (unit : m)

the Onagawa bay.

The examples shown in the preceding paragraphs seem to provide a lesson that it is absolutely necessary to make use of rubble or block mounds to protect the foundation of a revetment wall.

3) Sea Dikes

Most of the sea dikes found along the Sanriku coasts, except for those especially designed against tsunamis, invariably consist of a seaward face protected with a simple masonry or concrete wall, but of the landward face almost unprotected. The sea dike at the mouth of the Okawa river located in the Kesennuma bay, shown in Fig. 8, was overtopped by the tsunami of 1960 at the estimated level of 0.97 m over the crown which is T.P.+1.75 high. This was calculated from the traces found inland nearby, T.P. +2.72 m, since the dike itself did not retain any trace. A sluice was attached to the dike in order to drain the impounded water. However, the tremendous mass of water thrown behind the dike by the tsunami apparently began to flee through a gap existing between the earth dike and the sluice and brought about failure of the dike by gradually widening the gap as the breakthrough continued. Another failure of a sea dike occurred in the same manner at Kozumi of the Ojika peninsula, where a destruction started near the sluice resulting in the revetment stones dispersed seaward approximately 50 m. (No stone could be found beyond this distance because the sea started there).

There are indications that for a low dike the receding water overflows the crown level scouring the seaward base of the revetment; and that for an earth dike the overtopping water first tend to erode the landward shoulder and to cause a failure of the entire face of the landward slope as the inundation is prolonged. The patterns of failure vary in minor details according to the inundation level, the inundation period, the height of a dike, the drainage conditions of the protected land behind a dike, the directions of the receding water and the flow patterns. It is therefore suggested that those who are concerned with planning of the counter-tsunami measures should take into consideration the topographical conditions of the adjacent area in relation to the factors cited above.

4) Sea Walls

Some of the sea walls designed against a tsunami were overtapped by the 1960 tsunami. The sea wall shown in Plate 4 and Fig. 9 is located in Ozuchi, with the crown level T.P. +3.20 m. Considered from the trace level T.P.+3.70 m found at a house standing in front of it, the overtopping level of the tsunami is estimated to be 0.5 m over the crown of the wall. Because the level of overtopping was low, the inundation period must have been short, as a result the failing procedure of the landward slope being less severe. Until the failure of the landward slope started, the level of the overtopping water had already been reduced considerably, and consequently the invading water fell from the crowning concrete slab immediately into the base below causing a scour as shown in the picture. This process of failure seems to be confirmed by the facts that the houses located approximately 10 to 20 m behind the sea wall evaded destruction, and that the landward slope located in the

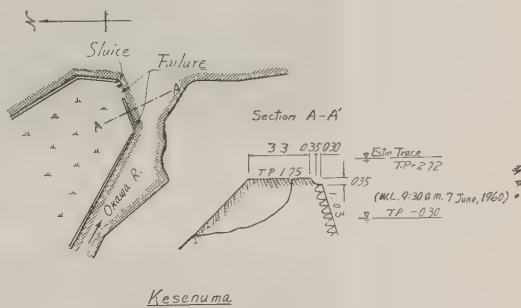


Fig. 8 Sea dike at Okawa Inlet. (unit : m)



Plate 4 Failure of the sea wall at Ozuchi shown with a scoured ditch on the landward slope. Houses remained unscathed. A counter-tsunami grove is seen yonder.

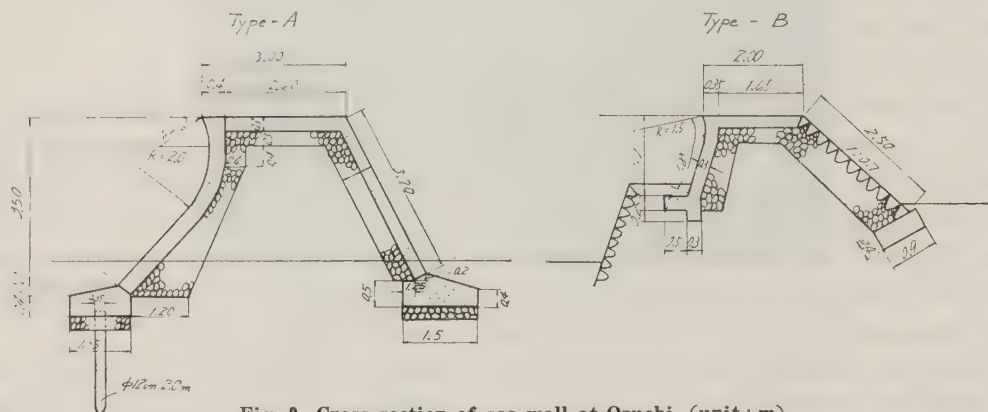


Fig. 9 Cross section of sea wall at Ozuchi. (unit : m)

shade of a hut standing in front of the sea wall remained intact.

To the north of Funakoshi and facing the Yamada bay was a sea wall with a counter-tsunami grove lying in front. Here, the failure started from an ill-maintained spot where a passage had been cut for traffic of trucks. At Osawa in the Yamada bay the tsunami took a round about path rushing upstream of a river which flanked the sea wall, overflowing into the protected area at a place where the embankment was relatively low, and then destroying the sea wall of a considerable height from behind. The wall was built of silty soil and protected with a masonry revetment on the seaward slope. This example shows that a sea wall of an adequate height alone is insufficient to guarantee the safety of the protected area unless the flanks facing a river is also equipped with an embankment of an adequate height. We have already experienced this type of disaster during the Ise bay typhoon in 1959.

5) Quay Walls and Lighter's Wharf

Plate 5 shows the failure of a quay wall capable of mooring 10,000-ton vessels at Ofunato where the backfilling was scoured. Plate 6 shows the failure of another quay wall of the Fuji Steel Co. at Kamaishi. The former had the crown level T.P.+1.65 m and was inundated for approximately 20 minutes by the tsunami with the maximum level of T.P. + 3.85 m, i.e. 2.20 m above the crown level. The next wave flooded the quay wall again



Plate 5 10,000 ton capacity quay wall at Ofunato with back fillings washed by receding water.



Plate 6 Fuji Steel quay wall at Kamaishi shown with sheet pilings overturned and backfillings washed.

about 0.70 m above the crown level, but the subsequent waves remained below the crown level.* The sheet piles, 15 m long and resting at the level T.P. - 14.35 m, had the embedment depth of approximately 11 m below the sea bed of T.P. - 3.35 m. The scour is attributed to the falling water during reflux which caused a scour at the front bed followed by suction of the backfilling soils through gaps of the sheet piles. The water level in front of the quay wall was less than T.P. - 2.35 m or 1 m deep during reflux. We may think of other causes of the scour such as piping action or slippage of saturated backfills along the circular surface of rupture, but further studies are necessary to determine the factor which is most responsible to the scour of the backfills. In this connection it must be pointed out that the scour occurring in front of a quay wall seems to be far more intensive than used to be imagined.

On the other hand the sheet piles of the Fuji Steel quay wall at Kamaishi were 11 m long with only 3 m of embedment depth. The construction of this wall dates back to 1937 and supposedly numerous unfavorable conditions had since been accumulated to reduce it

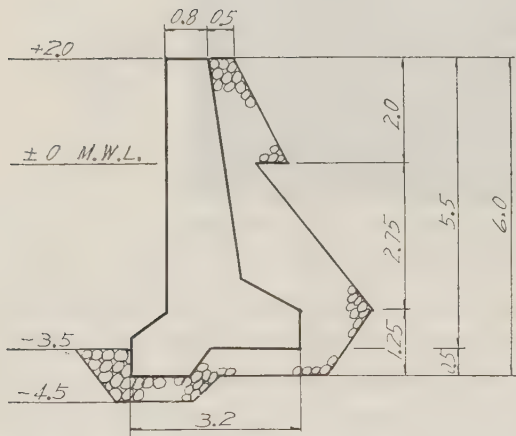
* This information was supplied by Mr. Koei Hashimoto of the Nissan Civil Engineering Co., together with photographic evidences.

vulnerable to a flood. It overturned toward the sea.

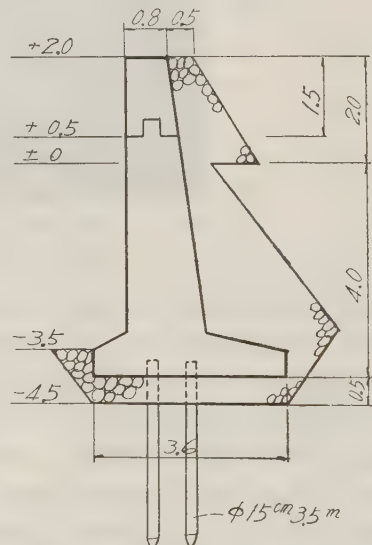
At the Hachinoe industrial sector, the quay wall built of reinforced concrete sheet piles had the backfillings washed, and collapsed due to lack of interlocking power of the sheet piles. At the Konakano fishery wharf of Hachinoe (See Plate 7 and Fig. 10.) the front bed was severely scoured due to raging water which rushed to and fro inside the anchorage basin. The wharf finally collapsed.



Plate 7 Konakano fishery wharf at Hachinoe collapsed after scouring of the front bed due to raging water which rushed to and fro inside the anchorage basin.



Section - A



Section - B

Fig. 10 Cross Section of Lighter's Wharf in Hachinoe. (unit : m)

Subsidence of the crown floor occurred at the quays of the Shizukawa, Onagawa and Kamaishi ports, due probably to suction of the backfilling soils.

6) Counter-tsunami Groves

The most prominent disaster of this kind was found at the well-known pine grove Rikuzen-takada. One of the authors had visited this place only in October last year, but was appalled this time at the transformation which befell upon the acquainted scenery. At

the central portion of this green belt of pines was an overflow weir built on the former mouth of the Kesen river, where the belt was narrower with relatively young trees sparsely planted. The weir position was a little lower than the adjacent areas. This very spot was broken through first by an onslaught of the tsunami, which swept the pines scouring the underlying soils. After repeated inflow and outflow of raging tides through this gap, the scour reached as great as 6 m at some places. When the authors visited the place, a troop of the Defense Corps were fighting the tide to stop the gap until the middle of July.

The tsunami of 1960 took a heavy toll of human lives at the Matsubara park in Shizukawa, and infrequent examples of the disasters connected with a counter-tsunami grove seemed to raise a doubt as to the effect of such a grove in deterring the blows of a tsunami. Professor Takeda of the Iwate University, Japan, states that an effective counter-tsunami grove should be as wide as 200 m. It is not useful unless densely planted with trees and lowlying bushes. Such an effective grove was found at Ozuchi which proved highly useful against the tsunami of 1960. A village at Ando which is located outside the lee of the grove suffered heavy casualties. Though a counter-tsunami grove must not be depended upon as a protection against inundation, it will still play an important role in ridding the tsunami of some its energy, or in preventing infectious destruction of houses. It was strongly felt that the reliability of a grove should be evaluated in the light of the strength, the resistance against an onrushing flow and the decelerating effect on a flow. A grove could be more effective if combined with other protective measures such as a sea wall.

7) Other Structures

At the port of Hachinoe, a breakwater near the river mouth subsided by 0.5 m; a lighter's wharf designed for a 10,000-ton vessel also subsided by 3.5 m in the midst of construction; and the base-protecting tetrapods were dispersed at a few places. As to minor disasters, the navigation channels and anchorage basins in and out of the port were either shoaled or scoured, notwithstanding damages of vessels, machines or office buildings. Similar to the disasters which occurred during the Ise bay typhoon at Nagoya, drifting timbers or vessels claimed some vital part of the disasters this time. We were bound to feel that the mooring techniques of timbers at the storage yard or factory should be revised with due consideration to such possible disasters.

We were unable to determine the effect of a breakwater against such a long-period wave as a tsunami. At Ryoishi the fishermen insisted that the tsunami was lower there and hence less destructive than that of 1933 because a breakwater 50 m long established at the bay neck partly reflected the tsunami toward the sea. However, the truth seems to remain still be confirmed by a further study.

IV. COUNTER-TSUNAMI MEASURES

The Sanriku coasts were invaded by a great tsunami in 1896 and again in 1933, which almost annihilated a number of villages taking a heavy toll of human lives as well. After these disasters were experienced the counter-tsunami measures against another possible hazard have become the vital problem for the local inhabitants of the northeastern coasts of Japan. Various measures have been devised and partly practised, such as (a) completion of an alert system; (b) removal of houses to neighboring highlands; (c) construction of refuge roads; (d) drilling for urgent evacuation; (e) plantation of counter-tsunami grove;

(f) construction of sea walls; and (g) frontage sheds or other facilities of a port sector built as solid permanent structures to shelter the resident area lying behind. However, economical difficulties menaced overall execution of these measures, since such a costly investment could pay little in the underdeveloped areas of the northeastern district of Japan, and since a tsunami disaster would not occur so often, namely once every 30 years. Worse still, the life on the highlands reduced the economical activities of the inhabitants extremely unfavorable, since they mostly lived on the sea. With the passage of time people began to crowd the lowlands near the beach again and most of them were practically helpless against another disaster when the tsunami struck them in May, 1960.

However, there are places, though limited in number, such as Yoshihama and Taro, where towering sea walls surround the towns ensuring almost permanent safety from the ruthless fangs of a tsunami (See Figs. 11 and 12.). Particularly the former proved highly effective against the 1960 tsunami. Yamada is guarded by a sea wall which runs right through the downtown district (See Fig. 13.). This ingeneous device will be very useful to such fishing ports or harbors where a high wall built along the waterfront may paralyze the normal function of the port facilities. In Iwate Prefecture, construction of a coastal sea wall is being planned and partly fulfilled at Akamae, Tsugaruishi and Takahama which are located in the recess of the Miyako bay. A certain defensive project is also under way for Fudai. We sincerely hope that at this crucial moment the government moves to shoulder every responsibility for establishing and executing a long-term defensive

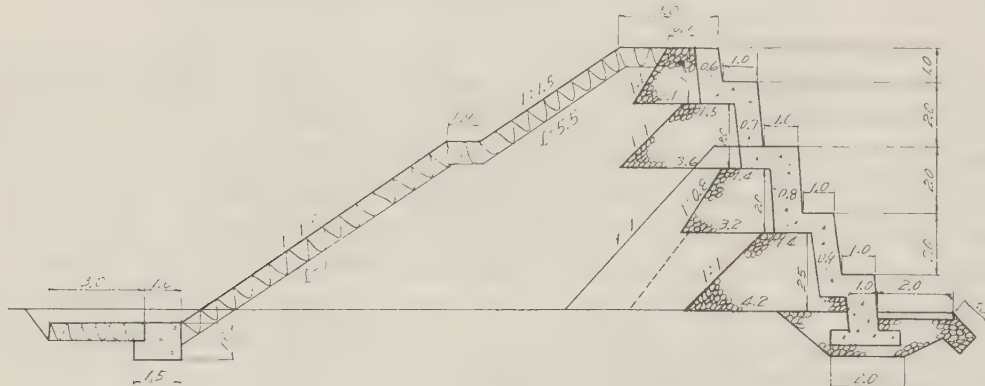


Fig. 11 Cross section of sea wall at Taro. (unit : m)

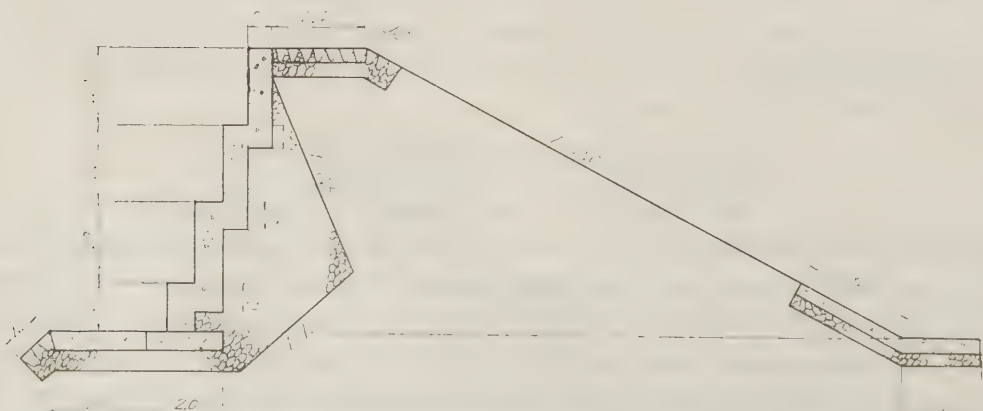


Fig. 12 Cross section of sea wall at Yoshihama. (unit : m)

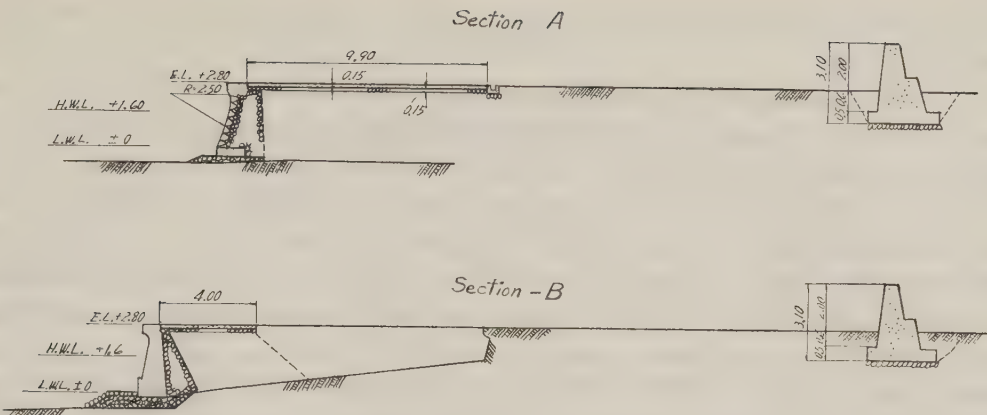


Fig. 13 (a) Cross section of sea wall at Yamada. (unit : m)

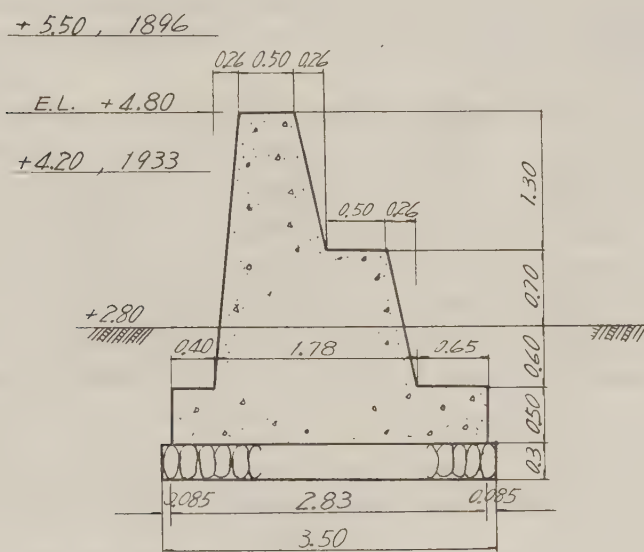


Fig. 13 (b) Cross section of sea wall at Yamada. (unit : m)

policy against tsunami hazards which may recur any time in the future.

From purely technical point of view, insurmountable difficulties exist as to defensive measures against a tsunami. As already discussed, it is practically impossible to determine the design height of a probable tsunami for each locality. The present practice of determining the height of a sea wall is based on the records of the past tsunamis. Now that the highest possible tsunami can not be forecast, even a sea wall possessing a height which should not be overwhelmed by any tsunami ever recorded, may not be an absolute guarantee. Consequently, the best policy available today to evade disasters lies in timely evacuation of human lives; and a sea wall must not be fully counted on. The inhabitants of the tsunami-haunted coasts of Sanriku are quite alert to a sign of a tsunami. However, the tension could not always be maintained at its best against such an infrequent disaster as a tsunami. It will help easing such an awkward situation if the engineers let them acquainted with the reliability of counter-tsunami measures such as a sea wall or a counter-tsunami grove. We fear that the policy of migrating the living quarters to the highlands would be a shameful failure, unless adequate allowances be made on the basis of under-

standing toward the situations of the inhabitants along the Sanriku coasts, who dominantly depend on fishery.

It is unfortunate to point out the deplorable lack of fact-giving data at the scenes of disaster. A good command over the facts is prerogative for establishing a workable policy against recurrence of the disaster. The greatest problem facing the engineers today is, curiously enough, the situation that they are devoid of actual data. In order to further engineering techniques as well as facilitate an economically feasible policy, efforts should be done continuously and at all times to clarify intricate processes of a tsunami. For instance, the first-line scientists of the district observatory have long been crying for a robot tidal station, but they are still badly in need of it today. During our visits to several observatories we were greeted with a complaint that they had to make risky trips between the observatory and the seaside tidal station several dozen times in the midst of the tsunami. We should like to call the public attention to such a deplorable situation before putting the blame on the observatory officials for having failed in forecasting the tsunami in time. A number of properly distributed and substantially built tidal gauges are needed right this moment.

The Earthquake Research Institute of the University of Tokyo has been bent on the time-consuming efforts of fact-finding to the utmost of its capacity, i.e., installing a tsunami recorder at Enoshima, Miyagi Prefecture, establishing an entrusted network of cine stations at Ofunato and Miyako, and setting up the brine-sensitive gauges at the Miyako bay also entrusted to the Miyako Meteorological Observatory, etc. We hear that such efforts have been paid to a great deal at the 1960 tsunami. In connection to this success which has been achieved by a far-sighted effort but by a very modest finance, we should like to hope that the government shows more enthusiasm toward this profitable project so that the disaster-ridden country of Japan could in the future look back on the grievous past with utter disbelief.

V. ACKNOWLEDGEMENTS

The investigation party was originally organized from the members of the University of Tokyo as a part of the combined study financed by the Education Ministry, with Professor Ryutaro Takahashi as chief representative of the project, with an objective of investigating the disasters inflicted on the civil engineering establishments along the Sanriku coasts of Japan. It was later joined by the Tohoku University. Our activities concurrently represented the Disaster Investigation Committee and the Coastal Engineering Committee of the Japan Society of Civil Engineers.

The party consisted, beside the authors, of Mr. Takashi Kataoka, Assistant Professor of Iwate University, Mr. Choule Sonu, M.S., postgraduate student at the University of Tokyo, and Mr. Akira Saito, postgraduate student of the Tohoku University. The paper contains some of the results which one of the authors had obtained in a previous expedition carried out in cooperation with Messrs. Kiichi Okubo, Yasusuke Samejima, and Akiichi Wachi from the Transportation Ministry.

We are deeply obliged to the civil engineering departments of Miyagi and Iwate Prefectures, the 2nd District Port Development Authority of Transportation Ministry, and other related personnel for invaluable cooperation and assistance provided to our investigation activities.

APPENDIX

SOME ADDITIONAL REMARKS ON THE CHILEAN-EARTHQUAKE TSUNAMI

*Kiyoshi Horikawa**

The mechanism of the tsunami which was generated on May 22, 1960, in Chile has not been explained definitely because of the complication involved in the phenomenon.

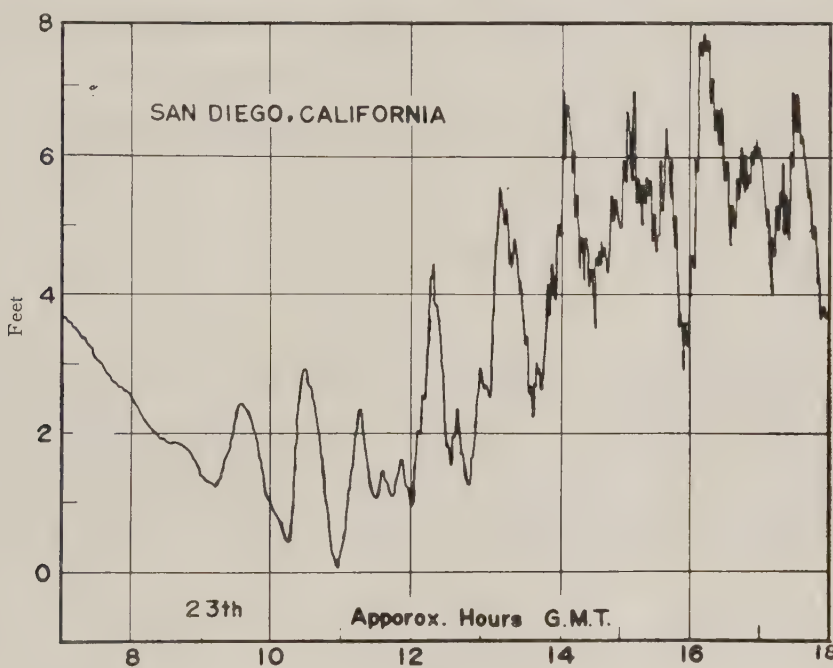


Fig. 1

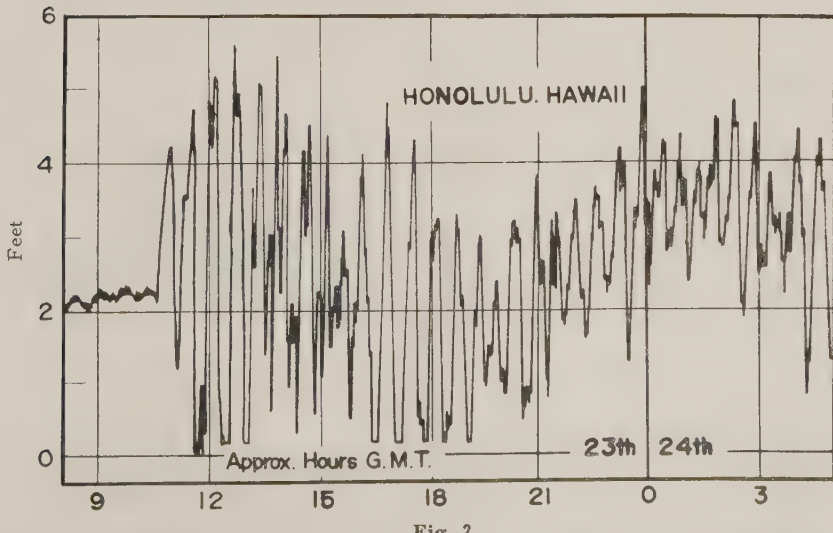


Fig. 2

* Assistant Professor of Civil Engineering, University of Tokyo.

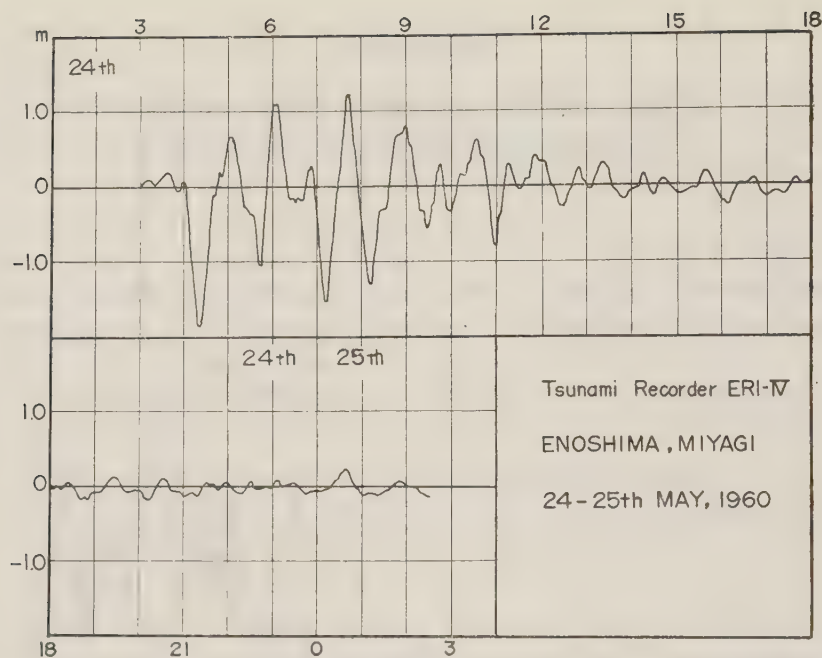


Fig. 3

According to the data collected by the author in Chile during October and November, 1960, the ground level was elevated in both the northern and the southern parts of the earthquake zone, while in the central part it was subsided. The tidal records obtained along the Pacific Ocean coasts in Peru, the United States and Canada show, as indicated in Figs. 1 and 2¹, that the first wave of the tsunami started at the flood. On the other hand, the tidal records obtained in Japan, namely at Enoshima (Fig. 3), show, quite to contrary, that the first wave started from the ebbs². This discrepancy in the tsunami characteristics, observed on both sides of the Pacific Ocean, may probably be attributed to the different features of crustal movements which occurred at the northern and central parts of the earthquake zone in Chile.

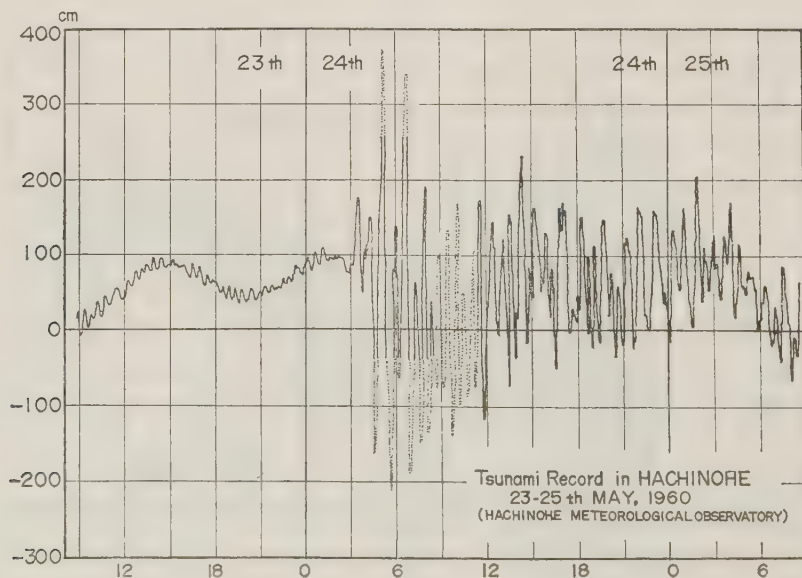


Fig. 4

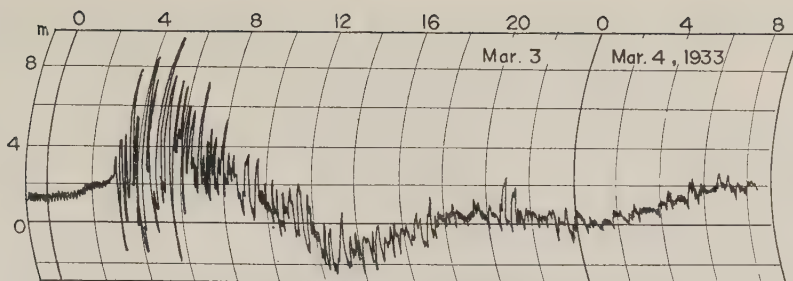


Fig. 5 Tsunami record in Hachinohe in Mar. 3~4, 1933

It is rather difficult to determine the exact periods of the tsunami waves from the obtained records, since the gauge which was mostly installed inside a bay recorded the normal oscillation of the bay induced by the tsunami as well as the tsunami itself. Figs. 4 and 5 are the tsunami records obtained in Hachinohe, Japan, in 1960 and 1933, from which you may recognize how difficult it is to distinguish the exact periods of the tsunami waves. A rough reading yields approximately 60 min. and 12 min., respectively. A Fourier analysis of these records is expected to shed light on the pattern of spectral ensemble of the tsunami in near future.

Another point worth mentioning is the probable occurrence of the tsunami hazards. The Pacific Ocean coasts of Japan are confronted with the notorious outer earthquake zone in the northwestern Pacific, which is responsible for most of the great earthquakes and tsunamis along the northeastern coasts of Japan. Naturally, the Japanese engineers were quite alert to the tsunamis which arrive from such nearby epicenters. However, the tsunami hazards caused by the Chilean earthquake in May, 1960, convinced us that a tsunami generated at the other side of the earth could be as disastrous as the one born at the nearby ocean floor. (Fig. 6).



Fig. 6 Refraction diagram (after K. Yoshida.)

From a careful study of old provincial records S. Ninomiya³⁾ has discovered at least 10 tsunamis which came from South America and caused damages along the northeastern coasts of Japan during the last 380 years. Among them, 6 were generated in Chile, 3 in Peru and 1 in Mexico. The author was informed by a Chilean engineer that he witnessed a tsunami which rose up to 2.4 m above mean sea level at the Pier of Compania de Acero del Pacifico

in Concepcion on November 5, 1952, incidentally the date of the Kamchatka earthquake.

REFERENCES

- 1) Symons, J.M. and B.D. Zetler : The Tsunami of May 22, 1960, As Recorded at Tide Stations, Preliminary Report, U.S. Dept. of Commerce, Coast and Geodetic Survey.
- 2) Investigation Groups for The Chilean Earthquake Tsunami : Primary Report, The Tsunami of May 24, 1960, July 1960. (In Japanese)
- 3) Saburo Ninomiya : A Study on Chilean Earthquake Tsunamis through the Historical Data in the Northeastern Region of Japan, Aug. 1960 (In Japanese)

WAVE OVERTOPPING ON SEAWALLS

*Tojiro Ishihara**
*Yuichi Inagaki***
*Hiroshi Mitsui****

I. INTRODUCTION

So far, criteria for seawall design have been based on the idea that the height of a seawall should be greater than that of wave run-up on the seawall face in order to protect the land area from erosion or damage due to wave action and flooding by preventing from wave overtopping completely. If such criteria are to be adopted, a very high and big body of seawall is required. Therefore, the scientific design should be made with consideration on the economical value of the background. From this view point, if a seawall is designed considering the economical effect and allowing overtopping which causes very few damages, the effective height of a seawall can be reduced. It is evident that the rate of overtopping becomes an essential factor in estimating dangerousness of the background and designing drainage facilities and pools behind the wall.

The rate of overtopping is affected by many factors, such as characteristics of incident waves, type and location of seawall, wall height from still water level, roughness of wall face, coastal configuration, wind and others. No theoretical analysis on these factors has been conducted because of complicated phenomena of wave overtopping. In this paper, the relations between the rate of wave overtopping and the factors described above are plotted based on the experimental results with two different kinds of scales conducted at Kyoto University and the laboratory data taken at the Beach Erosion Board and the University of California in U.S.A.

II. EXPERIMENTAL APPARATUS AND PROCEDURE

1. Experimental apparatus

The tests were conducted in two different apparatus ; one is the indoor wave tank at the Hydraulic Laboratory, Civil Engineering Department for the two dimensional analysis, and the other the outdoor fan-shaped wave basin at the Ujigawa Hydraulic Laboratory, Disaster Prevention Research Institute for the two dimensional and especially the three dimensional analyses when waves attack the seawall obliquely. These wave tank and basin are shown in the references 1) and 2).

The case of the indoor wave tank : The characteristics of the incident waves are tabulated in Table 1. The model of seawall was made of the plastics plate and the inclination of the wall face was changed in five cases ; 20°, 30°, 40°, 60° and 90°. The height of the wall was variable with every 2 cm for each inclination. The walls were located so that the water depths at the toe of wall were 0, 7 and 10 cm and the breaking point without wall was to be observed in this region.

The case of the outdoor basin : The heights, lengths and periods of the incident deep water waves were between 10.25 and 15.05 cm, 136 and 264 cm, and 0.935 and 1.300

* Professor of Kyoto University ** Assistant Professor of Kyoto University

*** Former Graduate Student of Kyoto University

Table 1. Characteristics of the incident waves for the case of the indoor wave tank

Wave No.	Wave Height H_0 cm	Wave Length L_0 cm	Wave Period T sec	Wave Steepness H_0/L_0
1	6.70	219.0	1.185	0.0306
2	7.46	185.3	1.090	0.0402
3	8.04	160.7	1.015	0.0500
4	8.07	140.8	0.950	0.0573
5	8.26	123.5	0.890	0.0668
6	7.23	110.1	0.840	0.0657
7	7.24	90.1	0.760	0.0803

sec respectively. The steepness of the incident deep water wave was changed in eight cases; 0.0389, 0.0507, 0.0610, 0.0728, 0.0827, 0.0904, 0.1055 and 0.1105 with the incident angles 45° and 90° for the vertical wall face.

2. Experimental procedure

In the indoor tank, the quantity of overtopping water was measured for the combinations of three cases of water depth at the toe of wall h , five cases of wall face inclinations θ , each elevation of the wall crest above still water level H_c and seven cases of deep water waves. The data were taken mostly from the sixth wave to the tenth wave after the generated waves reached the wall and became steady. At the same time, the reflection coefficient which may affect the rate of overtopping was measured by the Healy's method³⁾. Moreover, the high speed cinecamera was used to observe the condition of wave overtopping on the wall.

In the outdoor wave basin, the experiments were conducted in the same manner as in the indoor wave tank.

III. EXPERIMENTAL RESULTS AND ANALYSIS

1. Reflection coefficient

Fig. 1 shows an example of data on the reflection coefficient which are plotted against the ratio of the elevation of the wall crest above still water level to the deep water wave height H_c/H_0 with a parameter of the wall face inclination. It may be concluded from the figure that H_c/H_0 does not affect the reflection coefficient very much, and especially when H_c/H_0 is small, it is governed by the type of wall face rather than H_c/H_0 .

2. Rate of wave overtopping for vertical wall face

The case when the incident waves attack perpendicularly to the wall: In analyzing the experimental data for both indoor wave tank and outdoor wave basin, the Beach Erosion Board data⁴⁾ were additionally adopted to examine the scale effect. Of importance is how to express the rate of wave overtopping dimensionlessly so that the results of model experiments can be applied to the prototype of shore structures. Saville and Caldwell⁴⁾ established a dimensionless expression for the quantity of overtopping water by taking the ratio of the energy in the overtopping water to the energy in the incident wave.

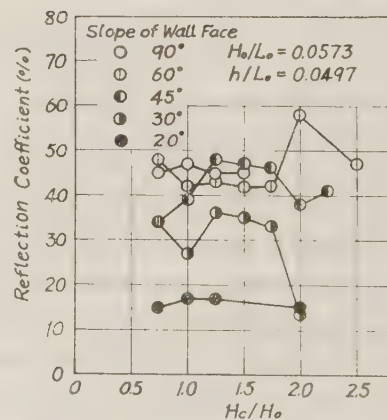


Fig. 1 Relations between the reflection coefficient and H_c/H_0 with a parameter of the wall face inclination

$$\frac{\text{Potential energy in the overtopping water}}{\text{Total energy in the deep water wave}} = \frac{\rho g Q H_c}{1/8 \rho g H_o^2 L_o} = \frac{8 Q H_c}{H_o^2 L_o} \dots\dots\dots(1)$$

in which Q is the volume of water overtopping the structure per wave period. This dimensionless expression is based on the idea that a part of the energy in the deep water wave transfers the potential energy in the overtopping water. However, Eq. 1 is not applicable to represent the quantity of overtopping water when $H_c=0$ because Eq. 1 includes H_c .

In the present paper, the ratio of the quantity of overtopping water per wave period to the quantity of water moving onshore per wave period is taken instead of Eq. 1 so as to make it applicable even when H_c is zero or less than zero such as a submerged structure.

Taking the x -axis along still water level in the direction of wave propagation and the y -axis upwards and vertically, the horizontal velocity of water particles at $x=L_o/2$ in the small amplitude theory for deep water wave is

$$u = \frac{\pi H_o}{T} e^{\frac{2\pi}{L_o} y} \sin\left(\pi - \frac{2\pi}{T} t\right) \dots\dots\dots(2)$$

On the otherhand the volume of water passing onshore through the vertical plane belt of unit width at $x=L_o/2$ per wave period Q_o is expressed, using Eq. 2, as

$$Q_o = \int_{-\infty}^0 \int_0^{T/2} u dy dt = \int_{-\infty}^0 \int_0^{\pi} \frac{H_o}{2} e^{\frac{2\pi}{L_o} y} \sin\left(\pi - \frac{2\pi}{T} t\right) dy d\left(\frac{2\pi}{T} t\right) = \frac{H_o L_o}{2\pi} \dots\dots\dots(3)$$

Therefore, the dimensionless expression for the quantity of water overtopping the seawall per unit width of wall and per wave period Q is written in form of

$$\frac{Q}{Q_o} = \frac{2Q}{H_o L_o} \dots\dots\dots(4)$$

Since the quantity of water overtopping the vertical wall is concerned with the characteristics of deep water wave, the water depth at the toe of the wall h and the elevation of the wall crest above still water level H_c , Q/Q_o will be put in form of

$$\begin{aligned} \frac{Q}{Q_o} &= \frac{2\pi Q}{H_o L_o} \\ &= f\left(\frac{H_o}{L_o}, \frac{h}{L_o}, \frac{H_c}{H_o}\right) \dots\dots\dots(5) \end{aligned}$$

Fig. 2 shows an example of the dimensionless plots of the data taken in the indoor wave tank and by the Beach Erosion Board based on Eq. 5.

In general, if the wave breaks on the wall face or in front of the wall, water splashes so high on the wall that wave overtopping is observed even when H_c is quite large. It is seen in Fig. 2 that when h/L_o is large, the value of $2\pi Q/H_o L_o$ increases rapidly with decrease in H_c/H_o , and on the other

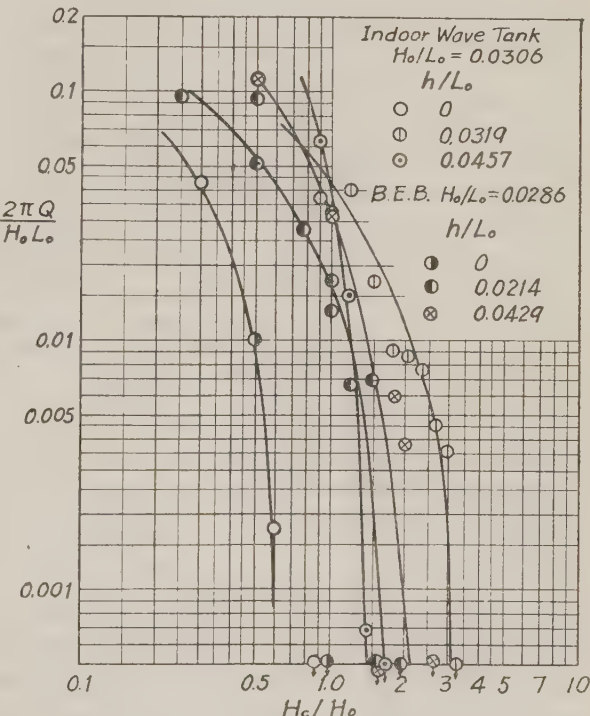


Fig. 2 Plots of the dimensionless quantity of overtopping water $2\pi Q/H_o L_o$ against H_c/H_o with a parameter of h/L_o for the cases when $H_o/L_o=0.0306$ and 0.0286

hand, when h/L_0 is small and therefore breaking wave overtops the wall, $2\pi Q/H_0 L_0$ increases slowly with decrease in H_c/H_0 . This fact will be caused by the effect of splash mentioned above.

The relation between the relative height of the wall H_c/H_0 and the shallowness h/L_0 is shown in Fig. 3 with a parameter of $2\pi Q/H_0 L_0$ for the case when H_0/L_0 is approximately equal to 0.07. The solid lines in Fig. 3 represent the mean lines drawn smoothly for each constant value of $2\pi Q/H_0 L_0$ considering the tendency of change in the $H_c/H_0 - h/L_0$ relation with change in wave steepness. Fig. 3 shows that the maximum relative heights of the wall are located at the left side of the breaking point obtained from the Breaker Index denoted as B.P. (at the shallower position than the breaking point), and that the convex curve becomes sharp with decrease in $2\pi Q/H_0 L_0$. The characteristics of wave overtopping for other steepness are quite same as those shown in Fig. 3. As is seen in Fig. 2 and 3, the experimental results obtained by the authors using the comparatively small models are approximately in agreement with those for as large scale model as the shorestructure in the field by the Beach Erosion Board. This fact is considered to verify the validity of the dimensionless expression for the quantity of overtopping water described previously.

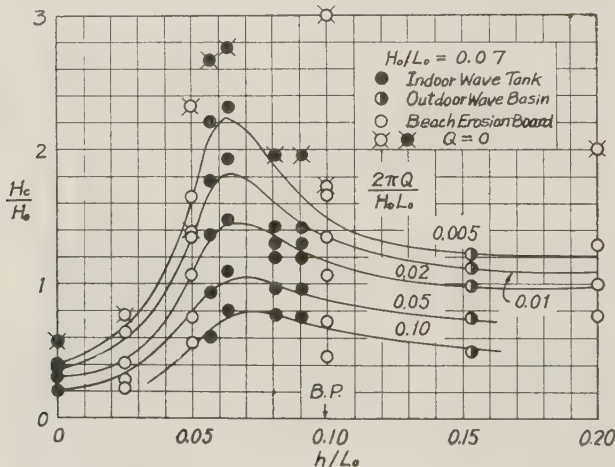


Fig. 3 Relation between H_c/H_0 and h/L_0 with a parameter of $2\pi Q/H_0 L_0$ for the case when H_0/L_0 is approximately equal to 0.07

It is found from the experimental results that the water depth at the toe of the wall is the most important factor which governs the quantity of overtopping water if the characteristics of deep water wave and the elevation of the wall crest above still water level are constant. In other words, for existing seawalls the water level which changes due to tides, wind set-up, seiches and others plays an important role to overtopping; therefore, the determination of water level becomes an important problem for design of actual seawalls. In customary design, the water level obtained by adding the past maximum deviation to the mean high water of spring tide is used as the design high water level. If, however, the seawall is designed to prevent from wave overtopping completely for the past maximum high water level in the storm tides which attacked often the Japanese coasts recently, a very high seawall is required and its construction is impossible economically. Consequently based on the idea of allowing wave overtopping to some extent, the storm tide will have to be treated from view point of the economical effect.

As the design flood in river planning at the present day, the statistical treatment of water level becomes necessary for design of the seawall too. In this case a lot of past data on storm tides are required such that a number of past data on flood are required for the study of flood statistics in hydrology and river engineering. Since for past ten years destructive typhoons attack Japan every year and caused enormous damages due to storm tides here and there along the coast, the whole tide stations in Japan were improved rapidly, and precise data are being taken. Therefore, the statistical treatment of the data became possible. In Japan, the noteworthy reports on the statistics of storm tides were published recently by Miyazaki⁵⁾ and Kishi⁶⁾ using the new data.

The case when the incident waves attack obliquely to the wall: For the case when the incident waves in deep water attack by 45 degree to the coast line, the experimental data taken by the authors in the outdoor wave basin are analyzed. In expressing the quantity of overtopping water in dimensionless form, as the incident waves refract until arriving at the coast, the wave at the position of the seawall must be transferred to the equivalent deep water wave which is assumed to progress straight shoreward, and the quantity of overtopping water must also be transferred to that per unit length of the wall perpendicular to the direction of progression of the equivalent deep water wave. Using the equivalent deep water wave height H'_0 instead of H_0 and letting the quantity of overtopping water per unit length of the wall be Q sec α , the dimensionless expression for the quantity of overtopping water for the case of oblique attack of wave is written as

$$\frac{Q'}{Q'_0} = \frac{2\pi Q'}{H'_0 L_0} = \frac{2\pi Q \sec \alpha}{K H'_0 L_0}, \quad \dots(6)$$

in which α is the incident angle, K the refraction coefficient, and the prime represents the equivalent quantity to the case when the wave progresses perpendicularly to the wall without refraction. Figs. 4 and 5 are the relations between $2\pi Q \sec \alpha / K H'_0 L_0$, $H_c / K H'_0$ and h / L_0 for the constant values of $K H'_0 / L_0$ corresponding to Figs. 2 and 3. In this analysis, the refraction coefficient K and the incident angle α were obtained by the small amplitude wave theory, and these values in the shore side beyond the breaking point were assumed to be equal to those at the breaking point K_b and α_b .

Although the experiment was conducted for only the case when the incident angle of deep water wave was 45°, as the incident angle of wave at the position of the seawall was ap-

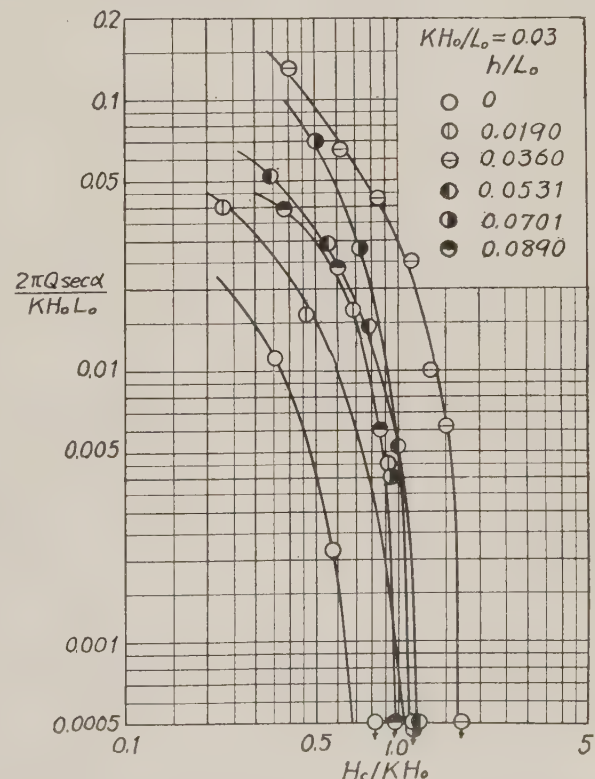


Fig. 4 Plots of dimensionless quantity of overtopping water $2\pi Q \sec \alpha / K H'_0 L_0$ against $H_c / K H'_0$ with a parameter of h / L_0 for refracting waves when $K H'_0 / L_0 = 0.03$

proximately between 20° and 40° , Fig. 5 can be applied to the wave with the incident angle of this region on the beach.

It is seen by comparing Fig. 5 with Fig. 3 that the quantity of overtopping water shown in Fig. 5 is less than that shown in Fig. 3 in every case. The cause of reduction in the quantity of overtopping water will be explained as bellow.

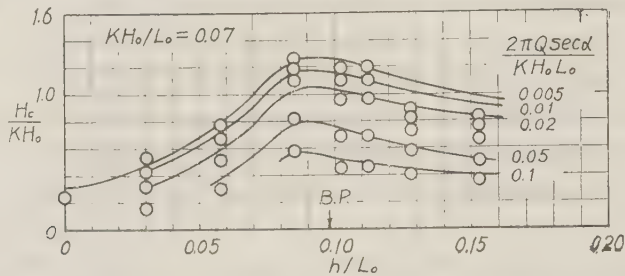


Fig. 5 Relation betwenn H_c/KH_0 and h/L_0 with a parameter of $2\pi Q \sec \alpha/KH_0 L_0$ for refracting waves when $KH_0/L_0=0.07$

When the incident wave strikes the wall obliquely with a certain angle and runs up the wall face or splashes on the wall, water particles have the velocity component in the lateral direction due to the oblique incident wave. Therefore, a part of wave energy to serve overtopping runs away along the wall, and then the quantity of overtopping water is reduced compared with that in the case of right angle incidence of wave. Reduction in the quantity of overtopping water is much in the onshore region beyond the breaking point rather than in the offshore region from the breaking point. From this fact, on the coast where the incident direction of wave is limited such as the coast in the bay having a narrow opening, the cost of construction may be saved if deciding the height of wall by Fig. 5. It should be noted, however, that if there is an obstacle, such as a jetty, in front of the wall, the quantity of overtopping water increases locally at that position. In this case, the height of the wall must be increased in the vicinity of the jetty.

3. Rate of wave overtopping for inclined wall face

Fig. 6 is an example of the dimensionless plots for experimental results by the indoor wave tank and represents the relation between $2\pi Q/H_0 L_0$ and H_c/H_0 with a parameter of the slope of wall face θ for constant values of H_0/L_0 and h/L_0 . The plot of H_c/H_0 against θ with parameters of $2\pi Q/H_0 L_0$ and h/L_0 for a constant value of H_0/L_0 is shown in Fig. 7. This figure contains the Beach Erosion Board data on smooth slope of 1 on 1.5, 1 on 3 and 1 on 6.

It is found from the experimental results refering to Fig. 7 that (1) in the case when the wall is located on the beach line, that is $h/L_0=0$, the effect of θ is not much though the quantity of overtopping water becomes

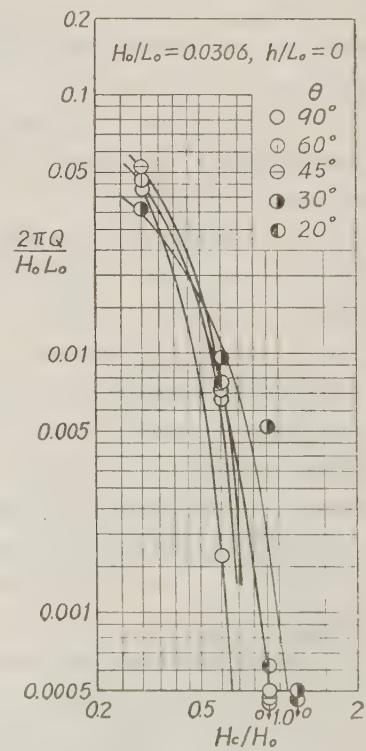


Fig. 6 Dimensionless plots of the quantity of overtopping water for inclined wall faces

maximum when θ is approximately 30° , and this result is independent of the steepness H_o/L_o ; (2) in the case when the wall is located a little shoreward from the breaking point obtained from the Breaker Index, the quantity of overtopping water becomes maximum when θ is approximately $30^\circ\text{--}45^\circ$; (3) when θ is less than 20° , the quantity of overtopping water is reduced rapidly with decrease in θ in the case when the wall is located in the vicinity of the breaking point, and is less than that for the vertical wall.

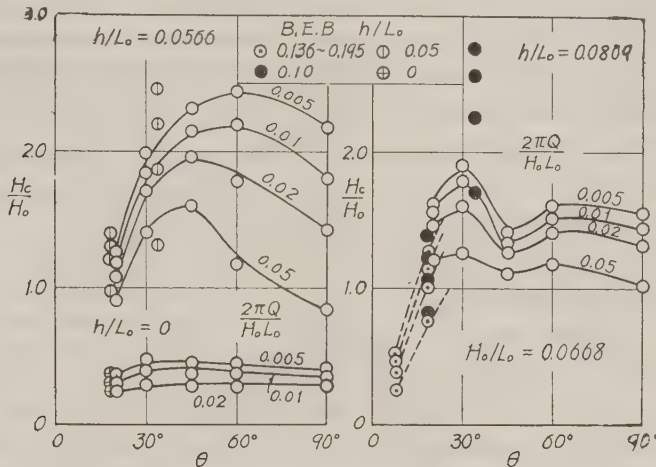


Fig. 7 Effect of the wall face slope, the height of wall and the water depth at the toe of the wall on the quantity of overtopping water

These results can be explained as follows. In the case of a vertical wall, water particles move up and down in front of the wall. Therefore, the quantity of overtopping water is relatively not much because less water flows over the wall crest resulting from the head difference between wave and wall crests or splash having small horizontal component of water particle velocity. Contrarily in the case of a sloping wall, the quantity of overtopping water is more than that for a vertical wall because the landward horizontal component of water particle velocity on the wall face is considerably large. If, however, the slope of wall face becomes smaller, as the distance of wave uprush becomes larger and much energy dissipates due to friction, the quantity of overtopping water decreases. When wave arrives at the wall after breaking, the quantity of overtopping water decreases so much because wave energy decreases before run-up or splashing due to impingement to the wall. Considering only from view point of wave overtopping, it may be concluded that a nearly vertical wall or the sloping wall with the angle of less than 20° is best. However, consideration of bed scour in front of the wall is necessary if a vertical wall is adopted. On the other hand, if the sloping wall with small angle is adopted, the cross-sectional area of the wall becomes large, and therefore, the cost of construction is much though the scour problem at the toe of wall does not occur, and wave force acting on the wall is smaller. Conclusively speaking, a vertical wall or a similar type wall to it is the most effective from view points of wave overtopping and construction cost if the foundation is of safty for scour and subsidence.

IV. CONSIDERATION ON THE EXPERIMENTAL DATA OF THE BEACH EROSION BOARD AND THE UNIVERSITY OF CALIFORNIA

1. Effect of sectional type of wall

The height of deep water wave and its period used in the test at the Beach Erosion Board⁷⁾ were from 90 to 360 cm and from 2.96 to 15 sec respectively. In this experiment, seven types of seawall models tabulated in Table 2 were tested by setting on the 1 on 10 slope beach as was done by the authors. For Type I, in addition, the case of 1 on 25 slope beach was tested to disclose the effect of beach slope.

An example of the dimensionless plots of the data for each type of the walls in Table 2 is shown in

Fig. 8, in which no data for Type II are plotted because they were not taken in the case when $H_o/L_o = 0.0286$. The experimental curves of Type V and VI are separated for 3 ft and 6 ft wave heights, and the dotted lines in Fig. 8 represent those for 3 ft wave height.

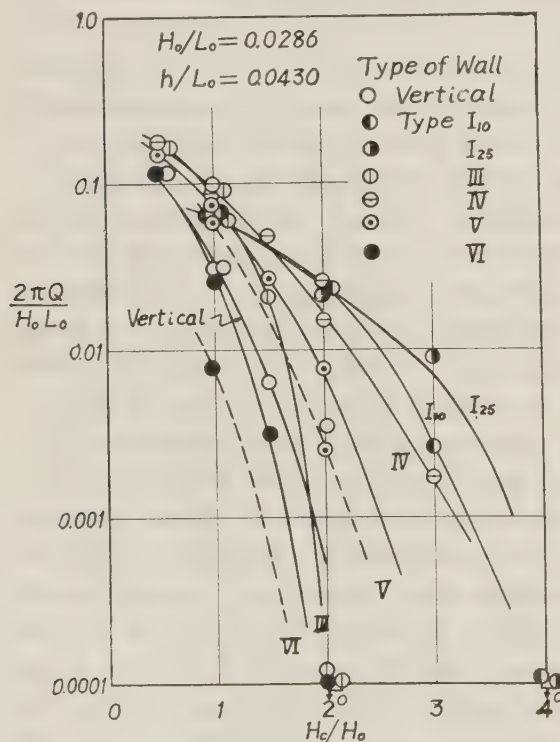


Fig. 8 Comparison of the quantity of overtopping water for various cross-sectional types of wall

Types V and VI walls, the effect of relative roughness can be found; that is, the dimensionless quantity of overtopping water for 3 ft wave height is less than that for 6 ft wave

Table 2. Test models of seawalls used by B.E.B.

Type of wall	Description of test section
Vertical	Vertical wall
I ₁₀	Curved-faced wall (Galveston type)
I ₂₅	Same as Type I ₁₀ except that the beach slope is 1 on 25
II	Recurved wall
III	1 on 3 smooth slope
IV	1 on 1-1/2 smooth slope
V	1 on 1-1/2 slope, step-faced wall
VI	1 on 1-1/2 slope, riprap cover

It is concluded from Fig. 8 that; (1) The quantity of overtopping water increases with decrease in the height of wall for all types of wall; (2) The Type I wall is not effective to overtopping when the wall is very high, but effectiveness increases quickly with decrease in the height of wall compared with other types of wall; (3) It is seen from other plots of data for different wave steepness from that shown in Fig. 8 that the effect of recurved top in Type II on overtopping is remarkable compared with Type I; (4) The Type III is more effective than the Type IV wall especially when the wall is high; (5) The Type V wall is more effective than the Type IV wall of which the face slope is same as that of the Type V wall except when the wall is very low; (6) The Type VI wall is much more effective than the Type V wall for all cases of the wall height; (7) For

height in the case of the same scale of the wall face roughness. This problem is discussed in the next article.

2. Effect of wall face roughness

In this article, Sibul's experimental results⁸⁾ are analyzed. The slope of wall face of the seawall models used in his experiments were 1 on 2 and 1 on 3, and as a roughness, strips having a rectangular cross section of 1" width and 1/4" height were arranged with a pitch of 3-1/2". The quantity of overtopping water in the case when the elevation of wall crest is below still water level was measured under the condition that water level in the landward side of the wall is same as that in the seaward side. Fig. 9 represents an example of dimensionless plots of Sibul's data, in which k is the equivalent sand roughness of the wall face obtained by the Johnson's method for open channels.

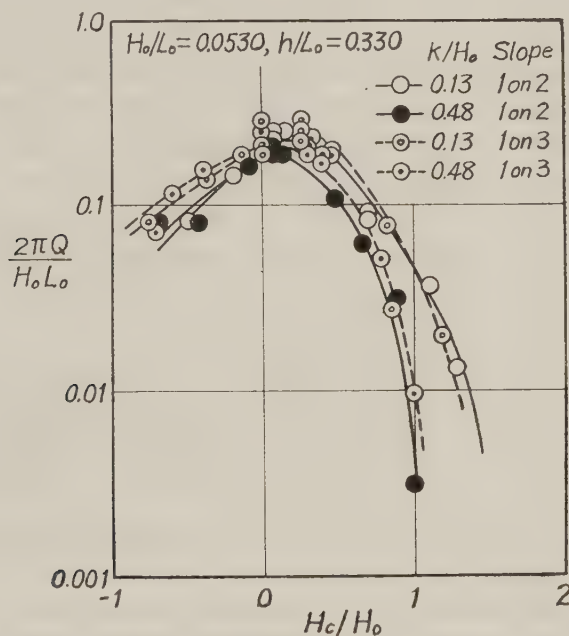


Fig. 9 Effect of wall face roughness on the quantity of overtopping water

As is seen in Fig. 9, the effect of wall face roughness on the quantity of overtopping water is remarkable when the effective height of wall H_c is large. However, when H_c is small, the effect of roughness disappears, and moreover when the wall becomes submerged, the quantity of overtopping water for the case of the rougher wall face tends to be more than that for the case of the other wall face. Further interesting fact is that there exists the critical wall height for the maximum quantity of overtopping water, and this value is 0.1-0.2 independently of the wall face roughness.

3. Effects of top width of wall, parapets and wind

The effects of the top width of wall and parapets were investigated by Sibul⁸⁾ and Sato and Kishi⁹⁾. The interesting fact found from Sibul's experimental results is that the effect of the top width of wall is remarkable when the height of parapet is greater than about a half of the incident deep water wave height.

The experiments on the effect of wind were conducted by Sibul and Tickner¹⁰⁾. It is found by comparing their experimental data on overtopping of wind-generated wave with

those presented previously by the authors that the smaller the slope of wall face, the more the effect of wind on overtopping. However, the experimental results can not be applied to the field quantitatively unless the hydraulic similitude on the effect of wind is made clear.

V. CONCLUSION

The effects of many factors which are considered to be concerned with the quantity of overtopping water have been discussed based on the experimental data presented by the authors, the Beach Erosion Board and the University of California. In analyzing the data, the authors have proposed a new dimensionless expression for the quantity of overtopping water and verified its validity by using the data for the various scales of the test models. It has been found from the analysis of data that one of the most effective factors on overtopping is the water depth at the toe of the seawall. It is needless to say that in applying the experimental results to the field, in addition to the water depth at the toe of the wall, the effects of the cross-sectional shape of wall, the coast and wind characteristics and other factors on wave overtopping must be considered as carefully as possible.

The authors are greatly indebted to the earnest assistance of Messrs. T. Sawaragi and H. Tsunashima. The present study is a part of the authors' study supported by the Science Research Expense of the Ministry of Education and thanks are due to the Ministry of Education.

REFERENCES

- 1) Iwgaki, Y., and T. Sawaragi : Experimental Study on the Equilibrium Slopes of Beaches and Sand Movement by Breaker, Coastal Engineering in Japan, Vol. 1, 1958, pp. 75-84.
- 2) Adachi, S., T. Sawaragi, and A. Ogo : On the Effect of Coastal Structure to the Littoral Drift, Coastal Engineering in Japan, Vol. 2, 1959.
- 3) Healy, J.J. : Wave Damping Effect of Beaches, Proc. Minnesota International Hydraulics Convention, 1953, pp. 213-220.
- 4) Saville, T., Jr., and Caldwell, J.M. : Experimental Study of Wave Overtopping on Shore Structures, Proc. Minnesota International Hydraulics Convention, 1953, pp. 261-269.
- 5) Miyazaki, M. : On Storm Tides which attacked the Japanese Coast Recently, Proc. of 3rd Conference of Coastal Engineering of Japan, 1956, pp. 1-8.
- 6) Kishi, T., M. Tominaga, and T. Oide : Weather and Water Level Deviation at the Mouth of Tone River, Proc. of 3rd Conference of Coastal Engineering of Japan, 1956, pp. 27-32.
- 7) Saville, T., Jr. : Laboratory Data on Wave Run-up and Overtopping on Shore Structures, Beach Erosion Board, Tech. Memo. No. 64, 1955, pp. 1-32.
- 8) Sibul, O.J. : Flow over Reefs and Structures by Wave Action, Trans. A.G.U., Vol. 36, No. 1, 1955, pp. 61-71.
- 9) Sato, S., and T. Kishi : Experimental Study of Wave Run-up on Sea Wall and Shore Slope, Coastal Engineering in Japan, Vol. 1, 1958, pp. 39-43.
- 10) Sibul, O.J. and Tickner, E.G. : Model Study of Overtopping of Wind Generated Waves on Levees with Slopes of 1:3 and 1:6, Beach Erosion Board, Tech. Memo. No. 80, 1956, pp. 1-27.

A STUDY ON THE VOLUME OF LITTORAL DRIFT

*Yasuo Mashima.**

I. INTRODUCTION.

The coast materials such as soil, sand, gravels and rocks will be continuously attacked by the force of the motions of sea water. If the active force surpasses the resistant force against the translation of the coast materials, the littoral drift will occur along the coast. As the author indicated in the previous report¹⁾, the motion of sea water arising the littoral drift includes the ocean current, tidal current and waves, the change of which effects complicatedly to the situation of translation or littoral drift. The translation of drifts take place in suspension, sliding, rolling, salation, etc. and they are combined each other according to the situation of coast, season, time and the materials. Accordingly the littoral drift at any position of coast will have to be characterised respectively. At the general coast, there are rip current drift or undertow drift, on-shore drift and long-shore drift with respect to the direction of translation. The long shore drift is classified into the right or left set drift facing to the offshore on coast.

Furthermore according to the position of drift there are breaking point drift, surf zone drift, offshore drift which includes normal beach drift and storm beach drift, rocky beach drift, and sandy beach drift. Generally at any coast, namely not only on the sandy beach, but also on the rocky beach there are littoral drift, and the deposit or the erosion of coasts will be occurred by the balancing relation of the supply and the outflow of coast materials. Under certain circumstances the balance will be established, or lost to develop the sandy coast by the deposition and the rocky beach by the erosion. If the sand beach maintains its figure and position during a long period, that is, any erosion or deposition will not be recognized at all, we can say that the coast is stable, because the relation between the inflow and the outflow of coast materials is balanced, but the sand particles themselves are continuously translating with the motion of sea water. As the translations of drift sand arise in the direction of the normal or the parallel to the coast line, the slope of the coast section and the plan figure of coast line are maintained as ever at any stable coast. The rocky coast where does not exist almost any movable materials can be recognized to be stable, since it does not change its situation and figure, but that is the case the outflow will be usually greater than the inflow. At such coast the sand deposit is occasionally developed according to the change of coast circumstances.

Moreover the diameter of the coast materials varies from that of very fine silt to that of cobble and these specific gravity varies from that of volcanic ash to that of iron sand, but the principal specific gravity is about 2.65, that is the value of common terrestrial rock. Drifting sea weeds or woods etc. are also translated or deposited and drift. The combination of the diameter of these drift sand has an approximately logarithmic normal distribution, so they have been effected by the sorting process. Namely the particles that have the diameter and specific gravity of the coast material lower than the certain limit will be translated and the higher will not be removed according to the motion of sea water. This limit will be influenced by the figure

* Dr. Eng., Civil Engineering Institute, Defence Academy, Yokosuka, Japan.

of particles, specific gravity, temperature of sea water, etc. If the state of littoral drift is provided, the limit of moving particles will be decided by a certain factor expressing the motion of sea water. That is to say, there are the smallest state of motion of sea water or the combinations of ocean current, tidal current and waves that can move the define particle will be exist according to each sand particle which has a definite diameter, specific gravity, figure, etc. respectively. Excluding the ocean and tidal currents, the motion will be able to be repesented by the critcal wave. The critical wave of a sand particle will decrease certainly along the coast prevailing the strong ocean current and tidal current. And then the critical wave of a sand particle will vary according to the state of littoral drift, that is, the position and the direction of littoral drift. For example the critical wave concerning the breaking point drift will be smaller than that concerning the surf zone drift. And the critical wave of rocky beaches is so very large that the beach cannot be transformed by the ordinary waves. But it is not yet sufficiently distinct that the critical wave described here is to be expressed by some factors which are to be decided hereafter. There are several methods, that is the critical wave is expressed by (1) the combination of wave height, wave steepness and period of wave, (2) the energy and steepness of wave and (3) velocity of longshore current.

In the above mentioned report, the author showed the limit of mean diameter of coast sand by the parameter of the velocity of longshore current. Johnson²⁾, Caldwell, etc. showed that the volume of littoral drift depends upon the longshore component of wave energy and the wave steepness. In addition, the waves at coast have no uniform wave height and period. The wave height will increase by the strong wind and the direction of wave propagation varies by the wind while the wave height will decrease by the weak wind. Such wave motions will be complicated by adding the periodical tidal current, ocean current and longshore currents. So the motion of sea water is the repetition of unsteady states and the accumulation of coast material is the layer of every diameter of sand. Accordingly the formation of the sand layer at coast will depend upon the strength of variation of waves, wave duration and the history of the coast. The development and the decay of waves depend upon the wind, that is, the variation of wind velocity, wind duration and the maximum wind velocity. These waves will be transformed by the submerged dikes, rocks, breakwater, coast topography and the water depth. These transformations will have influence on the stratum of coast sand, the volume of littoral drift and the critical waves.

On the above mentioned fundamental idea, various observations have been carrying out along the coast of Tokyo Bay, Miura Peninsula and Boso Peninsula from July, 1957. In this report, the relations between the supply and erosion of coast sands and the wind data observed at the coast Matsusaki, Yokosuka City are principally described.

II. INVESTIGATION COAST.

Matsusaki Coast between Isemachi and Mabori, Yokosuka City, is located near Cape Kannon at the entrance of Tokyo Bay as shown in Fig. 1 and Fig. 2. This is a sand beach of about 215 meters stretching between rocky points. Behind this coast, there is a road tunnel on the way from Yokosuka to Cape Kannon and Uraga which is penetrated in a soft rocks covered with thick sand strata and thin pebble layers. On this hill, the Deference Academy is situated. On 27 June, 1957, a heavy rain brought with Typhoon No. 5 overflowed from the concrete out-fall sewer on the hill and scoured so disastrously the sand layers that there formed a deep erosion valley and the mud flow from the valley fell to the coast from

TOKYO BAY

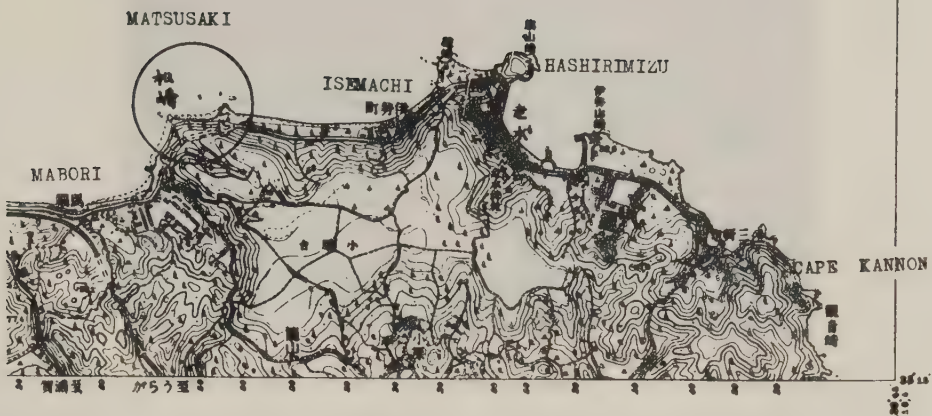


Fig. 1

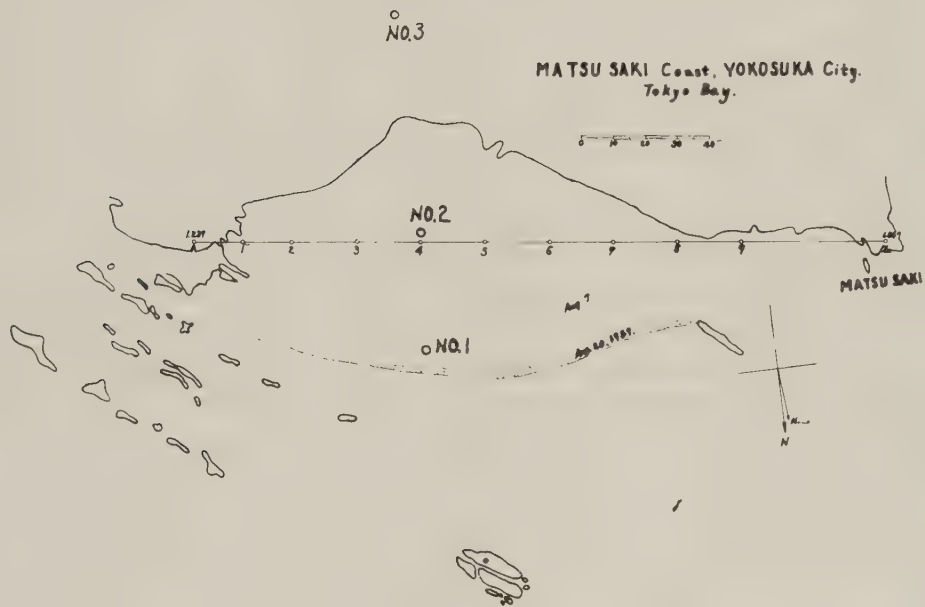


Fig. 2



Photo. 1 Alluvial cone at Matsusaki Coast, July 1, 1957.



Photo. 2 Alluvial cone at Matsusaki Coast Aug. 26, 1957.

about 6 meter height soft rock cliff under the sand layers and deposited a typical alluvial cone as shown in photograph 1 and 2.

Since that time, the constant sewage quantity from the purification tank flowed down intermittently from the demolished sewer, as if a constant water flowed out from the sand layer, and accelerated the erosion of the valley and the formation of the alluvial cone. In September 1957 a temporary sewer was completed, therefore the erosion of the sand layer ended, but the eroded materials of the cone flowed out to the coast. After the sewer was completely established in May 1958, the erosion of the strata and the cone by the sewage had stopped, but the beach line of the cone is being eroded by the attacks of sea waves and the surface of the cone is being weathered by the winds and rains the source of the littoral drift.

These circumstances were the actual examples of the hill side erosion, the formation of an alluvial cone, the supply of littoral drift by the repetition of river floods and the coastal erosion. The author is continuing many investigations on this coast immediately after Typhoon No. 5 in cooperation with the Soil Mechanics Laboratory, Civil Engineering Institute, Defence Academy, in order to investigate the relations mentioned above.

At present, about one year has passed, so the formation of the alluvial cone and its erosion are described here. The distribution of the sand strata at this coast is shown in Table 1, 2 and 3, which were collected at No. 1, No. 2 and No. 3 of Fig. 2. These soil

Table-1 No. 1 Remain Rate on Sieves

Sieve size	No. 1	No. 2	No. 3	No. 4	No. 5	No. 6	No. 7	No. 8	No. 9	Remarks
4.8 mm	—	—	1.55	—	0.2	1.18	—	—	—	Jan. 27
2.0	—	0.17	0.59	0.27	2.59	1.43	3.12	0.39	1.29	1958,
0.85	0.11%	3.06	2.58	4.24	20.69	13.25	2.97	7.31	13.64	Off shore
0.40	10.06	14.45	23.30	46.54	43.62	26.86	15.32	21.15	19.12	30 m from
0.25	45.78	28.55	26.65	29.64	19.04	27.01	30.61	33.04	13.91	base line
0.11	42.20	44.97	43.66	18.05	13.15	26.96	43.00	31.87	29.89	No. 4.
0.075	2.10	2.79	2.25	1.13	0.84	2.76	6.01	3.45	8.39	
Below	0.06	0.10	0.10	0.13	0.10	0.32	0.30	3.59	11.69	
Mean Dia	0.265	0.234	0.272	0.404	0.54	0.35	0.255	0.294	0.235	mm
Uniformity coefft.	2.26	2.48	2.50	2.94	3.20	3.19	2.44	2.79	5.24	d_{60}/d_{10}
Thickness	1 cm	1	1	1	1.2	4.8	5	5	5	
Depth from surface	1 cm	2	3	4	5.2	10.0	15	20	25	

Table-2 No. 2 Remain Rate on Sieves

Sieve size	No. 1	No. 2	No. 3	No. 4	No. 5	No. 6	No. 7	No. 8	No. 9	No. 10	No. 11	No. 12
4.8 mm	—	—	—	—	—	—	—	—	—	1.27	—	—
5.49	mm %	2.5 0.06	mm %	2.5 0.34	mm %	2.5 0.699	mm %	2.5 1.7	mm %	2.5 1.74	mm %	2.5 0.39
2.0	1.7	0.11	0.47	0.34	0.699	0.699	1.7	3.55	1.7	0.45	1.7	0.37
0.85	1.2	0.59	5.69	2.88	11.691	11.691	1.2	4.06	1.2	0.82	1.2	0.70
0.40	2.15	0.6	8.22	20.70	27.12	30.393	0.6	14.10	0.6	6.41	1.89	0.6
0.25	16.56	0.3	31.49	32.31	36.78	30.999	0.3	28.59	0.3	25.81	15.92	18.05
0.11	31.57	0.15	44.69	38.25	30.61	25.467	0.15	32.14	0.15	45.12	18.63	25.55
0.075	42.59	1.38	2.07	1.24	0.640	0.074	0.86	0.074	1.50	30.14	43.64	48.57
Below	0.28	0.074	0.85	0.51	1.03	0.112	Below	9.46	Below	18.34	2.30	4.15
Mean Dia.	0.27mm	0.26	0.28	0.31	0.35	0.35	0.24	0.36	0.26	0.24	0.24	0.24
Uniformity coeff.	2.21	2.54	2.41	2.87	3.00	1.80	4.00	2.38	2.15	2.33	2.33	2.32
Depth from surface	1-14 cm	18-31	30.5-43.5	50-63	68-81	84-97	98.5-111.5	113-126	126-139	139-152	154-167	173-190

Table-3 No. 3 Remain Rate on Sieves (Oct. 18, 1957)

Sieve size	No. 1	No. 2	No. 3	No. 4	No. 5	No. 6	No. 7	No. 8
4.8 mm gravel	0.84%							
2.0	2.67%	4.70						
0.85		1.83	4.7					
0.40 sand	73.03	13.39	81.3	25.99	13.021	93.0	1.10	0.2
0.25				25.43	34.672		12.11	27.7
0.11				16.36	44.034		66.0	61.8
0.05								
0.075 Silt	17.2	13.43	9.0	2.88	0.406	5.0	12.25	6.9
0.005								
Below Clay	7.1		5.0			2.0		1.19
0.001								2.541
Specific gravity	2.72		2.74	2.920		2.721	2.733	2.311
Mean Dia.		0.14mm	0.36	0.27		0.15	0.23	0.21
Uniformity coefft.	22.5		14.6			20.0	2.18	2.06

investigations are only a part of the detailed data of the coast geology carrying out now. Fig. 3 indicates that the sand neighbouring the beach line consists of some layer of several centimeter thickness from the surface this fact points out the remarkable sorting process of waves. In Fig. 3 the sand diameter of the lower part from the surface is more large. This is due to the sorting processes¹⁾.

Fig 4 shows that the soil behind the coast is sandy strata consisting of fine silt and sandy loam with some clay, but the soil of the alluvial cone that was formed by deposition of eroded soil by water flow consists of sands without fine part. When

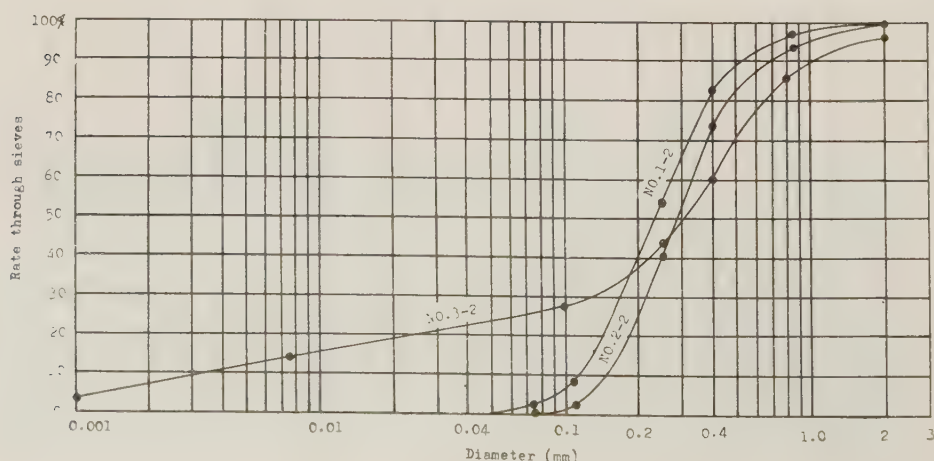
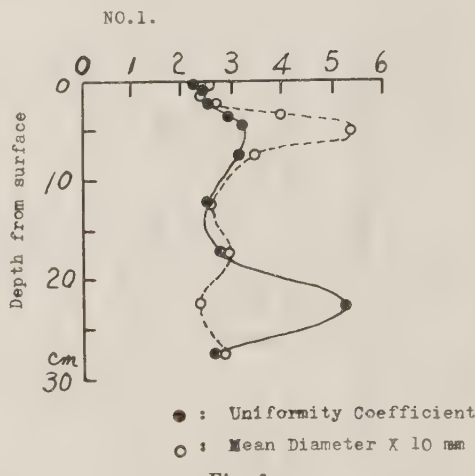


Fig. 4

the soil of cone at coast is attacked by wave action, it has a special strata by the different sorting process from the one of flow water.

III. FORMATION AND EROSION OF THE ALLUVIAL CONE.

As explained in the preceding chapter, the alluvial cone has been formed by the deposition of the eroded materials that were arisen by the flood flow of Typhoon No. 5 and the outfall from the sewage purification tank, and its growth was intermittent. When the flow was large, a small gulley developed on the cone surface and deepened its depth, but decreasing the flow quantity, the gulley lost its depth and the water flowed over its sides and flattened the cone surface. Every gulley from the outflow point has a different direction which distributes all direction uniformly on the cone surface and the cone gradually grew up.

The sewage volume from the purification tank was 25 ton every time and the mean number of the automatic valve opening was 28.96 daily, so that the flow quantity was about 721.6 ton per day. The max. number of flow times in a day was 49.7 and min. 14.7. The hill sand strata was eroded by this flowing out sewage from June 27, to Aug. 15, 1957 and the volume of the lower alluvial cone was increased. Since then the temporary sewer was completed, the deposited soil of the cone eroded by the sewage without any hill soil. If the erosion valley was assumed approximately a cone having its base area of the valley 1816 sq. m and max. depth 29.5 m, the eroded volume of the hill measured from the topographical map (Fig.

Table-4 TOTAL VOLUME (cu.m.) (Between A-9)

Date	No. of Max.		Above	Above	Above	Above	Above	Above	Above
	day	height	-1.0 m	-0.5 m	0 m	1.0 m	1.5 m	2.0 m	3.0 m
1957									
June	26	0	6209.76	3291.26	1802.51	559.75	265.00	94.25	4.50
July	23	26	4.0179			3728.94	2153.68	1152.83	183.58
	24	27	4.165				2403.78	1326.15	232.18
	25	28	3.919	13636.74	9709.99	3949.36	2230.61	1120.81	152.61
	26	29	5.384			4697.79	2893.26	1643.76	300.16
	29	32	5.655	15780.48	11567.23	5575.48	3692.73	2344.48	758.33
	30	33	5.722		11453.09	5581.79	3708.54	2350.85	748.35
	31	34	5.678		11794.72	5757.22	3849.47	2467.54	818.79
Aug.	1	35	5.692		11894.27	5906.77	3942.27	2513.88	813.17
	2	36	5.702			5680.74	3778.49	2386.09	714.64
	6	40	4.591		12434.55	6220.30	4150.55	2639.03	812.13
	7	41	5.925		12707.22	6272.47	4164.72	2657.05	858.31
	8	42	6.134			6681.16	4502.41	2941.05	1072.49
	9	43	6.112			6777.51	4497.08	2877.53	989.53
	12	46	5.952	18352.90	13738.40	6894.28	4599.44	2939.88	987.28
	15	49	5.938		13732.16	6903.91	4660.31	3029.81	1072.93
	16	50	5.984		14056.31	7136.81	4816.80	3151.98	1149.73
	20	54	6.160			6915.86	4598.92	2902.89	880.94
Oct.	2	97	5.997			6049.77	3964.89	2449.79	741.04
Nov.	1	127	5.932		12797.73	6387.73	4398.23	2919.42	1115.17
Dec.	6	162	5.937			6221.82	4294.55	2830.80	1034.93
	26	182	5.976		12571.46	6258.46	4330.08	2889.20	1079.02
1958									
Jan.	27	214	6.034	16635.57	12266.82	6102.32	4231.74	2813.49	1052.51
Mar.	1	247	6.085			6303.42	4413.29	2757.02	1009.93
Apr.	1	278	6.099		12038.00	6112.25	4234.50	2821.75	1031.50
	17	294	6.101			6037.67	4143.07	2748.32	978.95
May.	7	314	6.143		11502.27	5784.77	3977.77	2626.95	957.95
June	4	342	6.058		10992.83	5379.33	3613.89	2292.58	729.65
July	2	370	6.050	20880.14	15479.89	11438.89	5764.39	3952.44	949.19

Table-5 TOTAL VOLUME (cu.m.)

(Between A-5)

Date	Above -0.5 m	Above 0 m	Above 1.0 m	Above 1.5 m	Above 2.0 m	Above 3.0 m
1957						
June 26	1656.76	973.01	333.75	166.00	62.75	4.50
July 23			2458.64	1477.63	831.13	131.88
24				1758.53	1015.90	184.43
25	8308.67	6064.92	2647.92	1626.92	850.92	114.47
26			3349.04	2079.79	1230.29	237.54
29	10137.71	7653.46	3979.46	2722.46	1790.21	624.56
30		7629.61	4036.61	2796.86	1854.76	643.51
31		7926.43	4178.68	9210.68	1952.88	679.03
Aug. 1		7945.17	4266.67	2956.67	1957.83	680.58
2			4060.66	2783.16	1806.51	566.31
6		8467.70	4546.45	3128.70	2049.8	672.90
7		8705.55	4603.55	3149.55	2076.25	716.98
8			4751.89	3284.39	2199.40	841.34
9			4721.46	3245.21	2162.81	809.81
12	11555.67	8821.67	4687.92	3223.67	2130.41	767.66
15		8727.37	4640.37	3252.62	2190.02	828.89
16		8999.15	4827.40	3364.40	2274.13	877.13
20			4769.39	3273.89	2145.51	723.06
Oct. 2			3836.57	2600.14	1664.79	540.04
Nov. 1		7712.31	4151.81	3017.56	2120.62	900.62
Dec. 6			4028.04	2926.17	2050.42	845.30
26		7344.00	3993.75	2925.37	2078.99	886.25
1958						
Jan. 27	9571.52	7178.27	3889.52	2840.64	1993.14	825.66
Mar. 1			3876.16	2817.78	1954.26	790.42
Apr. 1		6968.40	3904.15	2878.15	2022.90	810.90
17			3764.77	2709.02	1868.52	708.52
May 7		6551.41	3625.66	2649.66	1853.22	756.49
June 4		6177.83	3270.08	2320.14	1544.33	542.90
July 2	8741.23	6556.23	3610.73	2619.98	1812.48	748.98

5) of the erosion valley was

$$1816 \times 29.5 \times 1/3 = 17857 \div 18000 \text{ cu.m.}$$

Since Typhoon No. 5, the variation of the topography of the alluvial cone was measured repeatedly by the longitudinal and transverse levelling referring a base line set parallel to the coast. From this survey, the deposited volume and the slopes of the cone were estimated, the results are tabulated in Table 4, 5 and 6.

The cone volume over -0.5 meter on Aug. 12, 1957 was

$$18352.9 - 3291.26 = 15061.64 \text{ cu.m.}$$

The cone volume over -1.0 meter on July 2, 1958 was

$$20880.14 - 6209.76 = 14670.38 \text{ cu.m.}$$

Assuming the deposited volume of the alluvial cone as about 15000 cu.m., about 83.3% of

Table-8 TOTAL VOLUME (cu.m.)

(Between 5-9)

Date	Above -1.0 m	Above -0.5 m	Above 0.0 m	Above 1.0 m	Above 1.5 m	Above 2.0 m	Above 3.0 m
1957							
June 26	3224.5	1634.5	829.5	226.0	99.0	31.5	
July 23				1270.3	676.05	321.7	51.70
24					645.25	310.25	47.75
25		5328.07	3645.07	1301.44	603.69	269.89	38.14
26				1348.75	818.47	413.47	62.62
29		5642.77	3913.77	1596.02	970.27	554.27	133.77
30			3823.48	1545.18	911.68	496.09	104.84
31			3868.29	1578.54	938.79	514.66	139.86
Aug. 1			3949.1	1640.1	985.60	556.05	132.59
2				1620.08	995.33	579.58	148.33
6			3966.85	1673.85	1021.85	589.23	139.23
7			4001.67	1668.92	1015.17	580.8	141.33
8				1929.27	1218.02	741.65	231.15
9				2056.05	1251.87	714.72	179.72
12		6797.23	4916.73	2206.36	1375.77	809.47	219.62
15			5004.79	2263.54	1407.69	839.79	244.04
16			5057.16	2309.41	1452.4	877.85	272.6
20				2146.47	1325.03	757.38	157.88
Oct. 2			5067.2	2213.2	1364.75	785.0	201.0
Nov. 1			5085.42	2235.92	1380.67	798.8	214.55
Dec. 6				2193.79	1368.39	780.39	189.64
26			5227.46	2264.71	1404.71	810.21	192.77
1958							
Jan. 27		7064.05	5088.54	2212.8	1391.10	820.35	226.85
Mar. 1				2193.26	1361.51	802.76	219.51
Apr. 1			5069.6	2208.1	1356.35	798.85	220.6
17				2272.9	1434.05	879.8	270.43
May. 7		6898.61	4950.86	2159.11	1328.11	773.73	201.46
June 4	9077.5	6727.5	4815.0	2109.25	1293.75	748.25	186.75
July 2	9076.16	6738.66	4882.66	2153.66	1332.46	777.71	200.21

the flowout volume of the erosion valley was deposited there and 16.7% arrived at sea water to supply immediately to the littoral drift. It is estimated that mean volume 3000/49 = 61 cu.m. was supplied daily to the adjacent coast or sea water in suspension, during 49 days up to Aug. 15. In Fig. 4, the lost volume 16.7% above described corresponds to the fine part volume smaller than sand of the No. 3 hill soil. The mean eroded volume was 367.3 cu.m. per day for the total volume 18000 cu.m. during 49 days. It is clear that the erosion of sand layer was so violent that the mud volume ratio of the mud flow was 50.9% and weight ratio was about 81.4% considering the sewage flow 721.6 cu.m. per day without Typhoon rain.

(a) Development of alluvial cone

The volume of alluvial cone formed by the mud flow relates approximately to the number

of days or the number of sewage flow, the max. height (h_0) of the cone and the height of base plane for volume survey as indicated in Fig. 6 written by Table 4, 5 and 6.

Assuming V_a as the deposited volume (cu.m.) over the height h meter and t as the number of days, and using the value of the survey between A-5,

The volume distribution against the height will be estimated by the formula (1), hence the volume of lower part of the cone is very large. The rise of the cone summit depends upon the number of days in the next formula (in meter unit)

$$h_0 = 1.5 + 3.636 t^{0.048} \dots \dots \dots \quad (2)$$

The coefficients of these formulae are estimated by the practical survey, and therefore in the case of different conditions of flow quantity, velocity and soil properties their values will vary correspondingly. In this survey, the datum level of the height is the mean water level of Tokyo.

One outflow of sewage to the alluvial cone is just like one flood, and at first the mud flow finds its way into a stream and up to the max. flow, the stream channel is eroded deeply, but at the decreasing flow, the stream channel is deposited in rising the water surface to over flow from its sides. Accordingly a stream bed is rised by the deposit at one outflow and the next outflow must find another stream channel. In such way, the cone is risen itself and formed uniformly from side to side from the center of flowout. In this case, as described above, most part of the flowing out mud deposits on the alluvial cone, and only one part attains to the sea. The formed topography is an almost perfect cone and its slope will depend upon the mud volume and water quantity of outflow, its intermittence and number of outflow, mean diameter and specific gravity of mud and sand, etc.. By this reason, the river in the region where it has a severe humid season and arid one alternately will be apt to meander and to form somewhat alluvial cone topography. Considering a very long time, the repetition of floods will result in the same circumstances. From such consideration, the cobble and larger stones will be transformed and deposited to the lower part of an alluvial cone. Therefore, the alluvial cone formed by a repetition of concentrated flow will have an almost uniform slope which can flow down the sand and mud containing water. Namely on the flatter slope, the sand and mud will deposit on the summit of the cone untill they can be transported. Thus the slope of the cone will correspond to the upper slope where the mud flow starts and therfore it will be able to estimate the state of upper erosive slope from the alluvial cone. In this example, the slope of the cone was 8 to 12%, from which a severe erosion on the upper valley will be reasonably conjectured. Besides when the flow from the upper valley

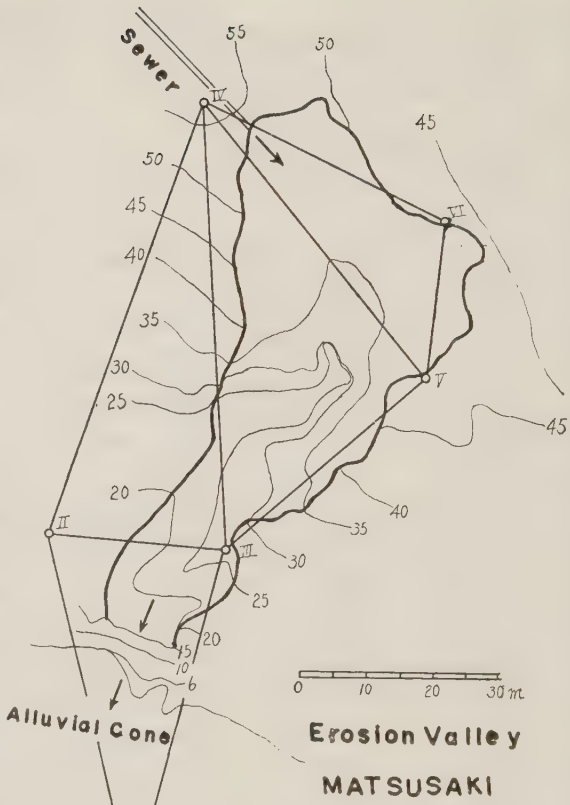


Fig. 5

does not contain any mud and sand, it will erode only the stream bed and fix a deep canal in cutting off the cone. Actually the completion of the erosion control on the upper part of the drainage area will result in the fixation of the river.

(b) Erosion of alluvial cone

Since Aug. 16, the deposition had stopped, and it entered in the period of erosion. In this period, the volume of the cone is decreasing gradually as indicated in Fig. 6.

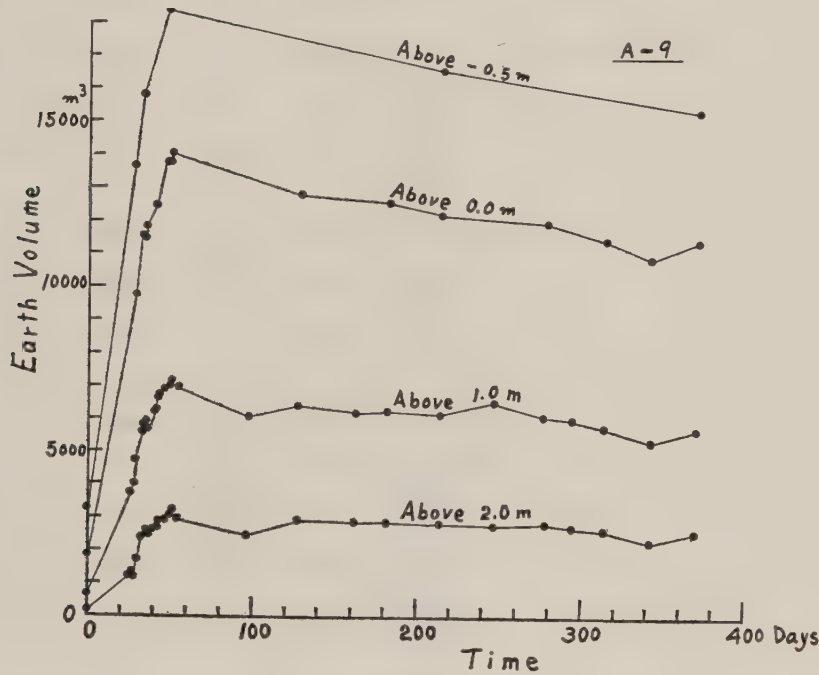


Fig. 6

If it is assumed that the volume of the cone varies proportional to the number of days,

where a : a coefficient

V_e : volume of the alluvial cone in cu.m.

t : number of days

Taking h (m) as datum plane, from Table 4

for $h = 3.0 \text{ m}$: $V_e = 900.6 - 0.9468 t$

$$h = -2.0 \text{ m} : V_e = 2120.6 - 0.7218 t$$

$$h = -1.5 \text{ m} : V_e = 3017.6 - 2.2841 t$$

$$h = -1.0 \text{ m} : V_e = 4151.8 - 2.7076 t$$

$$h = -0.0 \text{ m} : V_e = 7712.3 - 5.861 t$$

$$h = -0.5 \text{ m} : V_e = 11555.67 - 8.686 t$$

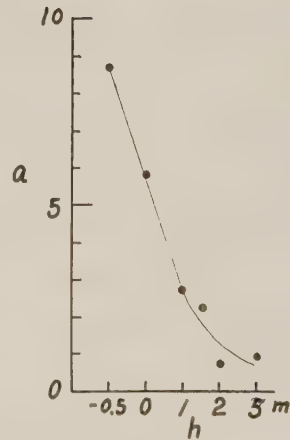


Fig. 7

Coefficient varies corresponding to the datum height of the survey as indicated in Fig. 7. These formulae show the volumes of the surface erosion on the alluvial cone and for h lower than 2.0 m they contain the volume of coast erosion along the beach line.

Assuming the surface slope of the cone is almost constant, the volume, surface area and base circumference of the cone can be expressed by the following formulae

Table-7 Slope and Radius of Alluvial Cone (Mean values)–(a)

Date	No. of days	Height -1.0 m	-0.5 m		0.0 m		+0.5 m		+1.0 m	
July 23	26				9.16	67.02	10.03	69.35	5.28 (20.45)	62.72
24	27				8.04	74.94	6.02 (12.71)	66.37	5.44 (9.43)	59.06
25	28		7.26	86.81	8.60	77.04	8.38	70.88	5.01 (11.62)	62.61
26	29						9.07 (11.43)	71.70	6.62 (47.74)	60.38
29	32	6.88 % 95.18 m	6.63	88.77	7.35 (8.37)	80.86	7.65 (9.71)	72.93	5.54 (7.84)	61.02
30	33		6.95	86.41	7.18 (8.80)	80.37	7.42 (9.55)	72.61	5.89 (11.18)	61.49
31	34		5.38	89.76	6.17 (8.14)	81.14	8.32 (10.36)	73.03	5.92 (10.53)	62.39
Aug. 1	35				7.68 (9.25)	79.97	9.74 (11.59)	72.39	6.00 (10.93)	62.74
2	36				11.32	64.26	8.86 (11.84)	72.20	6.46 (10.85)	62.48
6	40				8.51 (10.26)	80.34	9.07 (11.08)	73.86	7.21 (11.78)	64.20
7	41				8.42	83.02	7.77 (9.38)	75.41	5.95 (10.77)	64.65
8	42						7.77 (13.05)	78.42	7.86 (12.50)	65.65
9	43		3.74	96.60	7.03	86.67	8.70 (12.33)	76.52	5.97 (12.45)	69.51
12	46		7.22	90.42	7.50 (9.22)	84.73	7.58 (9.84)	77.41	5.87	66.24
15	49		8.67	89.35	8.08 (9.74)	84.31	10.37 (12.86)	77.77	6.32 (9.60)	69.31
16	50				7.25 (9.18)	82.82	10.44	75.06	7.66	66.59
20	54				5.74 (17.94)	97.78	5.71	75.86	6.45	66.41

Table-7 Slope and Radius of Alluvial cone (b)

Date	No. of days	Height -1.0 m	-0.5 m		0.0 m		+0.5 m		+1.0 m	
Oct. 2	97				5.23	78.75	7.68	75.86	6.63 (13.07)	67.75
Nov. 1	127				14.27	95.24	10.17 (11.32)	75.65	9.80	66.54
Dec. 6	162						(17.19)	(91.49)		
26	182		4.41	88.21	7.79	83.21	10.95 (12.34)	76.06	16.22 (25.93)	67.32
Jan. 27	214		5.08	89.54	7.41	81.93	10.42 (11.66)	75.94	13.55	66.31
Mar. 1	247				(1.39)	75.04	8.33 (10.06)	74.59	18.46	66.40
Apr. 1	278				7.18 (9.97)	80.22	11.63	74.19	10.33	67.17
17	294		3.00	93.39	7.47	78.43	11.45	74.28	18.61	67.00
May 7	314	6.36 108.96	5.67	89.38	7.11	79.72	14.02 (14.93)	72.28	38.64	66.30
June 4	342	4.85 101.76	4.46	88.34	8.33	79.18	12.42	73.17	26.87	65.56
July 2	370	4.02 100.88	4.30	89.51	8.78 (10.39)	77.08	15.02	71.82	13.47	65.96

Table-7 Slope and Radius of Alluvial Cone (c)

Date	+1.5 m		+2.0 m		+3.0 m		+4.0 m		+5.0 m		Remarks
July 23	5.55 (30.38)	53.69	6.29 (24.81)	35.46	6.42	19.43	9.13	13.12			Period of Erosion
24	4.97	42.35	5.93 (14.85)	36.54	7.06	21.94	11.43	12.81			
25	10.03 (35.52)	55.64	7.04	37.14	8.87	24.61					
26	5.51 (13.25)	49.32	6.56	39.70	7.30	25.08	10.12	14.14			
29	5.70 (17.89)	53.98	6.85	41.14	8.14	26.93	10.15	15.53			
30	6.99 (18.35)	54.38	7.82	41.56	7.91	27.59	8.08	20.17			
31	5.68 (16.72)	54.73	7.13	42.21	7.41	28.65	8.58	16.51			
Aug. 1	5.26 (11.75)	55.36	7.05	45.22	7.08	29.35	8.81	16.05			
2	5.20 (17.14)	55.10	7.16	42.72	6.41	28.34	10.13	15.36			
6	5.42 (19.42)	56.41	6.51	44.42	7.85	30.68	8.68	16.65			
7	5.39 (17.11)	56.52	6.75	44.73	7.36	30.68	8.21	17.42			
8	5.52 (24.52)	57.27	6.65	45.51	8.96	30.86	9.24	18.74			
9	6.87 (12.17)	59.61	6.96 (27.02)	46.19	7.88	31.15	8.18	18.28			
12	6.80	55.85	6.38 (23.13)	46.67	7.98	30.41	9.20	17.70			
15	8.49 (25.48)	58.70	6.88 (22.69)	46.54	9.92	33.00	8.09	18.49			
16	6.61 (12.65)	58.44	7.73	46.74	8.88	32.87	9.20	19.31			
20	6.70	56.63	6.83	47.34	8.08	34.18	7.09	18.02			

Table-7 Slope and Radius of Alluvial Cone (d)

Date	+1.5 m		+2.0 m		+3.0 m		+4.0 m		+5.0 m		Remarks
Oct. 2	7.20 (13.49)	58.52	7.50	46.74	7.49	32.38	8.92	19.73			Period of Erosion
Nov. 1	9.04 (25.39)	58.45	6.65	47.94	6.36	34.02	9.79	21.47	14.85	11.55	
Dec. 6											
26	10.12 (18.41)	54.66	6.93	47.61	6.55	33.21	9.68	20.46	21.36	11.53	
Jan. 27	7.77 (19.97)	54.32	7.92	47.18	7.57	33.13	9.00	20.64	18.57	11.80	
Mar. 1	10.80 (44.09)	61.67	7.72	46.83	7.42	33.68	9.06	20.02	36.90	11.55	
Apr. 1	8.24 (23.88)	57.02	7.48	47.41	9.10	33.59	9.35	20.53	19.80	11.80	
17	8.58 (27.91)	56.96	6.98	46.09	7.01	33.05	9.61	20.16	21.91	11.55	
May 7	9.90 (26.27)	56.90	6.48	46.65	7.58	33.12	9.38	20.25	20.74	11.85	
June 4	10.19 (49.47)	61.06	6.05	45.86	7.49	32.10	10.60	19.72	42.62	11.86	
July 2	8.43 (20.54)	57.46	6.57	45.93	9.89	32.26	9.86	20.59	15.86	12.50	

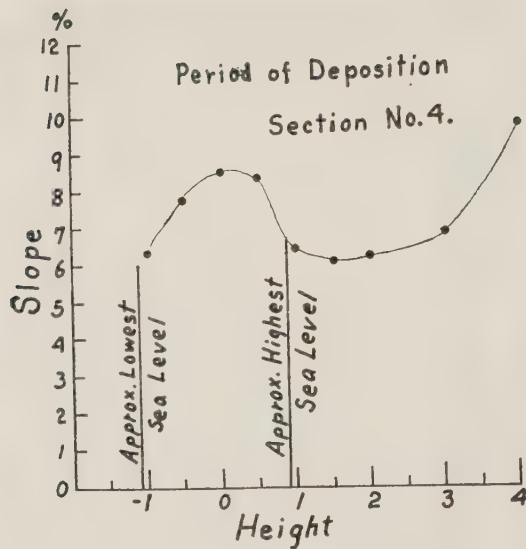


Fig. 8

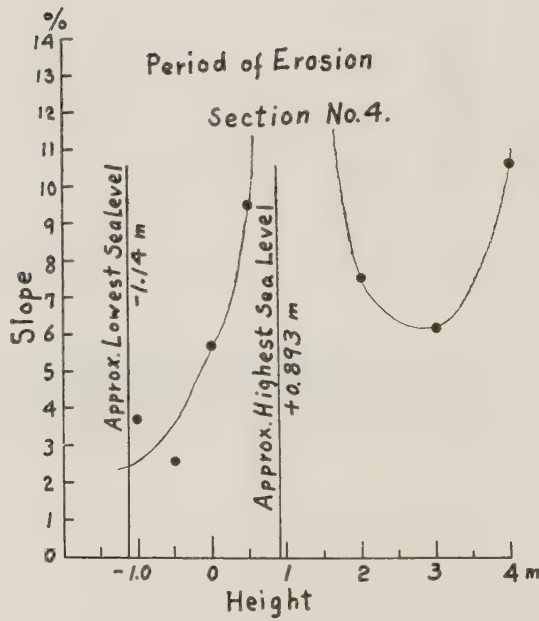


Fig. 9

$$V = \frac{\pi h^3}{6 i^2} \frac{\theta}{180} \quad \dots \dots \dots \quad (4)$$

$$S = \frac{\pi h^2}{i^2} \sqrt{1+i^2} \frac{\theta}{180} \quad \dots \dots \dots \quad (5)$$

$$L = \frac{\pi \theta}{180} \frac{h}{i} \quad \dots \dots \dots \quad (6)$$

where h : height of the cone (m),

$i = h/R$: slope of the cone,

V : volume (cu.m.)

L : length of the base circumference.

R : a radius of the base (m)

θ : central angle (degree)

S : surface area (sq.m.)

In this cone, $\theta = 123^\circ$, so

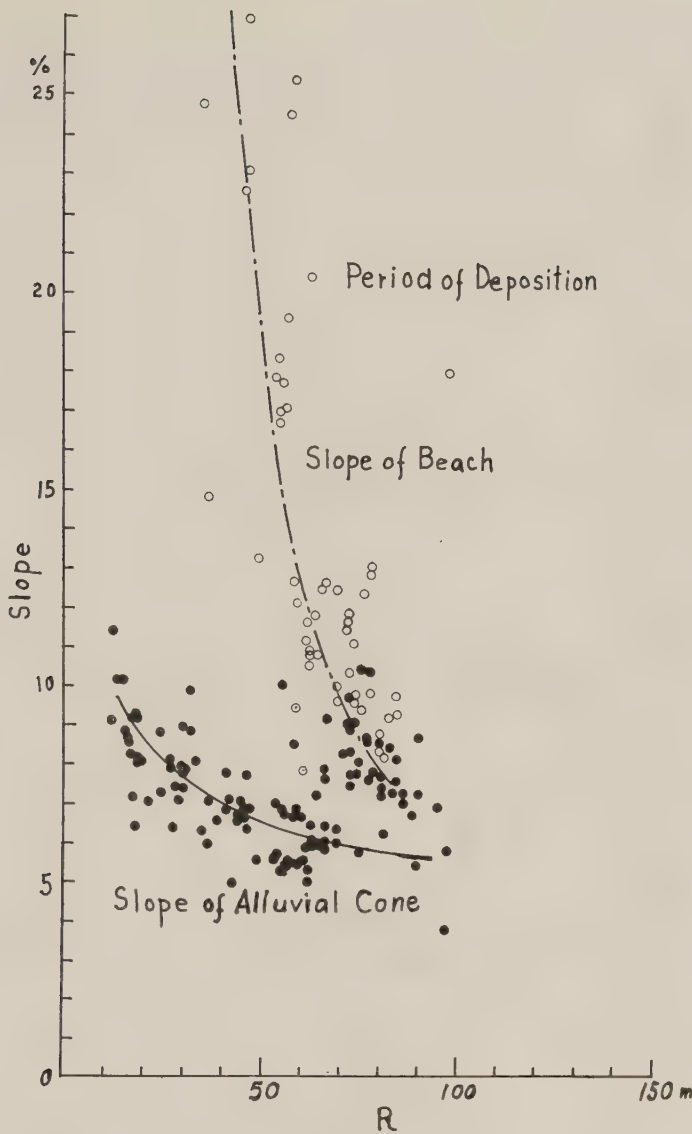


Fig. 10

Using V over $h = +1.5 \text{ m}$,

July 23, 1957 : $h = 4,017.9$ m $i = 0.1038$ ($5^{\circ}56'$)

Aug. 16, 1957 : $h = 5.984$ m $i = 0.126$ ($7^{\circ}11'$)

July 2, 1958: $h = 6.050$ m $i = 0.1416$ ($8^\circ 3'$)

The slope in the erosion period is steeper than that in the depositing period.

Using the values of longitudinal and transversal levels of the alluvial cone, and assuming it a perfect cone, the max. slope and the radius at every point and their mean values at each height were calculated as given in Table 7. The mean value of the max. slope at each height of the section No. 4 is indicated in Fig. 8 and Fig. 9.

At the points in the tidal range, the surface slopes are from 4.7% to 18.6% and their mean values have the variations as shown in these figures. Even in the depositing period

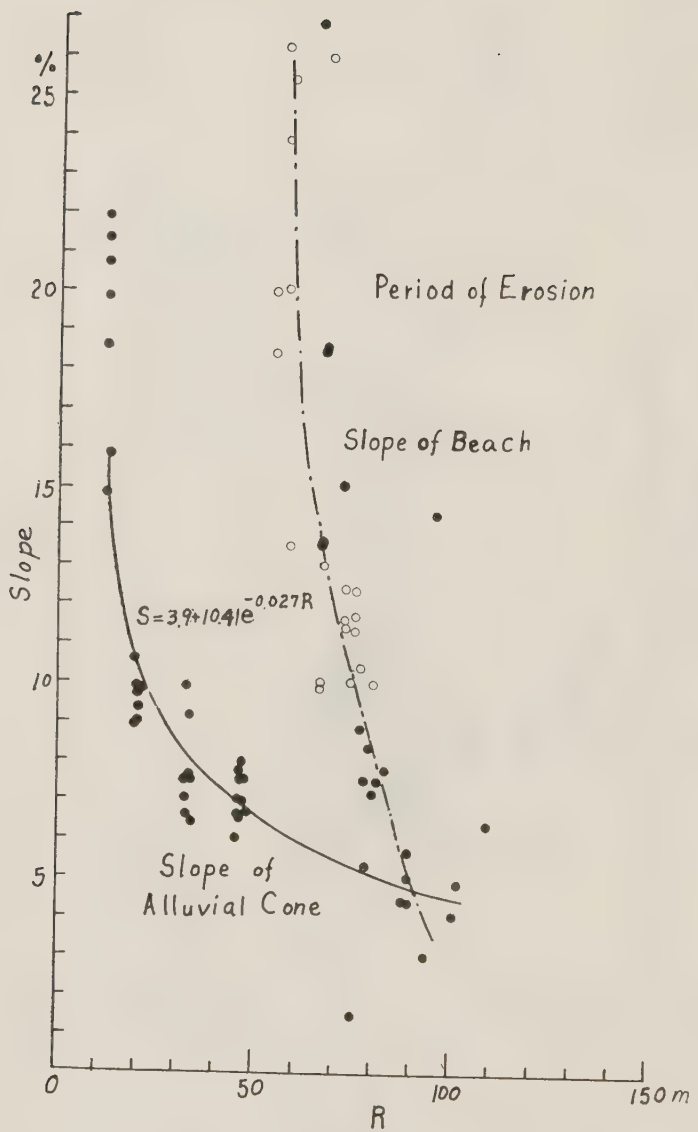


Fig. 11

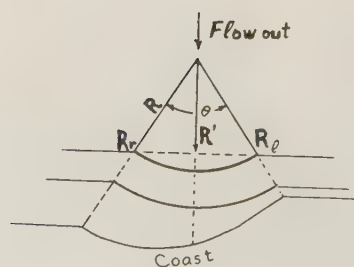


Fig. 12

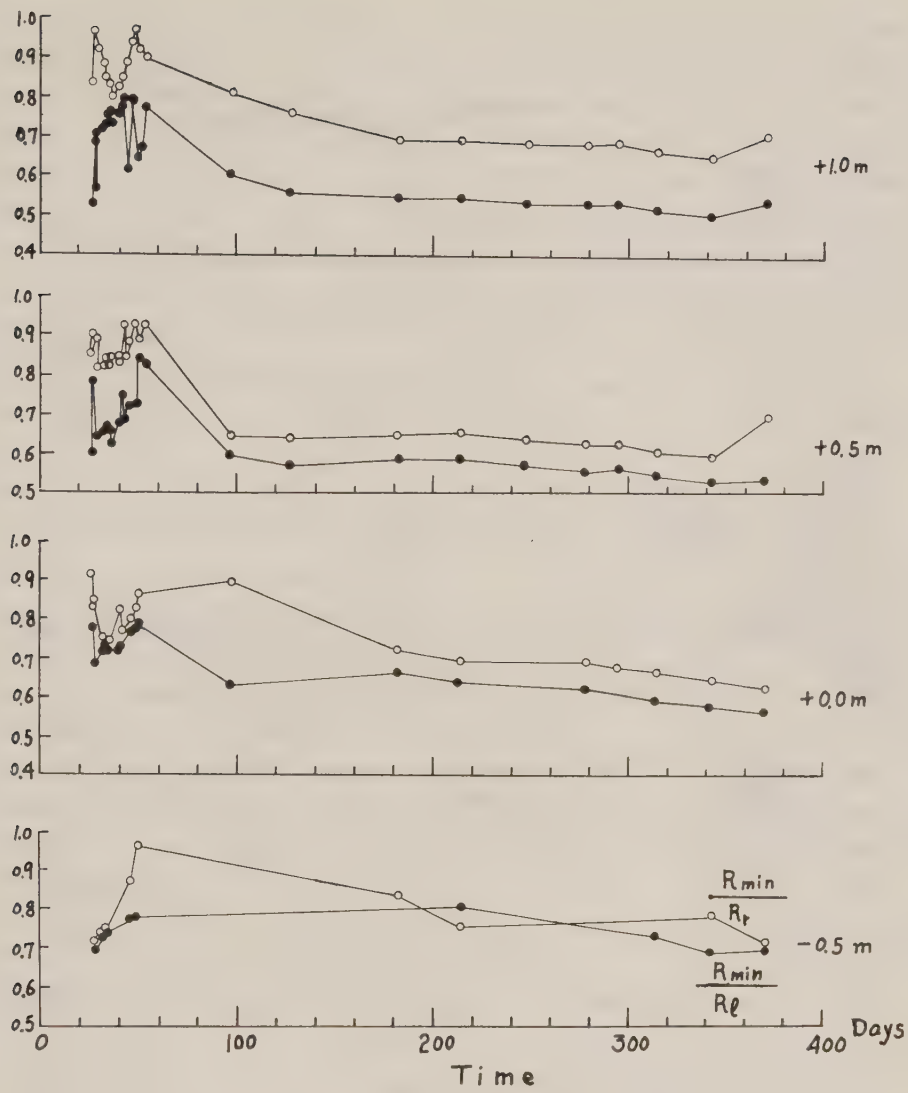


Fig. 13 (a)

of the cone, the slope near the beach will vary itself in response to wave action. And the height of the steep slope part over the max. water level will relate to the wave height. The slope of the alluvial cone at the erosion period becomes generally steeper than that at the deposition period. The part influenced by wave action has entirely different slope, that is: the upper end of the eroded part on the beach becomes steeper just like a cliff and the slope in the sea water flatter. When the waves are strong and the amount of flushed mud is small, the characteristic slope of the coast will be governed by the wave action. But if the wave action is small at the outflow period, the slope of the alluvial cone will maintain during the period. These situations are clearly shown in Fig. 11 obtained from Table 7.

If the radius R in the horizontal section of the cone at a given height is constant at any direction angle, the erosion of the alluvial cone will not contain the erosion by the coast process, but if R in the direction of the two equal division is smaller as Fig. 12 and $R' = R \cos \theta/2$, the coast line is straight and so the cone topography will be eroded by the coast process at all. Accordingly in this case

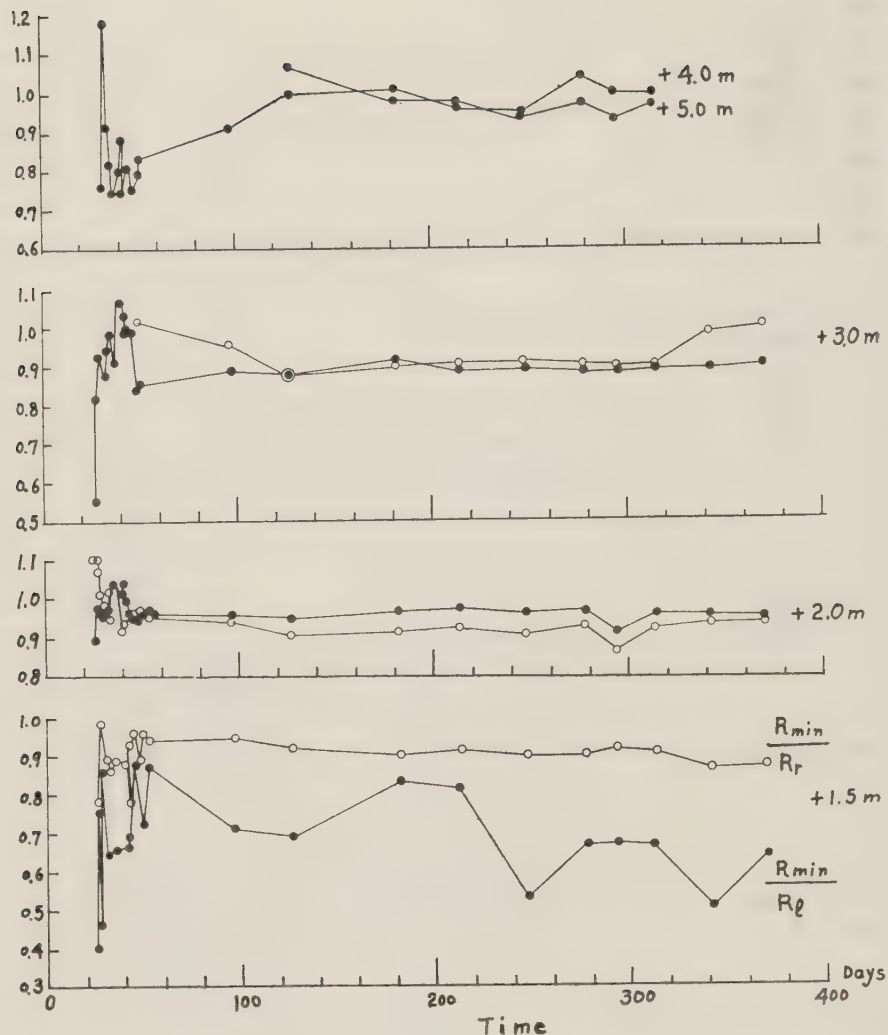


Fig. 13 (b)

$$\frac{R'}{R} = \cos \frac{\theta}{2}. \quad \dots \dots \dots (9)$$

The ratio R_{\min}/R of the minimum value R_{\min} of R to R , approaches nearer to $\cos \theta/2$, and the erosion will more advance. In our coast, $\theta=123^\circ$, $\cos \theta/2=0.4771588$.

Assuming the radius at the left side facing to the sea as R_l and at the right side as R_r , the ratios R_{\min}/R_l and R_l and R_{\min}/R_r will indicate the degrees of erosion at the left and the right side, respectively.

The results of the survey show in Fig. 13 that it is symmetric and the ratio is almost 1.0 at the height of 2.0 m or more, but on the level lower than +1.5 m it is somewhat unsymmetric and $R_r < R_l$ that left side is longer than the right. On the level lower than +1.5 m, the ratio decreases gradually, so that the coast line is approaching to a straight line.

IV. VOLUME OF LITTORAL DRIFT.

The volume of littoral drift is considered to be produced by the result of works

that due to the wave action at the coast. Shay, Johnson, Caldwell and Saville showed that the amount of littoral drift can be expressed by a function of the parallel component to longshore of the arriving wave energy, the volume of supply from the drift sources and the steepness of the arriving waves. Here in order to clarify the relation between the volume of coast erosion and the arriving wave characteristics, the one year data of wind direction and wind velocity hourly observed at Yokohama Meteorological Observatory from June 1958, are used by selecting the sea winds, mean velocity of which is above 5.0 m/sec. Then the wave heights, periods and the wave lengths generated by these winds are calculated from the diagrams of Moliter and Sverdrup. The formula of wave energy per unit wave length and width is

$$E = \frac{\omega L_0 H_0^2}{8} \left(1 - 4.93 \frac{H_0^2}{L_0^2} \right) \quad \dots \dots \dots (10)$$

and the wave power per unit width is

$$P = \frac{E}{2T} = \frac{\omega H_0^2}{16} \left(1 - 4.93 \frac{H_0^2}{L_0^2} \right) \sqrt{\frac{gL_0}{2\pi}} \quad \dots \dots \dots (11)$$

(After Sverdrup and Munk, Rossby 1947).

where H_0 : height of off shore wave

L_0 : length of off shore wave

T : wave period.

Assuming that these waves propagate in the same as the wind direction and neglecting of the wave refraction here, the parallel and normal components to the coast line of the arriving wave energy per unit length of coast are calculated. In Fig. 14, the parallel component of wave energy per unit length of coast is

$$\frac{E}{2} \sin 2\beta = \frac{E}{2} \sin 2\gamma. \quad \dots \dots \dots (12)$$

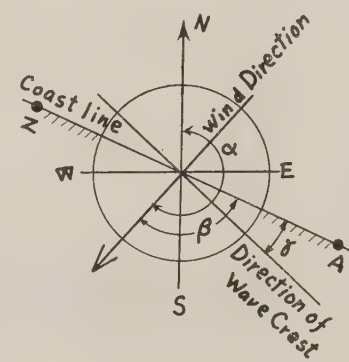


Fig. 14

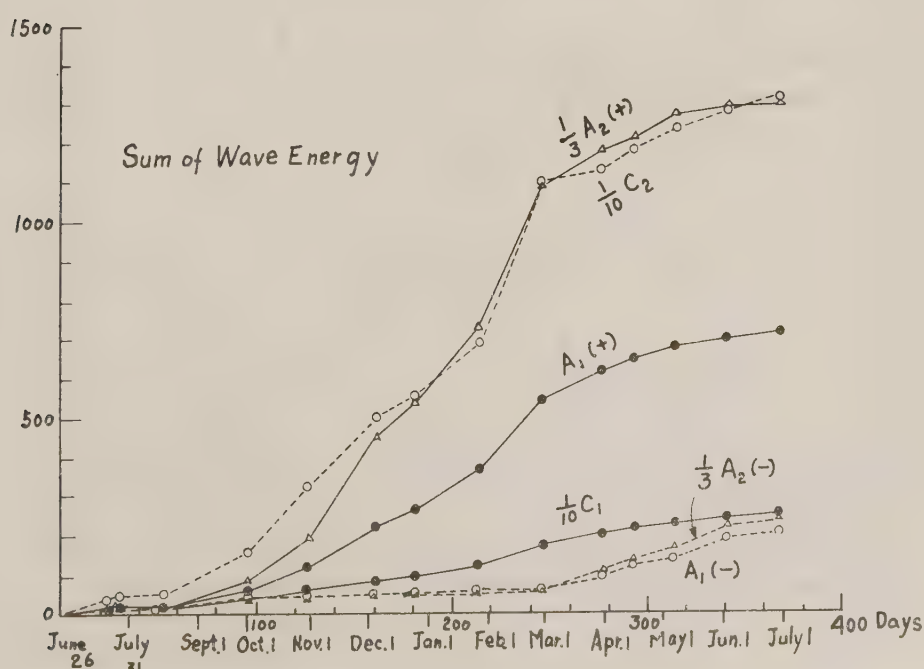


Fig. 15

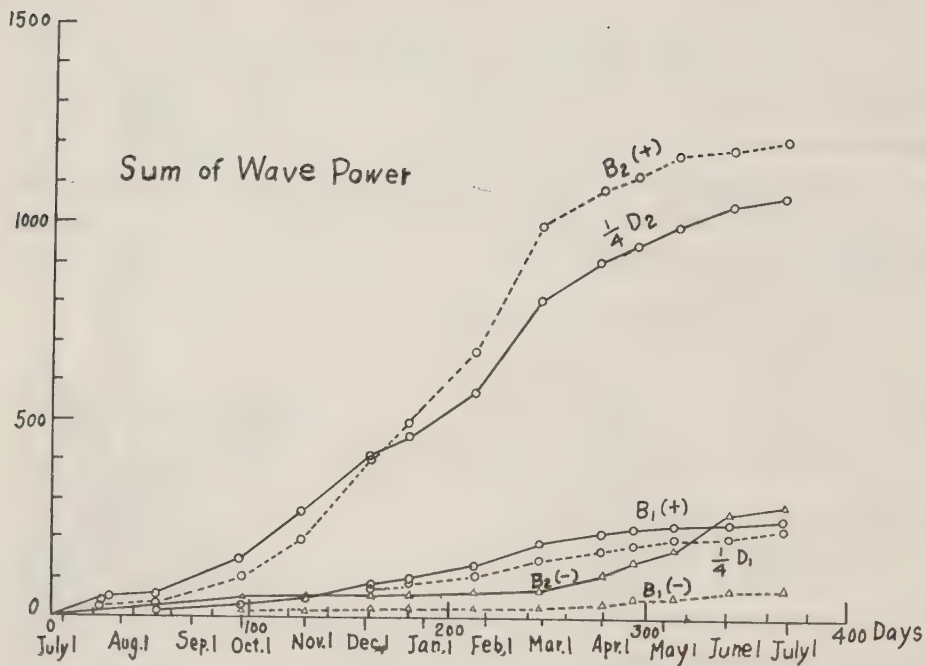


Fig. 16

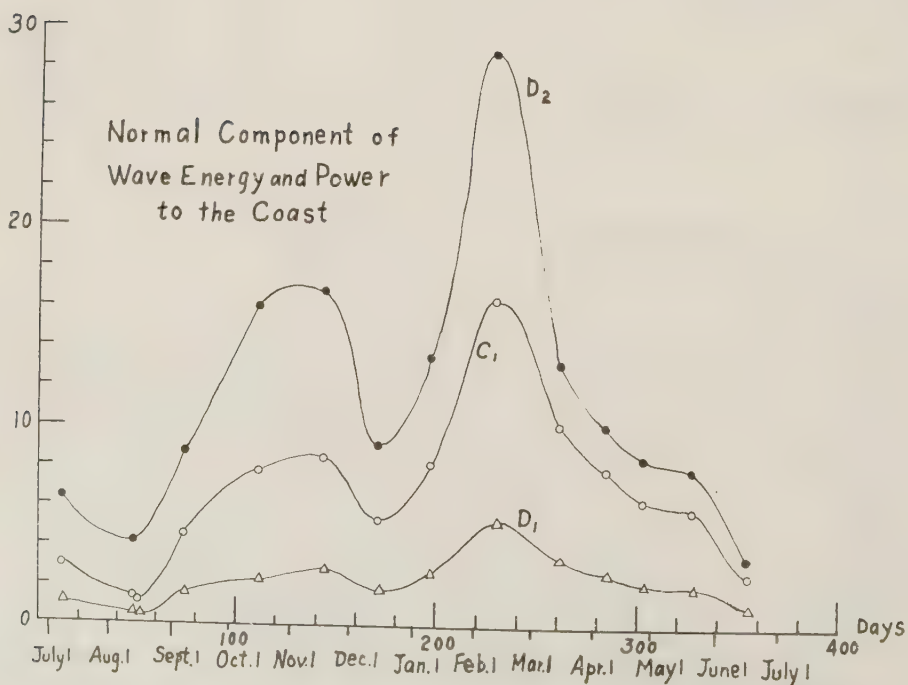


Fig. 17

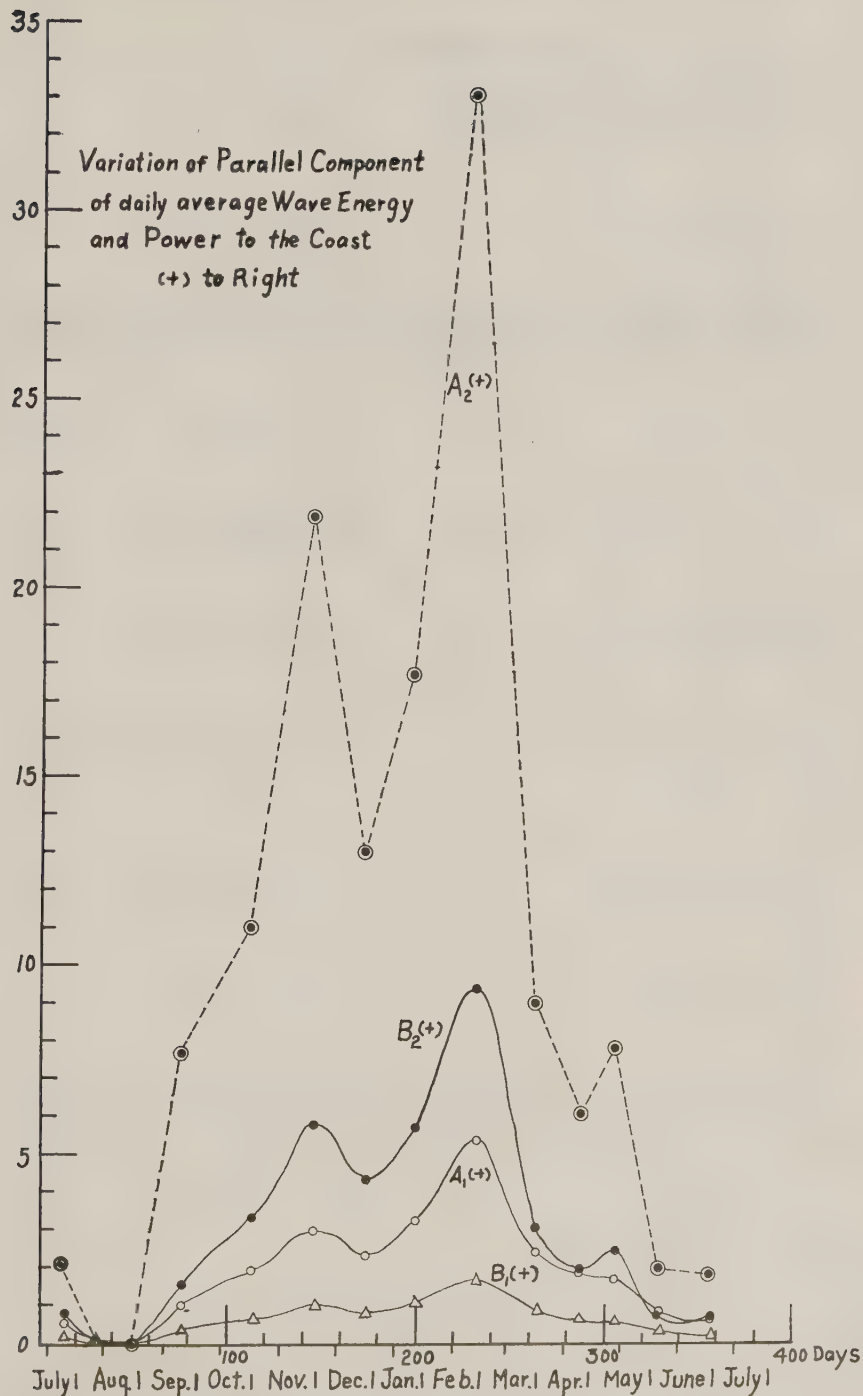


Fig. 18-1

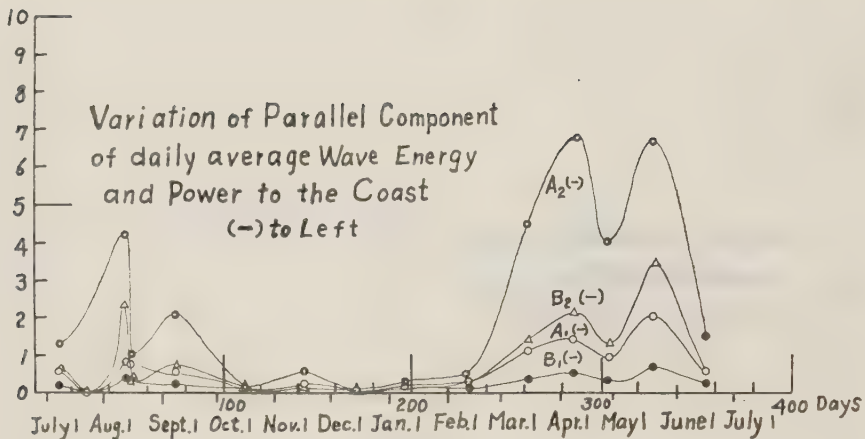


Fig. 18-2

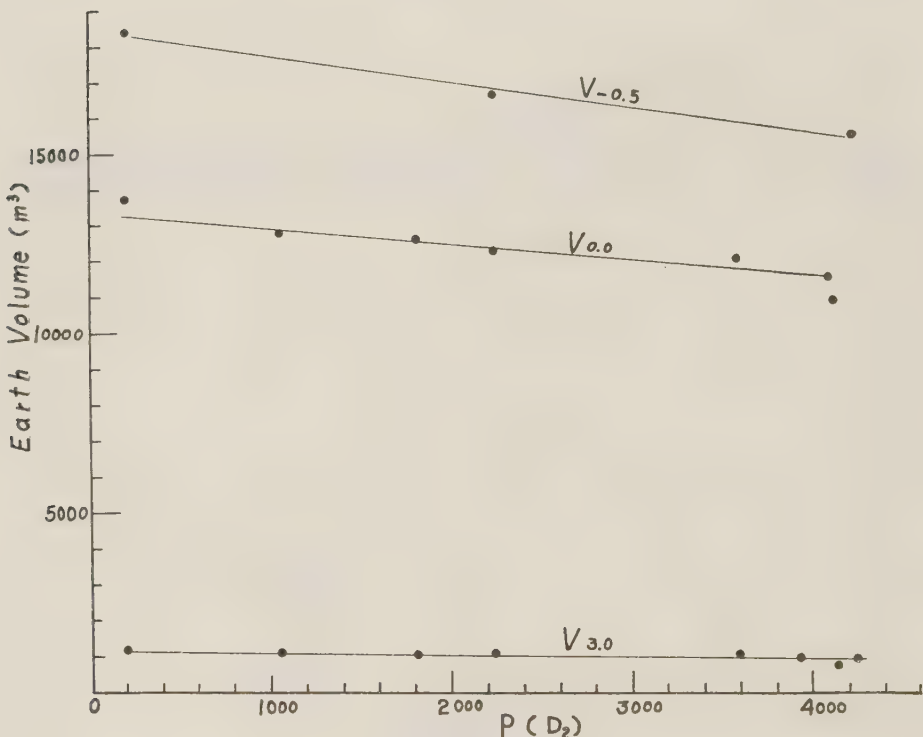


Fig. 19

Similarly the normal component is

$$\frac{E}{2} (1 + \cos 2r) = \frac{E}{2} (1 - \cos 2\beta). \quad \dots \dots \dots \quad (13)$$

The energy and power of waves will develop or continue during the time when the waves or the wind appears. So the total energy and work are estimated approximately by the products of energy and the power with the duration of wind. The result of these calculations are tabulated in Table 8.

The tendencies of these values during a year are fairly consistent as shown in Fig. 15 and Fig. 16.

The distributions of the total energy and work during a year are shown in Fig. 17 and Fig. 18.

Table-8-1 Parallel Component of Wave Energy and Power to the Coast (sea wind only) 1957-1958, at Matsusaki Coast.

Period	No. of days	Parallel Energy			Parallel Energy × Time								
		(+)	(+) Total	(-)	(-) Total	Alge. Sum	Total	(+)	(+) Total	(-)	(-) Total	Alge. Sum	Total
June 26-July 22	25	14,223	14,223	15,336	-1,113	-1,113	58,252	36,927	+21,325	-	-	-	+21,325
July 23	26	6,228	20,451	0,000	15,336	+6,228	72,541	0,000	+14,289	-	-	-	+35,614
July 24	27	—	—	—	—	—	—	—	—	—	—	—	—
July 25	28	—	—	—	—	—	—	—	—	—	—	—	—
July 26-July 28	31	0,716	21,167	0,000	—	—	0,716	73,257	0,000	—	—	—	+36,330
July 29-Aug. 14	48	—	—	—	—	—	—	—	—	—	—	—	—
Aug. 15	49	0,000	—	0,841	16,177	-0,841	—	—	—	—	—	—	+32,124
Aug. 16-Aug. 19	53	0,000	—	2,963	19,140	-2,963	+4,990	0,000	45,178	-4,206	+32,124	-4,045	+28,079
Aug. 20-Oct. 1	96	42,836	64,003	24,056	43,196	+18,780	+2,029	0,000	88,300	133,478	+102,490	+130,569	+48,451
Oct. 2-Oct. 31	126	55,908	119,911	2,529	45,725	+53,379	+20,807	190,790	264,047	136,907	+327,382	+327,382	+327,382
Nov. 1-Dec. 5	161	102,813	222,724	6,735	52,460	+96,078	+170,264	766,823	1361,281	18,300	154,907	+747,923	+1206,374
Dec. 6-Dec. 25	181	46,218	268,942	0,000	56,369	+46,218	+216,483	260,211	1621,492	0,000	—	+260,211	+1466,385
Dec. 26-Jan. 26	213	101,302	370,244	3,909	56,369	+97,393	+313,875	2189,677	568,185	161,288	+561,804	+2038,389	+2038,389
Jan. 27-Feb. 28	246	175,292	545,536	7,465	63,834	+167,827	+481,702	1949,050	3283,727	15,164	176,452	+1078,886	+3107,275
Mar. 1-Mar. 31	277	74,037	619,573	32,144	95,978	+41,883	+523,555	278,425	3562,152	136,307	312,759	+142,118	+329,393
Apr. 1-Apr. 16	293	29,300	648,873	22,248	118,226	+17,052	+580,647	97,074	3659,226	106,684	419,443	+9,610	+329,783
Apr. 17-May 7	314	34,881	683,754	19,179	137,405	+15,702	+546,349	164,581	3823,807	82,440	501,883	+82,141	+3321,924
May 8-June 3	341	21,083	704,817	53,048	180,453	-31,985	+514,364	52,306	3876,113	177,592	679,475	-125,286	+3196,638
June 4-June 30	368	14,734	719,551	13,869	204,322	+0,865	+515,229	50,564	33926,677	40,096	719,571	+10,468	+3207,106

A-1

A-2

Period	No. of days	Parallel Power			Parallel Power × Time								
		(+)	(+) Total	(-)	(-) Total	Alge. Sum	Total	(+)	(+) Total	(-)	(-) Total	Alge. Sum	Total
June 26-July 22	25	5,835	5,835	6,892	-1,057	-1,057	22,582	16,351	+6,231	-	-	-	+6,231
July 23	26	2,641	8,476	0,000	—	—	11,941	34,523	+11,941	-	-	-	+18,172
July 24	27	—	—	—	—	—	—	—	—	—	—	—	—
July 25	28	—	—	—	—	—	—	—	—	—	—	—	—
July 26-July 28	31	0,358	8,834	0,000	—	—	+1,942	0,358	—	—	—	—	+18,530
July 29-Aug. 14	48	—	—	0,396	7,288	-0,396	—	—	—	—	—	—	—
Aug. 15	49	0,000	—	0,354	8,642	-1,354	+1,546	0,000	2,376	-2,376	+16,154	+16,154	
Aug. 16-Aug. 19	53	0,000	—	9,865	18,507	+6,713	+0,192	0,000	1,865	-1,865	-1,865	-1,865	
Aug. 20-Oct. 1	96	16,578	25,412	9,865	18,507	+6,713	+6,905	66,922	101,803	31,890	52,482	+35,032	+49,321
Oct. 2-Oct. 31	126	17,747	43,159	1,198	19,705	+16,549	+23,454	200,444	1,198	53,680	+97,443	+146,764	+146,764
Nov. 1-Dec. 5	161	35,013	78,172	2,509	22,214	+32,504	+55,958	203,609	404,053	6,409	60,089	+197,200	+343,964
Dec. 6-Dec. 25	181	16,092	94,264	0,000	—	+16,092	+72,050	86,473	490,526	0,000	—	+86,473	+480,437
Dec. 26-Jan. 26	213	33,785	128,049	1,694	23,908	+12,031	+182,078	672,604	2,768	62,857	+69,747	+69,747	+69,747
Jan. 27-Feb. 28	246	55,459	183,785	3,078	26,986	+52,381	+164,522	310,571	983,175	6,151	69,008	+94,167	+94,167
Mar. 1-Mar. 31	277	26,092	209,600	11,151	38,137	+14,941	+171,463	93,943	107,118	12,159	111,167	+51,784	+965,248
Apr. 1-Apr. 16	293	9,713	219,313	8,078	46,215	+1,635	+173,038	31,048	1108,166	33,751	144,918	-2,703	+963,248
Apr. 17-May 7	314	12,068	231,321	6,796	53,011	+5,212	+178,310	51,341	1159,507	26,302	171,220	+25,039	+988,248
May 8-June 3	341	8,369	239,690	5,944	75,738	-8,414	+169,896	19,786	1179,303	92,061	263,281	-72,765	+916,022
June 4-June 30	368	5,506	245,196	5,944	-0,438	-0,438	+169,456	18,300	1197,603	15,395	+2,905	+2,905	+918,927

Remarks

+: To right facing to sea on the coast,

- : To left

*: To the west

B-1

The wave energy of one wave length against the coast line 1 meter is expressed in ton-meter by producing w/8 to the above energy values.

The wave power arriving at the coast line 1 meter is expressed in ton-meter per second by producing 1.249 w×60×60/16 to the power in the above table, where w is weight of sea water of unit volume or 1cu.m.

The total work done is expressed in ton-meter by producing 1.249 w×60×60/16 to the power in the above table, where w is weight of sea water of unit volume or 1cu.m.

B-2

**Table-8-2 Normal Component of Wave Energy and Power to the Coast
(sea wind only)**

Period	No. of days	Energy	Total	Energy x Time	Total	Power	Total	Power x Time	Total
June 26-July 22	25	82.659	82.659	446.346	446.346	34.270	34.270	173.423	173.423
July 23	26	22.135	104.794	72.305	518.651	8.685	42.955	27.370	200.793
July 24	27								
July 25	28								
July 26-July 28	31	1.247	106.041	1.247	519.898	0.624	43.579	0.624	201.417
July 29-Aug. 14	48								
Aug. 15	49	1.465	107.506	7.325	527.223	0.690	44.269	4.140	205.557
Aug. 16-Aug. 19	53	4.680	112.186	6.083	533.306	2.130	46.399	2.791	208.348
Aug. 20-Oct. 1	96	195.656	307.842	1066.474	1599.780	74.187	120.586	370.495	578.843
Oct. 2-Oct. 31	126	231.528	539.370	1699.629	3299.409	71.743	192.329	478.913	1057.756
Nov. 1-Dec. 5	161	293.210	832.580	1748.943	5048.352	100.242	292.571	582.641	1640.397
Dec. 6-Dec. 25	181	103.228	935.808	540.076	5588.428	36.272	328.843	178.813	1819.210
Dec. 26-Jan. 26	213	258.884	1194.692	1342.719	6931.147	86.526	415.369	428.623	2247.833
Jan. 27-Feb. 28	246	534.919	1729.611	3139.123	10070.270	169.299	584.668	942.195	3190.028
Mar. 1-Mar. 31	277	310.595	2040.206	1279.624	11349.894	102.775	687.443	404.438	3594.466
Apr. 1-Apr. 16	293	124.601	2164.807	521.791	11871.685	42.524	729.967	159.794	3754.260
Apr. 17-May 7	314	132.741	2297.548	544.713	12416.398	46.448	776.415	175.867	3930.127
May 8-June 3	341	157.264	2454.812	492.207	12909.605	54.909	831.324	211.842	4141.969
June 4-June 30	368	74.027	2528.839	259.085	13168.690	28.773	860.097	95.747	4237.716
		C-1		C-2		C-1		C-2	

Using these values, the relations between the volume of the alluvial cone in chapter 3 and the works are indicated in straight lines as shown in Fig. 19. These values are as follows:

$P(D_2)$	V_0 m	V above -0.5 m	V above 3.0 m
206	13732 cu.m.	18353 cu.m.	1073 cu.m.
1058	12798	—	1115
1819	12571	—	1079
2248	12267	16636	1052
3594	12038	—	1032
3930	11502	—	958
4141	10993	—	730
4238	11439	15480	949

These relations will be able to express by the following formula

$$V = a - bP \quad \dots \dots \dots \quad (14)$$

where P is the work done per 1 meter of coast line.

The coefficient b calculated by the least square method using the values of the normal component of work $P(D_2)$ and volume of cone on the upper table are as follows.

For V_0 , $b = 0.59618$

$V - 0.5$, $b = 0.71313$

V 3.0, $b = 0.05742$

It seems that the decrease of the cone volume above +3.0 m is the result of the erosion by winds and rains and it is not proper to express by the wave energy or power. Notwithstanding the relation is almost a straight line, because it will be eroded by the winds which produce the waves. This idea is certified by surface conditions of the cone and the deposit on the summit of the cone by the wind. Therefore the volume of erosion at the part from -0.5 m to +3.0 m is

This is the total volume along the coast line 170 m, so that the volume per 1 m of coast line is

$$V_e = (0.71313 - 0.05742)P/170 = 0.003857 P$$

At the part from 0.0 m to +3.0 m, it is

$$b = (0.54618 - 0.05742) / 170 = 0.48876 / 170 = 0.002875$$

That is to say, the erosion volume at the part from 0.0 m to 3.0 m was so larger than that on the part from 0.5 m to 0.0 m, and the ratio is as follows:

$$0.002875/0.000982 = 2.9 \text{ times.}$$

Moreover the relation between the cone volume and the parallel components of the wave energy and work are

$P(+B_2)$	$P(\pm B_2)$	$P(-B_2)$	V 0.0 m
35	+18.5	-21	13732 cu.m.
200	+147	-54	12798
491	+430	-60	12571
673	+609	-63	12267
1077	+966	-111	12038
1160	+988	-170	11502
1179	+916	-263	10993
1197	+918	-279	11439

◦ : sign on the figure

$$b = 2.05783$$

$$b = 1.99083$$

$b = 7.875829$: Coefficient of formula (14)

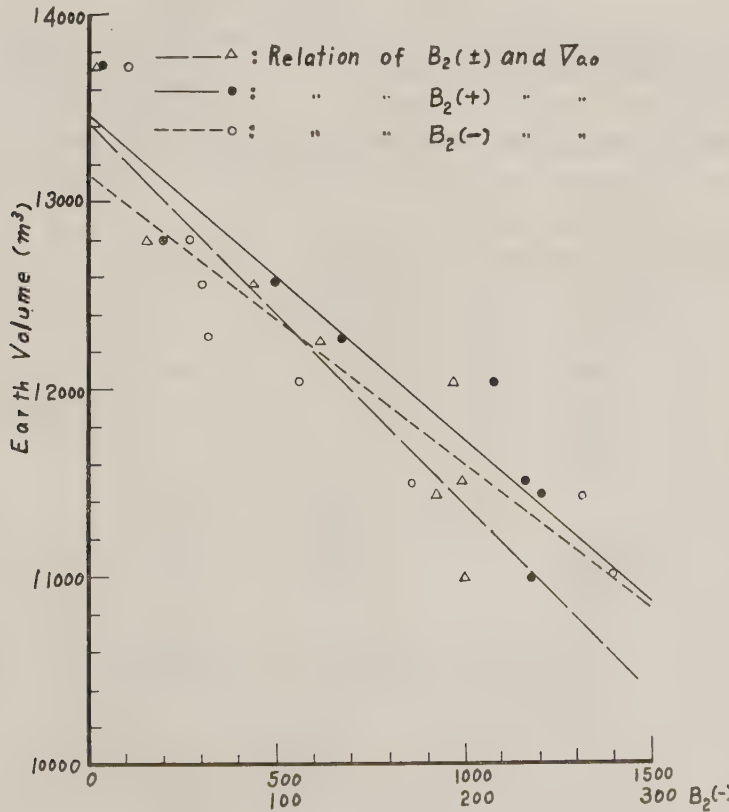


Fig. 20

The volume of coast erosion will be transported immediately to the same direction of wave energy as the littoral drift. But it will be easily considered that the erosion will be more decrease, the more straight the coast line is. In such case the volume of littoral drift will depend upon the amount of supply to the coast.

V. CONCLUSION.

In this study, the disastrous erosions on the mountain side by the flood of rivers which are the supply sources of littoral drift and the accompanied development and erosions of the alluvial cone are interpreted by the observation on the erosion of the alluvial cone arised by the Typhoon No. 5, June 1957. Moreover the actual relations between the volume of erosion at the erosive coast topography and the arriving wave energy and work are verified principally in this observation.

This study has been continued as a part of the cooperative research between the Water Works Laboratory and Soil Mechanics Laboratory, Civil Engineering Institute, Defence Academy concerning the littoral drift, coast geology and the coast water quality. The cooperators of this observation are Assist Prof. Yoshinori Odaira, Lecturer Masanori Naritomi, Assist. Masayuki Ikeuchi, Akira Koyama, Yasunao Kobayashi. The vehicles and boats of Administration Section, Defence Academy and helicopter of Tateyama Air Corps, Maritime Self Defence Force of Japan were utilized for this investigation. The expenditure of this study was partly supported by Science Experiment Research Fund of the Ministry of Education. The author appreciates heartily here to all of them.

REFERENCE LITERATURES

- (1) Mashima Yasuo; The study on the littoral drift and longshore current, Proc. of 2nd Conference Coastal Engineering in Japan, Nov. 1955. Japan Society of Civil Engineers.
- (2) Johnson, J.W.; Sand Transport by littoral current, Proc. of Fifth Hydraulic Conference, June 1952. State University of Iowa Studies Engineering Bulletin 34 No. 426.

THE EFFECT AND DAMAGE OF SUBMERGED BREAKWATER IN NIIGATA COAST

Naobumi Shiraishi*

Atsushi Numata*

Naoki Hase*

I. INTRODUCTION

The beach erosion is a very serious problem in Niigata Coast where the shoreline receded more than 300 m during the past fifty years. This tendency was accelerated after the completion of flood way of Shinano River which caused the remarkable decrease of sediment supply to this coast. The submerged breakwater was constructed for the purpose of protecting this eroded coast, about 500 m offshore from the shoreline. The height of this breakwaters was decided upon from the following points of view.

(a) It must have the sufficient height to prevent the incident wave and transmit as small portion of wave energy toward the shoreline as allowable. The transmitted wave may cause longshore or rip-currents inside the breakwater and prevent depositing of sand near the shoreline.

(b) It must not be so high that the wave force on the structure is dangerous and the scouring on the foot of the structure may be remarkable. After the discussion on these points, the crest level of the breakwater was determined near the mean sea level. In this paper the effect of breakwater on the wave transmission and on the deposit of sand were discussed by means of the results of field observations which were carried on by the Office of Shinano River Works, Niigata Prefecture.

II. EFFECTS OF THE SUBMERGED BREAKWATER ON WAVE TRANSMISSION

The main function of the submerged breakwater is to limit the transmission of wave energy into the beach area and to prevent the outflow of sand due to back wash action of sea water. Fig. 1 shows the general map of the western coast of Niigata city, locations of the observation stations and the arrangements of groins and submerged breakwaters. The wave was observed at the stations in the beach protected by submerged breakwater (say beach A, station I and II) and in the open beach (say beach B, station III). Each station is provided with posts and track cables for measurement of waves and transportation of measuring apparatuses. The

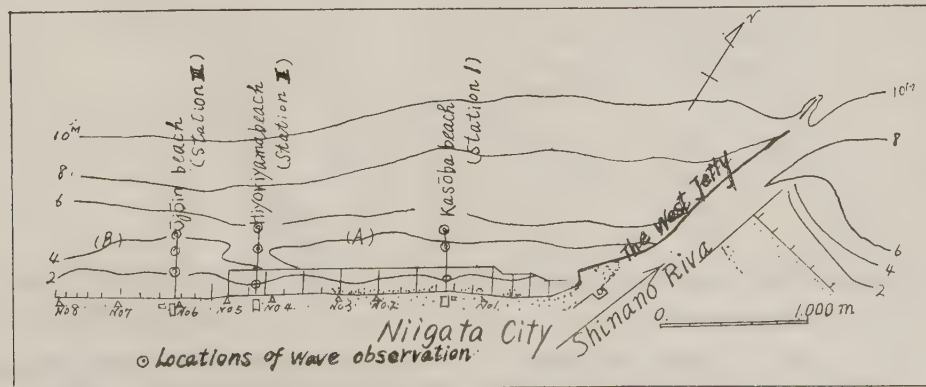


Fig. 1 Locations for wave observation.

* Ministry of Transportation, Niigata Harbor Construction Office.

unit : m

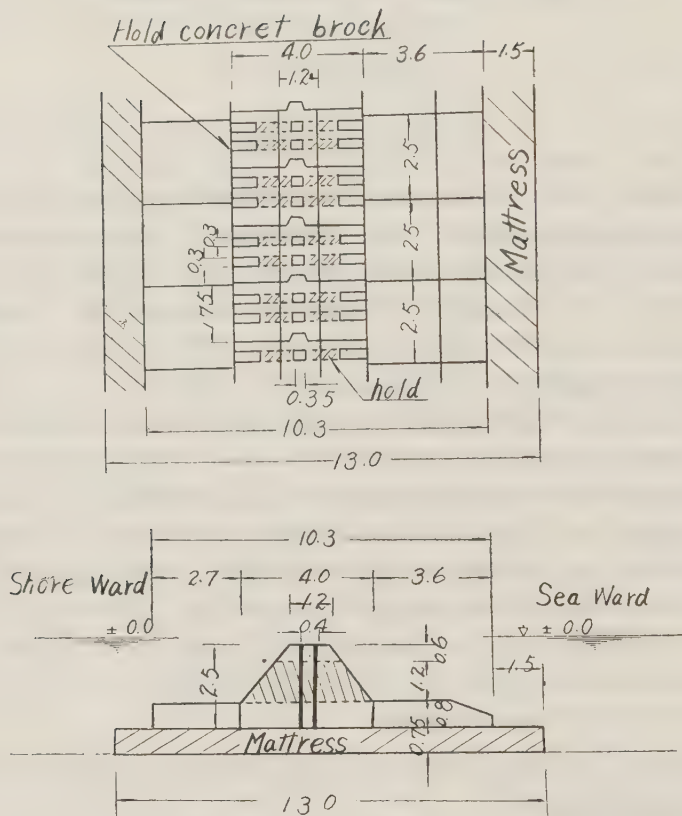


Fig. 2 Construction of submerged breakwater by holed concrete brock.

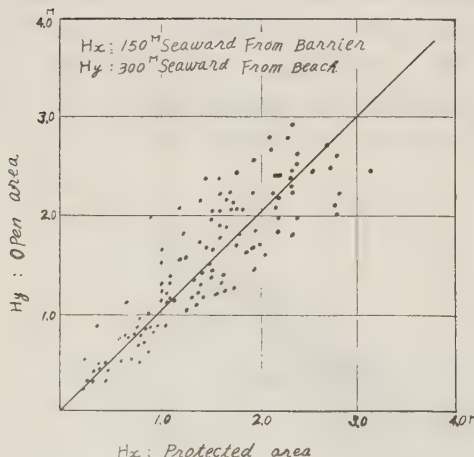


Fig. 3 Seaward wave height relationship in both protected and open areas.

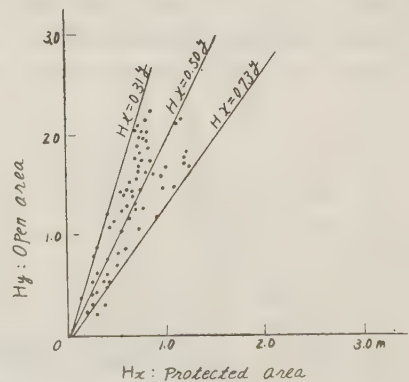


Fig. 4 Shoreward wave height relationship in both protected and open areas.

a) Open area

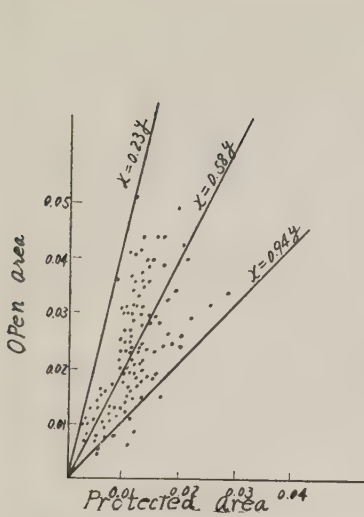


Fig. 5 Comparison of wave steepness at the protected and open areas.

[H_i : Wave Height of 150m Sea ward
 H_o : Wave Height of 300m Sea ward]

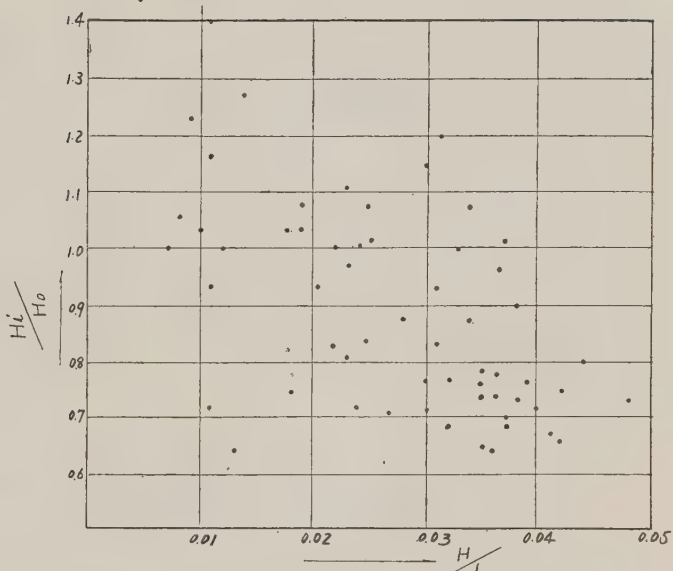


Fig. 6 (a) Relation between the rate of wave height decrease and wave steepness.

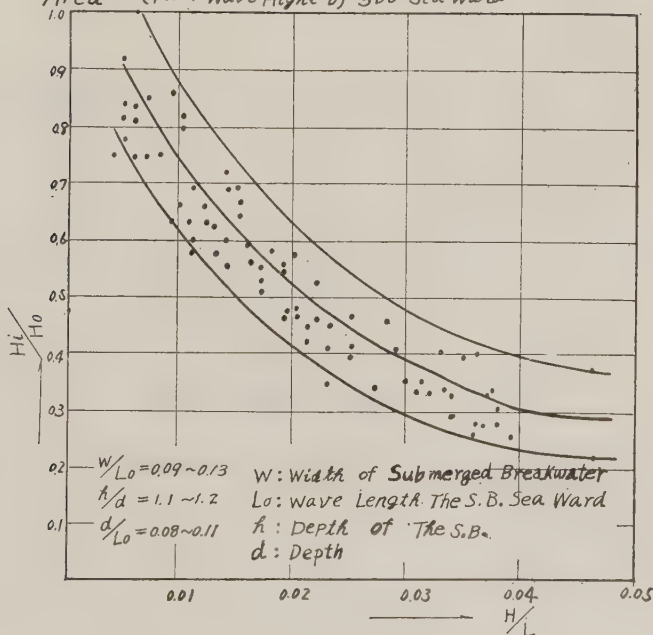
b) Protected Area. [H_i : Wave Height of 150m Sea ward
 H_o : Wave Height of 300m Sea ward]

Fig. 6 (b)

wave data used in this paper were obtained visual observation made three times a day and averaged for five minutes each time. Fig. 2 is a cross-sectional view of the submerged breakwater constructed in this coast.

The correlation between the wave heights at 150 m seaward from the breakwater (at the station I) and that at 300 m off the unprotected beach (at the station III) is plotted in Fig.

3. This figure shows that the correlation may be considered as nearly perfect. While the wave heights inside the breakwater at the station I are 30-70% of those 150 m off the unprotected beach at the station III as shown in Fig. 4, the wave profiles, i.e., the steepness of waves observed inside the breakwater are less than 0.03 and they are 10-80% of those observed 150 m off the unprotected beach (Fig. 5). The critical steepness of waves observed in this coast has been given as 0.017 according to the data obtained by the Shinano River Work Office.

The percentage of occurrence of waves steeper than 0.017 was 5.8 for the protected water and 68 for the unprotected water. These results may give a favorable answer for wave damping efficiency of submerged breakwaters built in this coast.

Fig. 6 shows the relationship between the steepness of offshore wave and the rate of decrease in wave height. For the open beach there seems to be no distinct relation, while for the protected area we can see a tendency that the rate of decrease in wave height rises with the steepness of wave.

III. CHANGES OF BOTTOM TOPOGRAPHIES DUE TO SUBMERGED BREAKWATER

The changes in wave elements mentioned above must affect the bottom topographies near the shoreline. It is generally believed that the bottom of a beach keeps a certain profil for a certain grain size of sediment under the effect of wave characters. Any change in wave elements must cause a change of bottom profile.

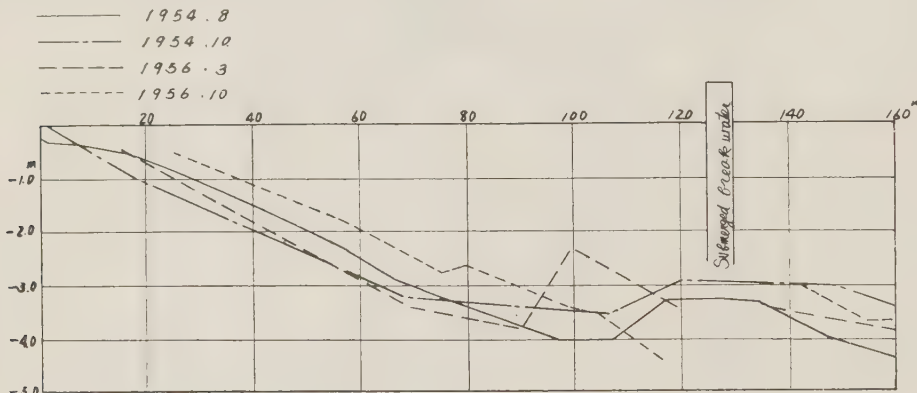


Fig. 7 Change of bottom profile

Fig. 7 shows the comparison of bottom profiles before and after the construction of submerged breakwater (the breakwater now in consideration was built in 1955). It may be seen from this figure that the shore profile in 1956 takes a little steeper slope than that in 1954 and that the shoreline advanced seaward. Further we can compare the nearshore slopes in the protected and open areas from the sounding data procured on the same day. The results are shown in Fig. 8, which also shows that the slope in the protected area is steeper than the others.

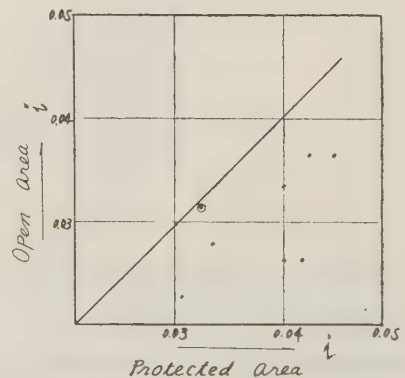


Fig. 8 Comparison of the bottom slopes in between open and protected areas.

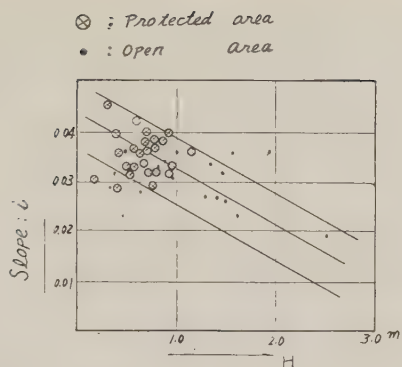


Fig. 9 Relation between the bottom slope and the wave height.

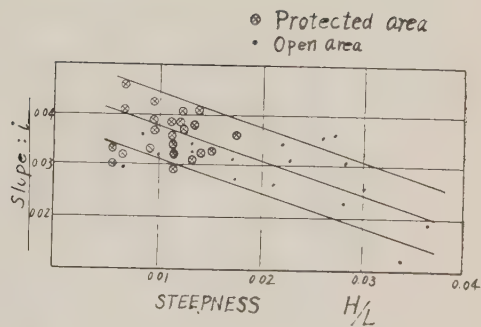


Fig. 10 Relation between the bottom slope and the wave steepness.

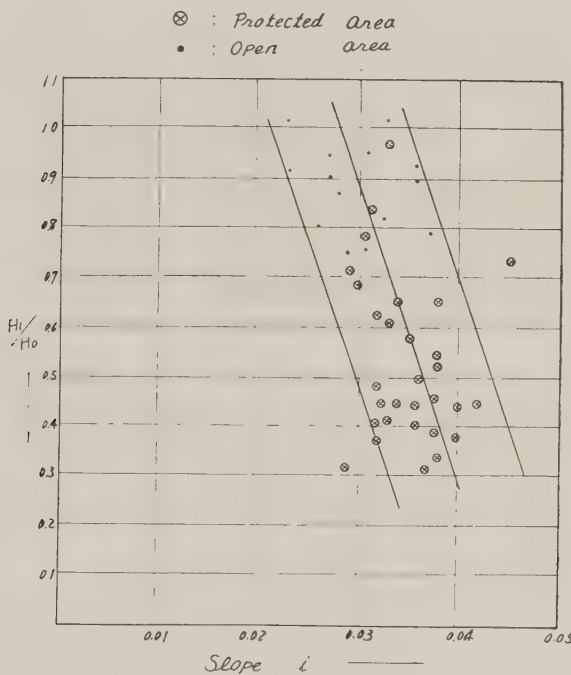
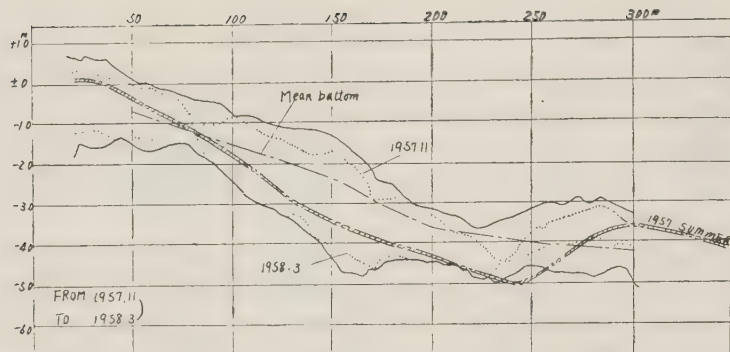


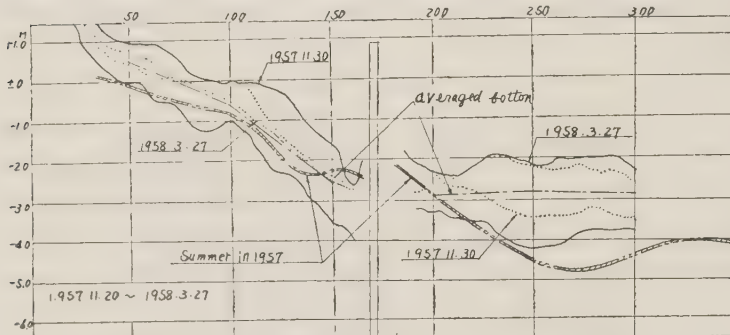
Fig. 11 Relation between the rate of wave height decrease and the bottom slope

Figs. 9, 10 and 11 show the relationships of bottom slope respectively with steepness, wave heights and decreasing rate of wave heights. They were examined for the purpose of finding a definite relation between the wave characteristics and the bottom slope of a beach shallow than the final breaking depth (that is 5.0–6.0 m in this coast). The observed data are still not sufficient to give a definite conclusion. It may, however, be conceivable that the bottom slope decreases with increase of wave height or steepness.

In this region the strong wind and violent wave predominate in winter season. Figs. 12 (a) and 12 (b) show the bottom profiles taken in some winter seasons for the open and protected areas respectively. The range of the change in bottom elevation inside the submerged breakwater is 1.1 m in average, while that outside the breakwater and that in the open area are much greater. This fact manifests that the submerged breakwater built here was sufficiently effective for the purpose of protecting the beach.



a) Open area.



b) Protected area.

Fig. 12 Diagram of the change of water depth.

In the open area maximum range of the change in bottom elevation took place at about 150 m off the shore line and its amount was 3.2 m. In the protected area, however, the maximum range was observed at about 50 m inshore of the breakwater and its amount was nearly half of that for the open area. It must be noticed that the location of the maximum range in the open area approximately coincides with the final breaker zone where submarine ridges always move according to the actions of various waves.

Table 1 gives the increase (+) and decrease (-) of the volume of bottom sand for some areas indicated in Fig. 13. The decreasing tendency inside the breakwater has gradually disappeared since 1952 when the breakwater was elongated and recently the increasing ten-

Table 1 Increase and decrease of bottom sand (m^3)

Area	Year	1951	1952	1955	1956	1957
A	2+3	-125000	- 72000	- 25951	- 4592	+71708
	2	- 60000	- 30000	- 6831	+ 7357	+69879
	3	- 65000	- 42000	- 19120	- 11949	+ 1829
A	4	- 6000	- 33000	(- 91825)	(+170700)	
B	4	+ 10000	+ 66000			
B	2+3	+371000	-130000	+151046	+344728	
	2	+241000	- 94000	+190850	+129680	
	3	+130000	- 36000	- 39804	+215048	

- : Erosion, + : Deposit, () : Sum of A and B area.

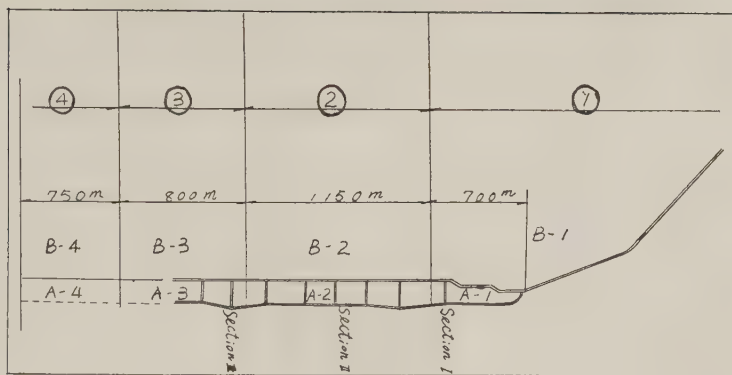


Fig. 13

dency is noticed. In the areas A-1 and B-1, there is a remarkable effect of dredged sand supplied across the jetty from the river estuary amounting to 500-800 thousand m³ per year. Such artificially supplied sand seems to affect also the area outside the breakwater. Beside that, there must be the influence of subsidence of this district. It complicates the problem even further, but any discussion concerning subsidence is beyond the scope of this paper.

IV. ADVANCE AND RETREAT OF SHORELINE

The recession of shoreline is the most vivid evidence of beach erosion. Fig. 14 shows the rate of recession of shoreline along this coast before and after the construction of submerged

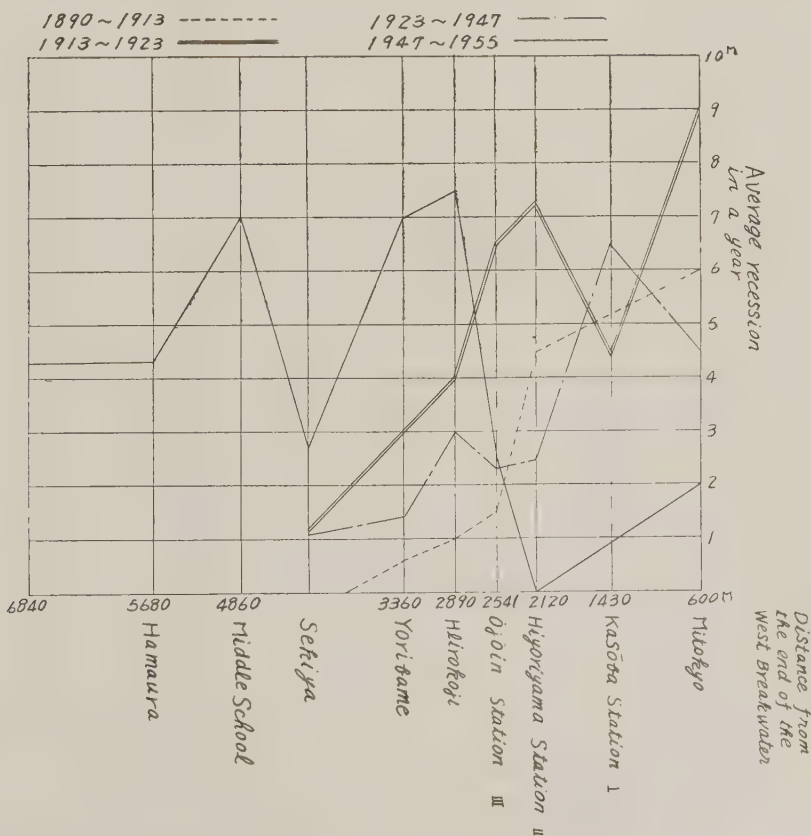


Fig. 14 Annual average rate of recession of the shore line.

Table 2 Variation of the shore line on the western coast

Area	No	1905 to 1947	1947 to 1954	1954 to 1955	1955 to 1956	1956 to 1957	Total
M I T O K Y O	1	-295	+10	-25	-10	+28	-297
	2	-320	+25	-35	-10	+33	-217
	3	-320	+ 5	-15	- 5	+33	-302
	4	-320	- 5	- 5	0	+12	-318
	5	-330	0	-15	0	+ 6	-339
	6	-280	-20	-20	+15	+ 2	-307
	7	-280	-25	-20	+30	-14	-281
	8	-290	-30	-15	+40	-15	-310
	9	-300	-20	-30	+30	- 9	-329
	10	-270	-25	-25	+45	-25	-300
	11	-250	-10	-15	+30	-18	-263
	12	-250	-15	-15	+10	-14	-284
	13	-220	-10	-25	+10	-15	-260
H I Y O R I Y A M A	14	-210	- 5	-25	+10	-24	-254
	15	-205	0	-20	+ 5	-15	-235
	16	-200	-15	-35	+ 5	0	-245
	17	-190	- 5	-15	- 5	+ 3	-212
	18	-180	-10	-25	0	- 8	-223
	19	-170	-10	-30	- 5	- 4	-219
	20	-155	-10	-15	- 5	- 6	-191
	21	-140	-10	-30	0	-11	-191
	22	-125	-10	-35	+ 5	+12	-153
	23	-125	-30	-25	+ 5	+15	-160
	24	-135	-45	-15	+ 5	- 7	-197
	25	-145	-50	-10	0	-10	-215
Y O R I I	26	-155	-45	- 5	-10	- 9	-224
	27	-135	-45	0	-15	-10	-205
	28	-110	-50	- 5	-20	- 2	-187
	29	- 90	-40	- 5	-20	+ 3	-152
	30	- 80	-35	-15	0	- 4	-134
	31		-30	-10	+10	-13	-43
	32		-25	-25	0	-17	-67
	33		-25	-30	+15	-12	-82
	34		-20	-20	+ 5	-10	-45
	35		-10	-40	- 5	-20	-65
	36		-20	-25	0	-32	-77
	37		-35	-10	-20	-32	-97
	38		-25	0	-30	-15	-70
	39		-15	0	-30	0	-45
	40		-10	-15	-20	+ 1	-44
S E K I Y A	41		-15	-15	-25	- 3	-58
	42		-15	0	-30	-11	-56
	43		-25	0	-20	-21	-66
	44		-30	-10	-15	-16	-71
	45		-20	+ 5	-30	- 1	-45
	46		-10	- 5	-30	+ 2	-43
	47			-20	-10	- 9	-39
	48			- 5	-20	- 5	-30
	49			+20	-40	- 8	-28
	50			+15	-35	+ 2	-18
	51			0	-20	+ 8	-12
	52			+ 5	-30	+ 6	-19
	53			+ 5	-20	- 8	-23
	54			0	-15	-17	-32
	55			0	0	-18	-18
	56			+10	0	-13	- 3
	57			+10	-20	- 6	-16
	58			+15	-20	- 5	-10
	59			+15	-15	+ 7	+ 7
	60			+20	-25	+ 8	+ 3
	61			+25	-20	-11	- 6
	62			+20	-25	- 8	-13
	63			+20	-35	0	-15
	64			+20	-40	-16	-36
	65			+15	-30	-35	-50
	66			+15	-15	-25	-25
	67			+10	-10	-25	- 5
	68			+15	-25	-22	-32
	69			+ 5	-10	-27	-32

note : + : advance of shore line

- : recede of shore line

Table 3 Slumping condition of

Type of S.B.	NO.	Year of Const.	Length (in m.)	Crown Height just after Const. (in m.)	Crown Height (in m.)			
					1954	1955	1956	1957
T-shaped	1	1946		—	—	—	+0.81	—
Hold block	2	1955	75.7	—	—	+0.64	-0.39	—
T-shaped	3	1947		—	—	—	+0.67	—
Hold block	4	1955	72.5	—	—	+0.72	-0.54	—
T-shaped	5	1949		planed (+0.90)	—	—	+0.28	—
Hold block	6	1955	58	—	—	+0.72	+0.62	—
T-shaped	7	1949		planed (+0.50)	—	—	+0.27	—
Hold block	8	1953	78	-0.42	—	—	-1.42	—
T-shaped	9	1948		planed (+0.50)	—	—	+0.37	—
Wire cylinder	10	1950	232	-0.18	-1.52 (-1.27)	—	(-2.20)	—
Rubble-mound		1951	12	-0.27	-0.22 (-0.57)	—	(-1.06)	—
Hold block	11	1955	(200)	—	—	+0.54	+0.01 (+0.06)	(-0.12)
Hold block	12	1951	80	-0.22	-0.70	+0.94	-1.04	-0.10
Cellular block	13	1951	145	-0.45	-0.66	-1.25	-1.38 (-1.39)	(-1.61)
Hold block	14	1953	220	-0.04	-0.28 (-1.27)	(-0.66)	(-0.88)	(-1.02)
L-shaped block	15	1953	220	-0.73	-0.13	-0.33	-0.43	-0.61
L-shaped block	16	1954	128	-0.15	—	-0.12	-0.23	-1.11
Hold block	17	1952	108	planed (±0.00)	-0.86	-1.62 (-1.28)	(-1.91)	(-2.27)
Hold block	17	1952	92	planed (±0.00)	-1.60	-1.86 (-1.78)	(-2.00) (-1.50)	(-2.02)
Hold block	18	1954	112	-0.95	—	+0.61	+0.31 (+0.37)	(+0.05)
Hold block	19	1955	220	—	—	+0.55	+0.31 (+0.32)	(+0.20)

breakwater. From this figure it is recognized that the point of most remarkable recession gradually moves to the west with the progress of coast protection works. The recession of beach was surveyed at 69 sections located at 100 m intervals along the beach starting from the root of the west jetty of Shinano River. Table 2 gives the rate of annual recession at each station. Since completion of the breakwater and beach protection works (1955), the shoreline in the protected area has been nearly stable. While in the coast extending to the west which is still left uncared, the amount of recession increased to as large as 7-16 m per year.

Proceeding to further details, in the area of sections 1-6 where the dredged sand has been supplied from the river any remarkable deposit of sand has not been observed. The reason is presumably due to the slump of the breakwater which amounts to 1.0-2.0 m and resulting reduction in the wave damping function. In the areas of sections 7-8 and 14-19 the breakwater was covered by tetrapods to the height of 0.5 m above the sea level in 1957. Table 2 shows the advance of shoreline in these areas and the erosion in other areas.

V. SLUMPING OF SUBMERGED BREAKWATER

The protection works in this coast came into practise after the big coast damage in 1945. In the begining of these works some sorts of groins or submerged breakwater were executed

the submerged breakwater

		Sinking (in m.)		
just after Const. to 1954	1954 to 1955	1955 to 1956	1956 to 1957	Total
—	—	—	—	—
—	—	* -1.03	—	—
—	—	—	—	—
—	—	* -1.32	—	—
—	—	—	—	—
—	—	-0.10	—	—
—	—	just after const. to 1956 -0.23	—	—
—	—	just after const. to 1956 -1.10	—	—
—	—	just after const. to 1956 -0.13	—	—
* -1.70	—	1954 to 1956 (-0.93)	—	-2.38
-0.49	—	1954 to 1956 (-0.49)	—	-0.98
—	—	-0.53	(-0.18)	-0.66
* -0.9 _{cs}	-0.24	-0.10	-0.06	-1.32
* -1.11	-0.59	-0.13	(-0.22)	-2.05
-0.32	(-0.39)	(-0.22)	(-0.14)	-1.06 (0 to -3.0)
* -0.86	-0.20	-0.10	-0.18	-1.34
—	-0.27	-0.11	-0.88	-1.26
—	-0.76	(-0.63)	(-0.36)	-1.41
—	-0.26	(-0.22)	(-0.52)	-0.42
—	-0.34	-0.30	(-0.32)	-0.90
—	—	-0.24	(-0.12)	-0.36

in trial in the eastern part of the beach, and after 1952 the submerged breakwater of special concrete blocks (holed blocks) was built in a long stretch to the west from the station II. The whole construction of nearly 2.3 km length was completed in 1955.

Though the effect of the submerged breakwater seems to be satisfactory, the body of the breakwater itself began to slump into the bed sand. Table 3 shows the progressing rates of slump of many sorts of construction which were used for the body of breakwater. From this table we may estimate the features of slump for each sort of construction. For example, L-type block breakwater which was built in 1953-1954 shows 0.45 m as the annual mean slump and 0.90 m as maximum rate. On the other hand, the special block (holed block) breakwater which stretches over a thousand meters show 0.38 m as the mean annual slump. The amounts of slump mentioned above include the depression by the scattering of block under the wave action.

VI. CONCLUSION

(1) The height and the steepness of waves transmitted over the submerged breakwater are 30-70% and 10-80% of those of incident waves respectively. The frequency of occurrence of waves steeper than the critical wave steepness of 0.017, the value of which was observed in this area, was 6% for the protected area.

(2) In the protected area, the rate of decrease of wave height increases with the increase of steepness of incident waves.

(3) The bed slope in surf zone becomes steeper with the decrease of height and steepness of waves. At the same time the shoreline advances and the range of the change of bed elevation decreases.

(4) After the completion of breakwater, the remarkable recession of shoreline and bed erosion disappeared in the protected area. While in the west of this area, the beach erosion became remarkable. The elevation of breakwater crown shows the visible effect of sand deposit in the area protected by it.

(5) Any kind of construction practised as breakwater in this coast is not free from slump. Among them the porous construction with deep pile foundation shows the best resistance.

As mentioned above, the submerged breakwater may be considered as an effective work against beach erosion, while its maintenance cost is very high for the inevitable phenomena of scouring and slumping. These problems are still left for further researches.

A STUDY ON BEACH EROSION AT THE SHELTERED BEACHES OF KATASE AND KAMAKURA, JAPAN

*Masashi Homma**
*Kiyoshi Horikawa***
*Choule Sonu****

I. INTRODUCTION

This paper presents the results of the investigation on the causes of beach erosion and related coastal processes occurring at the beaches of Katase and Kamakura, Japan. These beaches are located at the northeast corner of the Sagami bay, partly sheltered from the Pacific Ocean. (Fig. 1 and the photographs in the first page)

The investigation was carried out by the authors under auspices of Kanagawa Prefecture in two separate operations, the first one from September, 1956, to February, 1957, and the next one from June, 1957, to January, 1958.

At the onset of the investigation, the authors were greatly harassed by the lack of the records explaining the history of the highly publicized erosion at these beaches. As far as the progress of erosion was concerned, the only information available was, as invariably common to almost any urban coast subjected to erosion, the claim that the rate of erosion was likely to have been accelerated in recent years. However, it was doubtful whether it tells the true story, or it merely looked that way because the erosion was not clearly visible until it began to threaten the coastal establishments recently or because the recent boom of beach recreation including construction of a beach drive way had crowded the beach area. No reasonably quantitative data were available concerning winds, waves, littoral currents and other important factors, except for a brief geomorphological study made by the geologists of the Hydrographic Office¹⁾²⁾.

Accordingly, we were bound to develop our own method of investigation, which consists essentially of : (1) exploring whatever library data available on the investigation area from various approaches including geography, geology, oceanography and meteorology, (2) interviewing the elder inhabitants and local fishermen, and (3) conducting in parallel a series of field investigation as to winds, waves, littoral currents and drifts, beach materials in and out of the investigation area. The sounding data were provided by R. Komukai of the Japan Hydrographic Office, who was in charge of bottom deposits and seasonal soundings as parts of the entire project of investigation.

Another difficulty encountered was the fact that the field investigation during the summer season was practically impossible because of the swimming crowd on the beaches. Therefore our study failed to cover the effects of typhoon storms.

Nevertheless, the results of our investigation seem to have achieved some degree of success in exposing the predominant factors which have been contributing to the persisting erosion on these beaches, namely crustal action, deterioration of the sources of supply, and artificial barriers constructed along the path of sediment transport. They have also shed light on the characteristics of a beach process found along a sheltered bay on the Pacific Coast of Japan.

*Dr. of Engr., Professor University of Tokyo

**Assistant Professor University of Tokyo

***M.S. Postgraduate Student, University of Tokyo

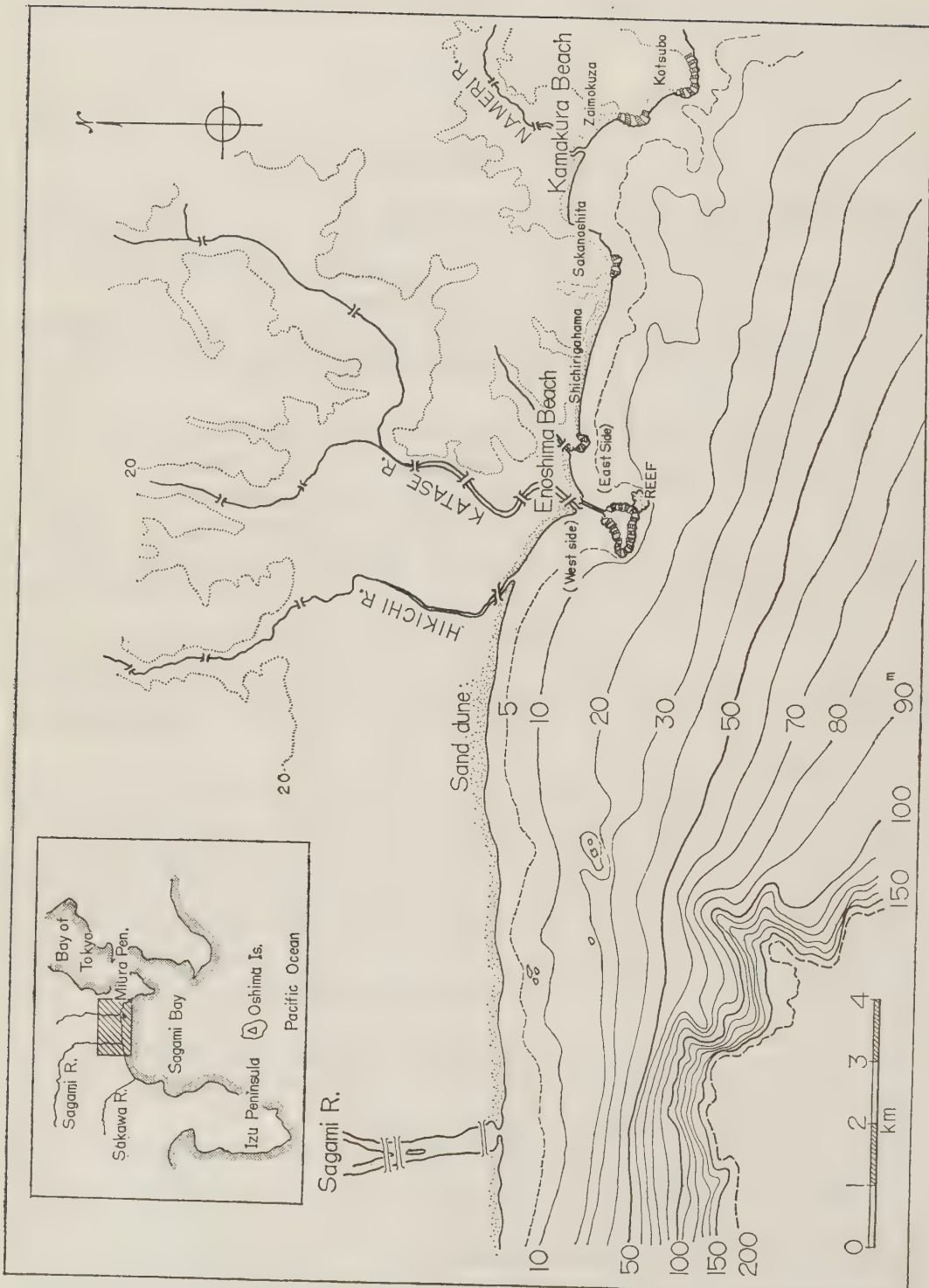


Fig. 1 Location of survey area.

II. DESCRIPTION OF THE AREA

1. Shoreline configuration

Our erosion areas are the beaches of Katase East and Kamakura. They both consist of a fairly narrow strip of sand confined at both ends either by promontories or a tombolo. The beach of Kamakura is approximately 2 km long; located at a deep recess between two promontories, Points Inamura and Kotubo, it is partly sheltered from the westerly gales. The beach of Katase East is approximately 0.9 km long, and here again Point Koyurugi and the Katase tombolo mark the ends of the shoreline. The sheltering effect is even better here due to the existence of the Enoshima island.

It is said that our beaches have been retreating as a whole, and that the most severe erosion has been occurring at the east end of Katase East and the west end of Kamakura. A general regression of shoreline has also been recognized at the Shichiri beach which lies between our beaches. On the other hand, it is also said that there has been general accretion of sand at the beach of Katase West. Further west, the shoreline is an almost straight sand beach extending approximately 10 km as far as the Sagami river. It was revealed by our interviews with the local fishermen that there has been a steady regression of the shoreline between Katase and the Sagami river mouth. It must be added that in the east of Kamakura the shoreline is a succession of small pocket beaches separated from each other by promontories.

During 1945 to 48, a two-lane beach drive way was constructed along the beaches of Katase, Shichiri and Kamakura, separating the dunes from beach zones completely.

2. Fetches

Our beaches are located at the northeastern corner of the Sagami bay, with the fetches exposed only toward the west-south quadrant. The length of the westward fetch is limited

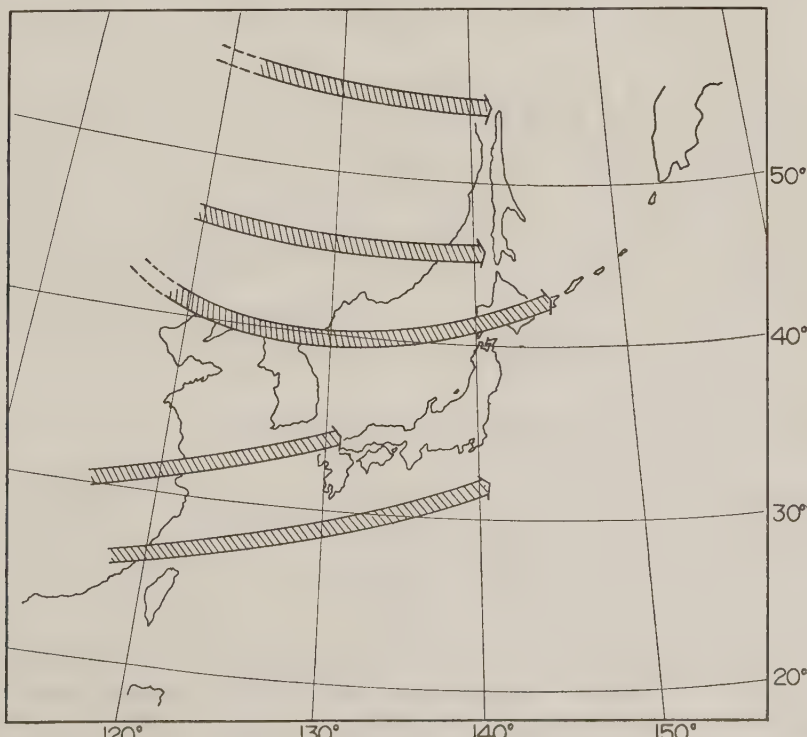


Fig. 2 Main low pressure pathes.

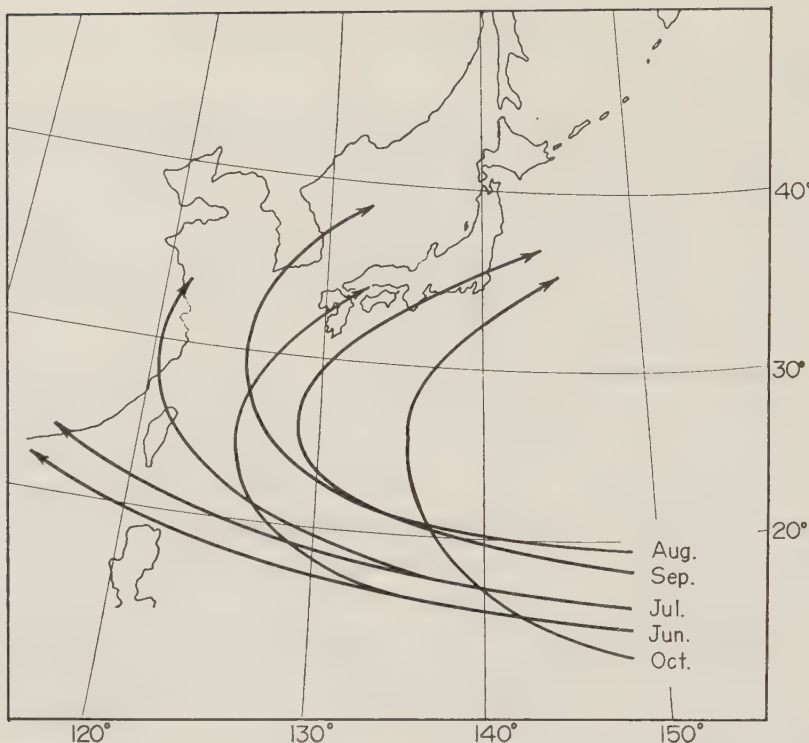


Fig. 3 Main paths of typhoon.

by the Izu peninsula, and over this fetch approximately 40 km long the strong westerly gales prevail during winter.

Toward south the bay continues to the Pacific Ocean beyond two straits around the Oshima island. The effect of Oshima as a fetch limiting factor is not yet to be determined conclusively. However, it is most likely that the swells generated by the migrating cyclones, (Fig. 2), or typhoons in the Pacific Ocean (Fig. 3), will arrive at our beaches all but unhindered. It is important to note that the Sagami bay is frequently hit by typhoon storms causing storm surges as well as formidable waves. For instance, it is reported that the wave plus surge height sent in by Typhoon Kitty, 1949, reached as high as 6 to 7 m above the mean sea level at the western part of the bay coast. However, the water in the vicinity of our beaches is generally calm for the rest of the year, and frequently gentle waves approximately 30 cm high break immediately at the shoreline.

3. Geological background

The Sagami river has developed a large alluvial delta which is bordered in the south by the shoreline extending from the river mouth to the Katase beach and in the north by a bluff line running northwest to southeast and ending at Point Koyurugi near Katase. A group of sand dunes cover the shoreline regions and the base of the bluff line, and at Katase East where these lines meet we find the sand dunes just behind the beach.

Characteristics of the sand dunes, outlet orientation of tributaries and size distribution of beach materials seem to suggest a predominant eastward migration of materials both as eolian and littoral processes. One of the geological studies on the characteristics of the sand dunes³⁾ indicate that they were formed by sand materials blown toward east and slightly inland. Still today, though the rate must have lessened due to recent development of

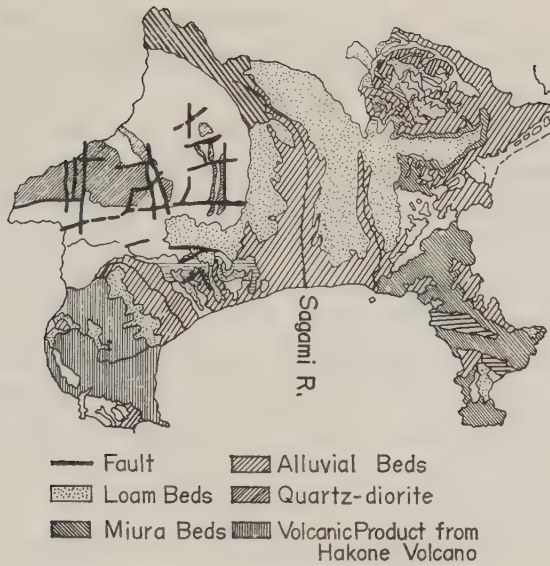


Fig. 4 Geological structure of Kanagawa Prefecture. (after)

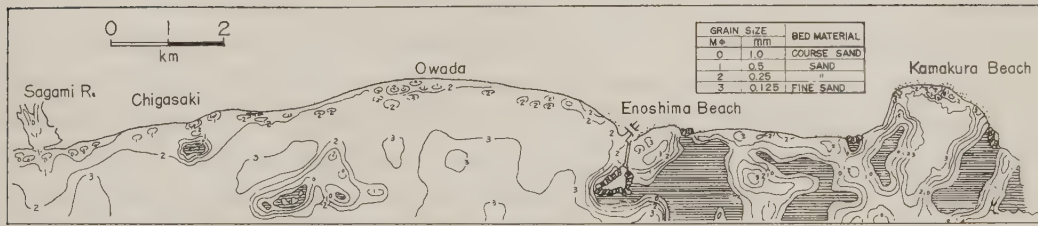


Fig. 5 Distribution of medium diameter of bed material (in 1956)
(after Hydrographic Office in Japan).

vegetation works and population increase, we observe a strong eolian movement of dune sand toward east during the gale season in winter. Along the shoreline, on the other hand, the outlet of the Hikichi gully as well as the Sagami river mouth tends to deviate toward east. This fact is interpreted as suggesting that there is a net eastward migration of materials along the littoral zone. According to the results of the recent investigation by the Hydrographic Office, there is a strong evidence that the average grain size of the beach materials decreases progressively toward east.

These facts undoubtedly combine to show that the Sagami river is the principal source of supply to the beaches lying between the river mouth and the Katase area.

Apparently, the beach of Katase is a part of the delta formed by the Katase gully. However, a review on the geological background will confirm the predominant role of the Sagami river as the principal and primary source of supply to these beaches. In fact, the gully is too small to erode any appreciable amount of materials from its own watershed and contribute it to the adjacent beaches. The gully was merely able to wash and carry the dune sand accumulated at the northern bluff line which originates from the beaches adjoining the Sagami river mouth. Naturally the sand thus supplied must be considerably fine in size and hence liable to erosion when exposed to a rough sea. However, the existence of the Enoshima island then took up the sheltering role and helped to form a tombolo by reflecting, diffracting and refracting the waves.

The general eastward migration of beach materials is unlikely to reach beyond this tombolo. It is presumed that the littoral drift is slowed down as it approaches the tombolo area resulting in deposition of sediment on the shallow floor or on the west slope of the tombolo. This trend seems to partly explain the steady growth of the beach of Katase West.

The topography in the east of Katase presents a sharp contrast to that in the west. This region is covered with mountainous topographies and the shorelines are separated into small segments by clifffed promontories. The tributaries are usually so small that they fail to make up a source of any appreciable amount of beach sediment. The shore-to-shore interchange of beach sediment is seriously interrupted by promontories. They are fringed by wave-cut bluffs at the outer ends and subside into submerged rocky terraces down to the depth of approximately 10 m. Not a strip of sand is found at the base of the bluff or on the rocky floors adjoining it. It is therefore assumed that the beach of Kamakura is essentially isolated from the adjacent beaches as far as the littoral process is concerned.

At the beach of Kamakura the outlet of the Nameri gully tends to deviate toward east during winter and at times the deviation amounts to approximately 150 m. However, this fact does not seem to suggest an allout eastward migration of beach materials, since the grain size decreases toward both ends of the beach and is at its maximum in the vicinity of the outlet.

Consulting the ancient pictures we find that there was once a rich sand beach at Kamakura. However, the present beach was formed by the great Kanto earthquake in 1923 which caused an elevation of the earth level by as much as 100 cm at Kamakura. Prior to the earthquake the beach had been severely eroded. This apparent cycle of erosion, elevation and then again erosion seems to suggest a theory explaining the origin of this beach which has otherwise but scant supply of materials to rely upon. Our assumption is that the beach of Kamakura is a shoreward extremity of a submarine canyon which runs in V-notch section immediately off the Nameri gully and is harbored between two promontories, Points Inamura and Kotsubo, and their adjoining rocky beds. In the geological age the entire region subsided to form approximately the present shoreline configuration and to reduce considerably the capacity of sediment supply of the Nameri gully. The gully then slowly filled the bottom of the valley notch over a long period of time until the sand floor was built up to the present beach. The capacity of sediment supply of the gully was so small that the beach processes depended principally upon the crustal movement rather than the source of supply. When the earth level was elevated there was a beach. But it was steadily and slowly eroded due partly to lack of supply and partly to inactive beach process until another crustal movement occurred to rejuvenate the dwindling beach.

The Sagami bay region is famed for active crustal movement. It has the history of numerous earthquakes, and even the prehistorical records of active crustal movement are observed everywhere along the surrounding topographies as well as on the sea floor. Some geologists counted five or six submerged terraces extending from the nearshore floor to the extreme edge of the continental shelf.^{1), 2)} A recent investigation by the Hydrographic Office reports that there is a fault line running at the depth of 15 m from Kamakura to Katase.⁴⁾ A survey conducted immediately after the great Kanto earthquake revealed a submergence of a sea floor amounting to apporoximately 400 m at some part of the Sagami bay and an elevation of the coastal region as much as 2 m.

III. DISCUSSION ON THE CAUSES OF EROSION

1. Crustal movement

The existences of the fissured blocks and confused faults in the surrounding mountainous areas and of the terraces along the river banks and coastal region show the frequent occurrence of the crustal movements in this area. The great Kanto earthquake in 1923 is believed to have its epicenter at the mouth of the Sakawa river situated at the North-West coast of the Sagami bay, and caused the land elevation of 80 to 100 cm in the area of our investigation.

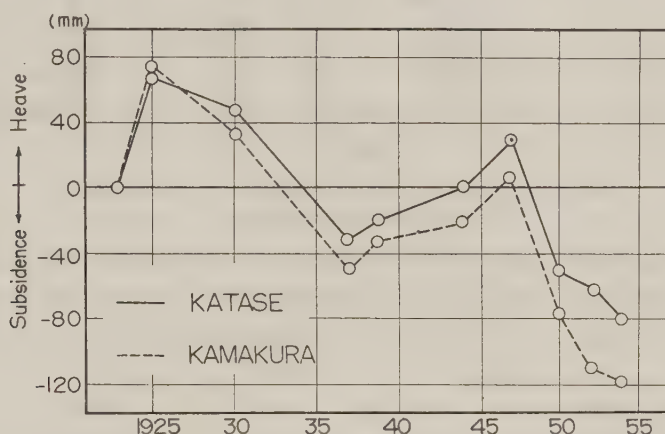


Fig. 6 Crustal movement after great Kanto earthquake in the investigation area.

The variations of earth level at Katase and Kamakura area since the occurrence of the great Kanto earthquake have been surveyed by the Geographical survey in Japan as shown in Fig. 6. The total amount of subsidence during the period of 7 years between 1947 and 1954 is about 10 to 12 cm, hence the annual rate of subsidence being 14 to 17 mm. The total amount of subsidence until 1954 is approximately 10% of the elevation caused by the great Kanto earthquake. However, it is quite difficult to evaluate the role of this subsidence on the regression of shoreline on the basis of the results mentioned above, because of the lack of detailed information on the recent regression of the shoreline.

According to the statements made by elder inhabitants in this area, the beaches along Katase and Kamakura, which were quite poor prior to the great Kanto earthquake, were formed as a result of the earth elevation. The beaches along the Sagami bay were commonly constructed by the same cause, and thereafter the regression of the shoreline has also commonly progressed there. The geomorphological interpretation of these beach processes is as follows. As observed in the tectonic terraces of rivers, the activities of natural forces were rejuvenated as a result of the earth elevation, therefore the beach, the width of which was wide enough, would be gradually eroded to a narrow beach. The nearshore sand would be transported to offshore and deposited there until the bottom profile is reestablished corresponding to the characteristics of bottom materials, waves, and topographical conditions. Owing to the fact that the earth level in this area had changed upward and downward alternatively in the geological ages, the present beach erosion could also be recognized as a stage of erosion cycle. The crustal movements used to accompany the great earthquakes, whose frequency and magnitudes are shown in Fig. 7. Some of the great earthquakes which attacked this area have been dropped from the above data, because of the lack of the clear

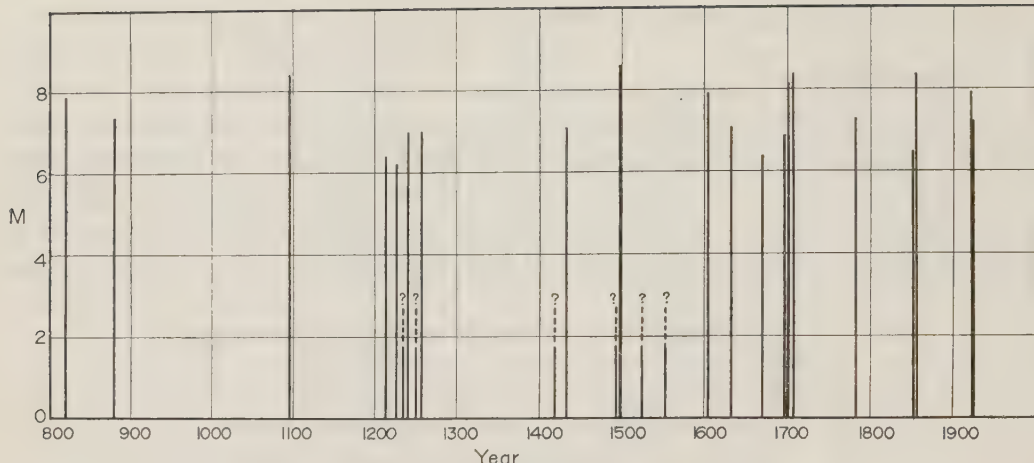


Fig. 7 Great earthquake frequency in the survey area.
M : Richter Gutenberg's scale.

statement in the records through which the magnitude of the earthquakes could be evaluated. It would be awfully difficult and dangerous to determine the period of occurrence of the great earthquakes, but the 70-year cycle stressed by some elder inhabitants seem to be well-founded especially in the last few centuries.

2. Devastation of the source of supply

As stated in the previous chapter, the Sagami river is assumed to be one of the main sources of supply to the beaches facing the Sagami bay. The river had supplied a tremendous volume of materials to the coast as a result of collapse of the mountain area until two dams, namely Yose and Tsukui dams, were constructed in 1940's at the upstream sites of the river. Recently the amount of materials moving down to the coast has been greatly reduced due to the flood control by dams, water supply to Tokyo and Yokohama Cities and also the increasing amount of sand and gravel produced from the river bed to meet the increasing demand for construction materials.

The amount of water drained away from the Sagami river in 1954 reached more than 20% of the ordinary discharge of the river, 4,000,000 m³, or little less than twice of that in 1951. This rate of 20% will be stepped up to 25% after completion of a new plan for water supply by 1961.

The volume of sand and gravel dug out from the Sagami river and its tributaries, the Doshi and Nakatsu rivers, has tended to increase sharply; 40,000,000 m³ per year in 1952, and then 120,000,000 m³ per year in 1956. But, as they are official figures, the actual amount should be more than 200,000,000 m³ in 1956.

The exact volume of transported materials by the Sagami river is quite difficult to predict at the present state, however in considering the volume of only 500,000,000 m³ of loose material stored in the valleys of Nakatsu and Doshi rivers, it would be easy to recognize the enormity of 120,000,000 m³ dug out in 1956 from the bed of the Sagami river.

In consequence of the fact stated above, the actual depression of the river bed which appeared in many places along the river shows that the amount dug out must be much more than that of supply.

The capacity of sand supply from the Katase gully is negligible, and the materials therefrom contain a fairly large percentage of fine sand which may not be able to remain nearshore.

In conclusion, the Katase gully can not be an important source of materials to this investigation area. The severe erosion at the beach of Chigasaki, located at the east side of the Sagami river, is also attributed to the deterioration of source materials at the Sagami river.

3. Interference by artificial barriers

First of all a highway constructed recently along the coasts of Katase and Kamakura should be mentioned as one of the artificial barriers. The highway runs along the seaside slope of the coastal sand dunes and bordered on the shoreside by the revetment. Therefore the beach width was apparently narrowed by the barrier, and also the waves at the rough weather send swashes against the revetment accelerating the scouring along the foot of structures. Besides the incident waves to the Kamakura bay are used to reflect completely from the revetment at westside of the Kamakura bay, and the reflected waves tend to concentrate on the part of the west side beach of the Nameri gully inducing a strong eastward current. Therefore the shore materials tend to move eastward along the eastern part of the beach.

The mouth of the Katase gully would often flow into the Katase East beach, but now it is completely fixed to the Katase West beach due partly to the land barrier constructed in 1949 by banking the northside of the tombolo behind the Enoshima, and partly to a jetty at eastside of the Katase gully. Thereafter the Katase East beach has been isolated in view of the supply of beach materials, because the eastward sand drift by marine as well as aeolian agents from the West beach was stopped by the above barriers.

4. Effect of storms

The storm waves erode and the ordinary waves build up the beaches; that is our common knowledge on the beach processes. As stated in the previous chapter, the storms caused by typhoons or cyclones hit this area fairly frequently, while the ordinary waves are considerably calm because this area is sheltered from local winds by an island and peninsulas. The shortage of moderate waves, which are mostly credited for active building of beaches, would delay recovery of the shoreline once badly hit by extraordinary waves. These characteristics of natural conditions may be counted as the secondary reason for beach erosion in this area.

IV. MOVEMENT OF COASTAL SEDIMENT

1. Methods and equipments of field investigation

The field investigation consisted largely of sediment sampling, longshore current measurement, and simultaneous observation of waves and tides in the same area.

(a) Sediment sampling

Three different samplers were used, classified as A-1, A-2, and B, which were nearly the same as that used at Tomakomai by H. Fukushima and H. Mizoguchi⁵⁾.

Sampler A-1 (Fig. 8 (a)) consists of a total 20 mesh-walled pipes, each 15 cm long and 1.8 cm in diameter. They are screwed into a steel frame, five pipes in each of the four directions and on five different echelons. The mesh opening is 0.075 mm in diameter. Sampler A-1 is tied to a concrete block to add weight and sink in waters of different depths while carefully adjusting its orientation by a compass held on a boat. The quantity of sediment arrested by sampler A-1 would tell the relative rate of the movement of suspended sediment with respect to the directions and heights above the sea floor. The heights of the open ends of the pipes on the lowest and highest echelons are 18 cm and 58 cm respectively.

Sampler A-2 consists of four mesh-walled pipes attached in four directions to a rectangular concrete block (Fig. 8 (b)). The structure of the trapping pipe is similar to that of sampler

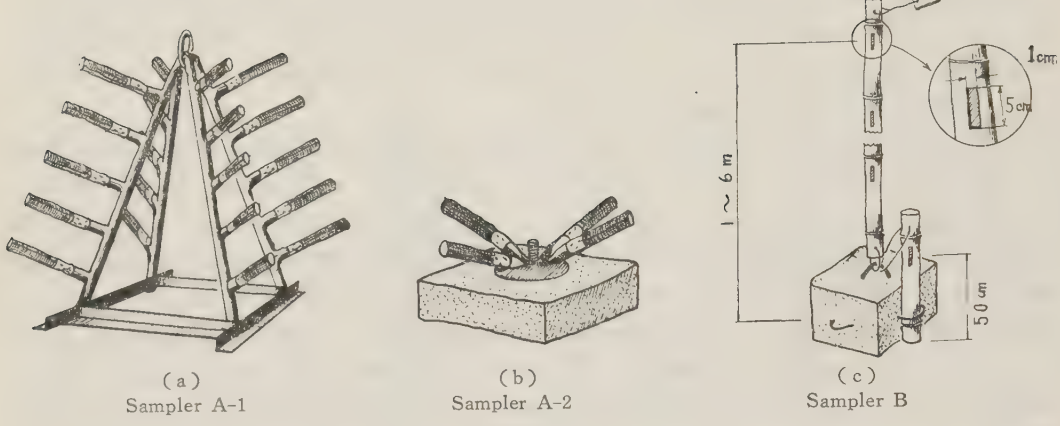


Fig. 8

A-1 except for the length, 20 cm. This has been designed to be used for arresting sediment in the surf zone where the sediment movement is expected to be far more active than outside the surf zone.

The open ends of the installed pipes were slightly directed upward to ensure that the arrested sediment may not be washed away and lost by disturbance caused either by waves or in the course of recovering operation.

Sampler B is a bamboo pole equipped with a rectangular opening 5 by 1 cm at every other joint (Fig. 8(c)). The intact joints would add buoyancy to the pole to keep it upright in water against wave action. This device is capable of arresting suspended sediment in differential levels beyond approximately 50 cm above the sea floor up to the surface.

Each run of sediment sampling operation consisted of 3 or 4 equally spaced lines either for sampler A-1 and A-2, or for B, named "Survey Line", drawn in the north-south direction. A survey line contained 4 or 5 samplers of the same type placed in 1 m-depth intervals. Sampler A-1 was recovered in about a day or two; sampler A-2 in about a day or less; sampler B in about a week. Three runs of sampling were performed both in the Katase East beach and the Kamakura beach.

(b) Longshore current measurement

To measure the longshore current accurately, which fluctuates considerably in time and space, the highly required functions of instruments are reliability as well as sensitivity and durability.

The means actually accepted consisted of a propeller type current meter, a wooden cross with a concrete block as weight (Fig. 9 (a)), a float made of a rubber ball (Fig. 9 (b)), and dye material such as potassium permanganate. The effective measurement could not be conducted with a propeller type current meter because of the difficulty of fixing the meter in the surf zone. The wooden cross, which had a great advantage of measuring the velocity in an arbitrary depth layer by a simple adjustment, could not be used in the rough seas owing to the difficulty of throwing it into the desired offshore depth.

Therefore a float consisting of a volley-ball attached with a tiny concrete block as a weight was used for measuring the surface current velocity, and the potassium permanganate was used to measure the middle layer current velocity. Both methods were quite effective for the present purpose, even though they had some disadvantages.

In order to measure the velocity at the bottom, a volley-ball was used as a float after filling it with sea water. However, minor configuration at the bottom such as ripple marks affected

the movement of the float when the velocity was small. During rough weather, waves uplifted the float as far as the sea surface. Such were the main difficulties encountered during measurement.

Originally the transits were operated to follow the float, but afterwards an observer was assigned to each float to perform a simultaneous observation along the entire shoreline.

(c) Observation of waves

The wave heights and periods were measured by reading the positions of the crest and trough of the wave train on the scaled staff installed in the water of known depth. The staff for the offshore waves is a thick bamboo pole anchored by concrete blocks to the depth of 8 to 10 m. The staff for the nearshore waves is a long wooden pole rigidly attached to a concrete block and placed in the depth of 1.5 m, approximately. The observation was made continuously for about 10 min. of the heights and corresponding periods simultaneously at the offshore and nearshore zones. The staffs were placed where the effect of refraction seemed least probable.

Every effort to determine the exact directions of wave orthogonals proved a failure, but careful observation seemed to show that most waves enter the basins from the south, and that waves break parallel to the shorelines.

After completing the schedule of the field observation, a pressure type wave recorder was installed in the basin of the Katase East beach at the depth of about 10 m. But, unfortunately, the data are not yet available for analysis.

(d) Miscellaneous observations

In parallel to the above observations, an extensive study has been conducted with respect to the minute characteristics of foreshore topographies such as beach cusps, foreshore slopes, changes of the tributary outlets, and the distribution of grain size on the foreshore.

2. Weather and wave conditions

The available data concerning the wind condition in this area are those obtained at Suka at the estuary of the Sagami river. Fig. 10 shows monthly averages of the occurrence of wind directions expressed in percent of the entire number observed, where "N" denotes the land wind from the N, NEN and NW directions and "S" the sea wind from S, SES, and SWS. The predominance of the southerly wind during three months from June through August is presumably indicative of the influence of the typhoons which passed over the China Sea and northwest Pacific during this season. The data failed to include the maximum wind velocities caused by a typhoon, and as a result a hindcast of characteristic waves due to typhoons is impossible.

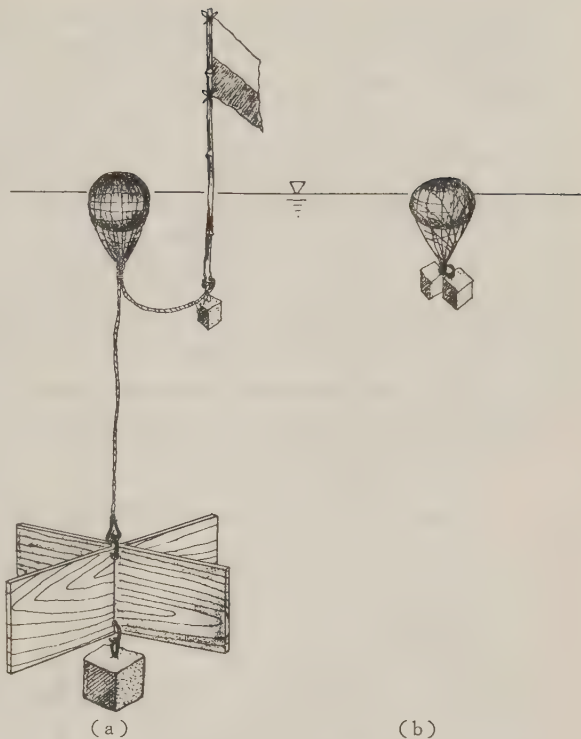


Fig. 9 Floats used for longshore current measurements.

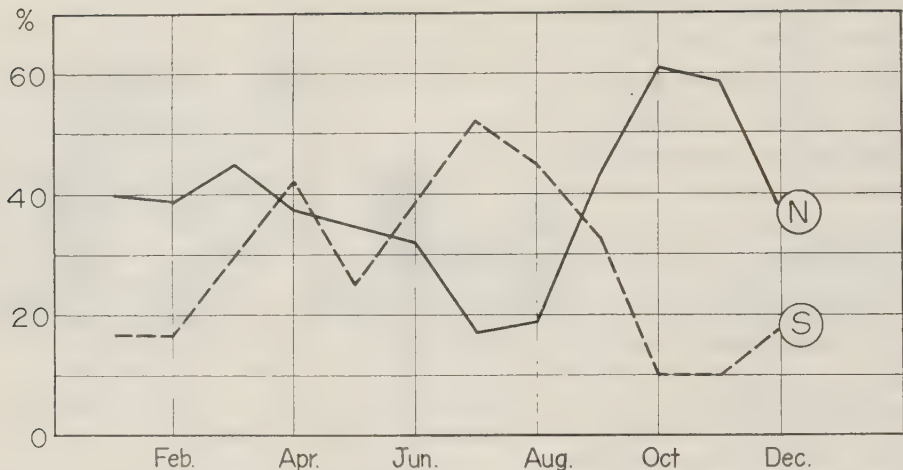


Fig. 10 Monthly average of predominant wind direction at Suka. (1950-1954)

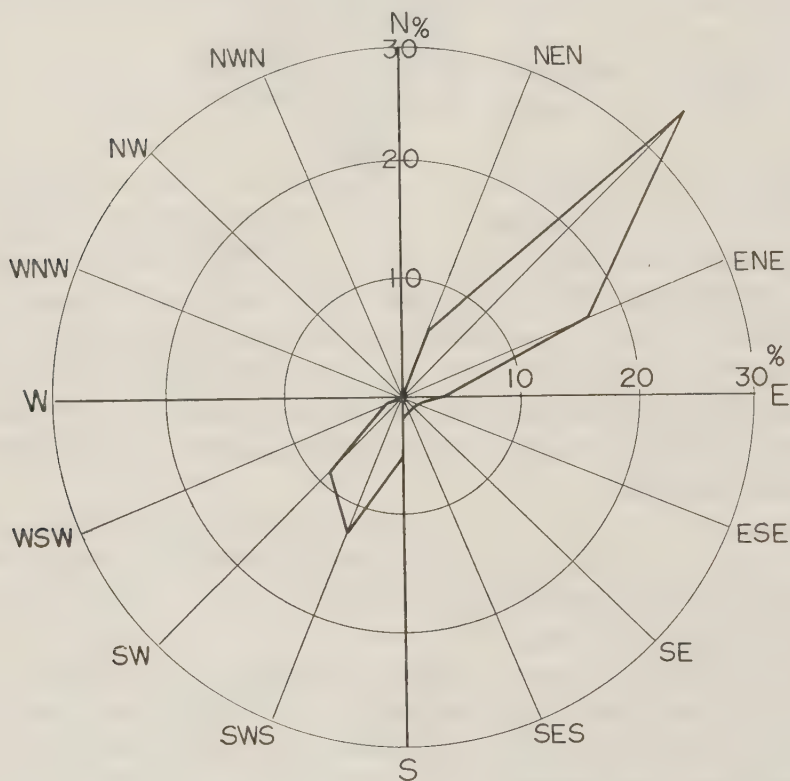


Fig. 11 Frequency diagram of wind velocity larger than 5 m/sec at Oshima Observatory.

In order to supplement the above data, the wind records obtained at the Oshima observatory in the period of 1953 to 1954 were analyzed. Part of the results is shown in Fig. 11. The remarkable fact is that the southerly winds predominate for about 3 months per year; most notable is the SW winds which predominate for 2 months a year.

According to the study by S. Unoki⁽⁶⁾, the prevailing winds are due primarily to cyclones in the Japan Sea, and secondly to the cyclones in the Pacific Ocean. Both migrate in the direction of northwest. The effect of a typhoon can not be ignored, since it generates the highest possible waves in this region.

Since the investigation area is sheltered by an island and two peninsulas, the ordinary waves are as low as 50 cm, and the wave periods are around 9 sec. The predominant wave direction is likely to be from south, but local winds and bottom topographies may complicate the incident patterns of the shallow water waves.

The wave data obtained during our investigation represent the ordinary characteristics which prevail in this area except for the typhoon season. The wave heights range from 20 to 50 cm, occasionally reaching 70 cm; the periods from 5 to 10 sec; and the wave steepness is 0.005 on the average.

In order to examine the distribution of breaker heights along the shoreline the refraction diagrams have been constructed by utilizing the sea charts and the results of the recent survey by the Hydrographic Office. The wave was assumed to arrive from SW, S, SWS, and WSW, with the periods 6, 8, and 10 sec. Some of the results are shown in Figs. 12 and 13.

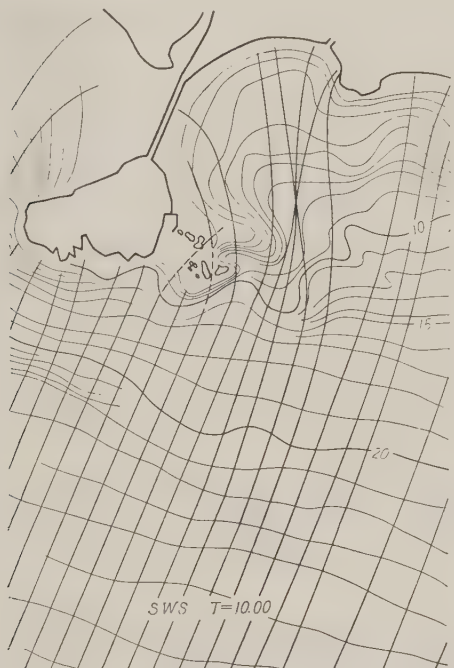


Fig. 12 Refraction diagram at Katase east beach.



Fig. 13 Refraction diagram at Kamakura beach.

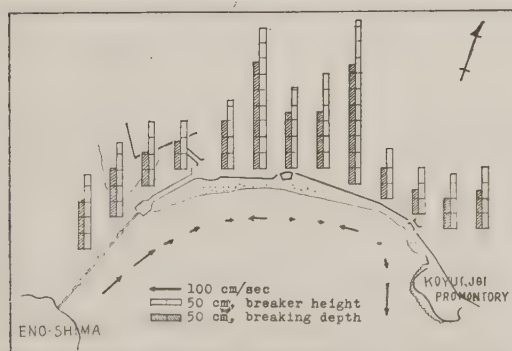


Fig. 14 Breaker height distribution and resulting littoral currents by refraction diagram, Katase.

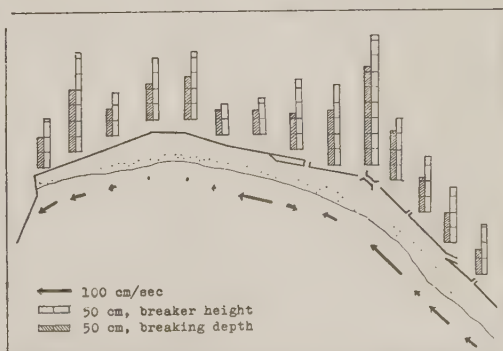


Fig. 15 Breaker-height distribution and resulting littoral current by refraction diagram, Kamakura.

Figs. 14 and 15 present part of the calculated breaker heights along both beaches. Generally speaking, the agreement between the predicted and observed values is good. However, the effects of diffraction around the reefs of the Enoshima island or of the reflection from the westside revetment at the Kamakura beach should be superposed on the above result in order to get more reliable prediction.

The effects of varying breaker heights along the shoreline are important. The higher breakers may cause stronger disturbance or scouring of the bottom sediment in the surf zone; larger amount of sand is thus set in suspension and subjected to transportation by littoral currents. Different rate of mass transport by breakers may cause differences in water level inside the surf zone, result in littoral currents due to surface gradient and transport the sand away from where the breakers are higher.

3. Longshore currents

The currents were measured by using floats and potassium permanganate at the water depth of 1 to 2 m just outside the breaker zone and in the surf zone. At the same time the breaker heights were measured along the shoreline.

The characteristics of the longshore currents observed are summarized as follows:

1. The locations where a strong longshore current occurred did not always coincide with the positions of higher breakers. The above result permits the following assumptions: 1) The incident waves are noticeably refracted owing to the topographic features of the basins of Kamakura and Katase East, as shown in the refraction diagram (Figs. 12 and 13). Hence the orthogonals cross the bottom contours almost at right angles at the breaking point. 2) The longshore current is caused mainly by the gradient of the water level in the surf zone owing to varied distribution of refraction coefficients.

2. The direction of the bottom current was not always the same as that of the surface and middle layer currents. It tends to deviate toward offshore.

3. The current direction outside the breaker zone was found fairly stable, while in the surf zone it fluctuated violently influenced by irregular swashes. Most intensive fluctuation occurred when the current velocity was below 5 cm/sec, but they decreased as the velocity increased.

4. Generally speaking, the greater the wave heights, the greater the current velocities.

5. Under the similar wave conditions the pattern of the longshore current changed depending on tidal conditions.

6. The rip current occurred as a pulsating outflow of turbid water mass; on one occasion two or three zones of turbid water were observed to spread into the offshore water at Kamakura.

7. A current directed offshore occurred frequently in the vicinity of the mouth of the Nameri gully. This was apparently not a rip current fed by longshore currents, but a secondary current induced by the existence of fresh water contributed from the gully.

8. The current directed offshore was decelerated with distance from the shoreline.

Most of the current measurement were conducted in the calm wave conditions. The observed deep-water wave heights were less than 1 m; the width of the surf zone was often very narrow; and the sea water was comparatively clear. Therefore, the velocities measured were mostly below 1 knot.

However, on December 19, 1957, the south-westerly wind of over 10 m/sec swept over the

Sagami bay area, generating waves of 1.5 to 2.0 m high in the deep water. At this time the current velocity attained 1 knot. On another occasion, July, 1958, the current velocity amounted to about 2 knots owing to the rough sea caused by the Typhoon No. 11, the wave height being between 2.0 and 2.5 m at breaking.

The current direction was mainly dependent upon the incident wave characteristics, but when the wave height was not so large, two currents flowing toward opposite directions induced a stagnation zone. The longshore current observed on December 19, 1957, was directed almost uniformly toward east, coinciding with the directions of winds and waves. After the Typhoon No. 11 passed away in July, 1958, the longshore current was directed westward without any influence of winds, although the swells broke perpendicularly to the shoreline.

Lack of data and inadequacies of instruments prevent us from giving any further remarks on the general pattern of longshore currents along these beaches. Accordingly, the following summaries are based merely on the data obtained.

Kamakura beach

The westward current predominates in front of the Nameri gully owing to the prevailing southwesterly winds in the period of June to January. During this period the mouth of the Nameri gully is shifted by about 150 m eastward. On the other hand, the westward current is predominant when the large swells approach perpendicularly to the shoreline and at the same time the current directed offshore occurs at the west end of the beach.

Katase East beach

When the southwesterly winds blow, the current is directed east in the whole area, but the current directed offshore or westward takes place at the east end of the beach. The latter must be generated by higher water level in that zone.

When low swells approach here, the current is observed mainly in the east half of the beach. When large swells arrive here, the westward current predominates in the whole area.

The eastward or westward current was observed at flood or ebb tide, respectively, as far as the wave heights were small. However, when large waves occurred, the current direction was not influenced by tide levels any longer.

4 Sediment movement

Sampling operations were impossible at rough weather conditions. Therefore the following results only represent the characteristics of the ordinary weather conditions.

(a) Horizontal movement of suspended sediment

An examination of samples obtained by sampler A-1 in all depths has revealed a definite relationship between the relative quantities of sediment arrested in the traps and their heights from the sea floor. Denoting the height of the trap from the sea floor by z , that of the highest echelon (58 cm) by z_0 , the quantity of sediment by m , and that of the lowest echelon (18 cm) by m_0 , we obtain (Fig. 16) :

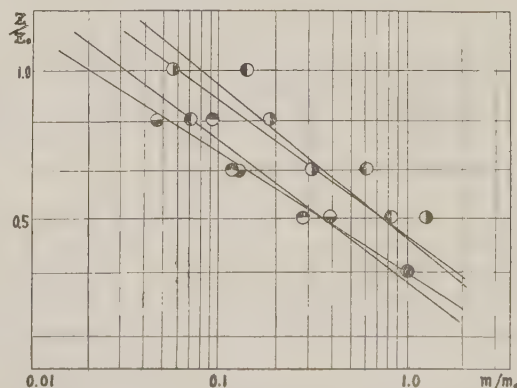


Fig. 16 Vertical distribution of suspended sediment in relation to height, for sampler A-1.

$$\frac{z}{z_0} = a \log \frac{m}{m_0} + b, \quad \dots \dots \dots \quad (1)$$

where a and b are presumably the constants depending upon wave characteristics, depths of samplers, grain sizes, specific gravities and fall velocities of suspended sediment. Determining the values of a and b from figures, the result is,

for the Katai East beach:

$$\frac{z}{z_0} = -0.41 \log \frac{m}{m_0} + 0.36 \quad \dots \dots \dots \quad (2)$$

for the Kamakura beach :

$$\frac{\tilde{z}}{z_0} = -0.37 \log \frac{m}{m_0} + 0.38 \quad \dots \dots \dots \quad (3)$$

It is questionable, however, whether the lowest samples consist purely of suspended sediment or include a portion of the disturbed bed-load due to possible settlement of the sampling frame. Nevertheless, the relationships show a similar pattern of sediment distribution for each sampler, regardless of the depth and direction. Accordingly, the samples on the lowest echelon may be considered as representing the relative quantity of suspended sediment in the corresponding directions. It should also be noted that the values of a and b are only related to ordinary weather conditions.

Figs. 17 and 18 show the examples of the distribution of the samples on the lowest echelon,

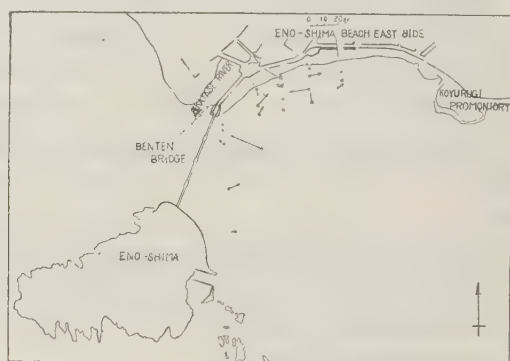
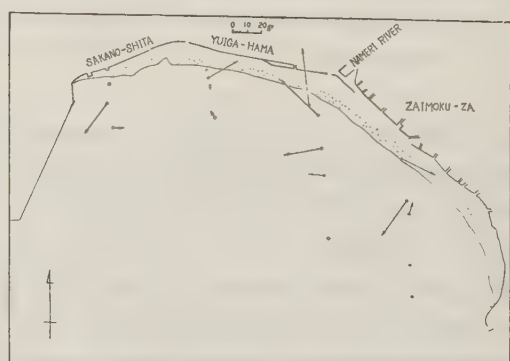
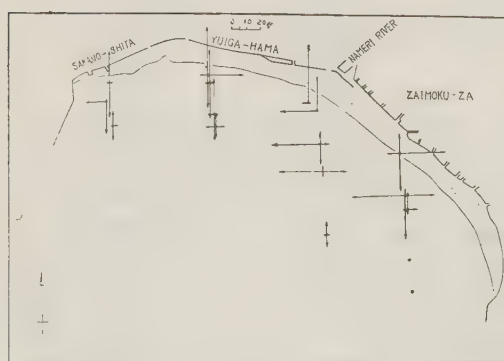


Fig. 17 Horizontal distribution of suspended movement for samplers A-1 and A-2, Katase East



(a) (b)
Fig. 18 Horizontal distribution of suspended movement for samplers A-1

m_0 obtained in unit sampling. Figs. 17 (a) and 18 (a) show the net quantities in each trap, and Figs. 17 (b) and 18 (b) the resultant quantities and their corresponding directions. Investigating the above results, it will be recognized that the predominant direction of sediment movement is perpendicular to the shoreline, that is, onshore and offshore directions.

(b) Vertical distribution of suspended sediment

Figs. 19 and 20 show the vertical distribution of suspended sediment measured by sampler B continuously over a period of about a week. It should be noted that the manner of distribution differs depending on their depths. The distribution in the depths greater than 4 m and less than 2 m are essentially the same. This can be explained by the fact that in the breaker zone, usually 2 m deep at ordinary wave conditions, the breaking waves cause a uniform disturbance of water throughout the entire depth from surface to the bottom, while in water as deep as 4 m or more, the disturbance by ordinary gentle waves is only capable of keeping a small amount of fine sediment particles in suspension.

The median diameters of sediment particles obtained in the surf zone, accordingly, scatter closely around 150μ , while the average grain size in depths greater than 4 m is 70μ .

The distribution of sediment in the intermediate depths, from 2 to 4 m, is in general similar to that of the river sediment. In the very shallow water, normally less than 1 m, no definite rule was found to apply to the pattern of distribution.

The data also show that the sand movement is especially active in the central portion of the beach of Katase East side, and in the vicinity of the Nameri outlet at the Kamakura beach.

5. Characteristics of foreshore deposits

(a) Foreshore slopes

Figs. 21 and 22 show the foreshore slopes along the beaches of Kamakura and Katase East. The fluctuation of foreshore slope is small at both ends of the Kamakura beach and near the tombolo at the Katase East beach. At these places the beach slopes are gentle because of little supply of materials, and are subjected to small waves.

The fluctuation of slope is large at the places of large slope, namely, the middle part of the Kamakura beach and the east half of the Katase East beach. These places are also characterized by coarseness of the beach materials, which include shell fragments. This

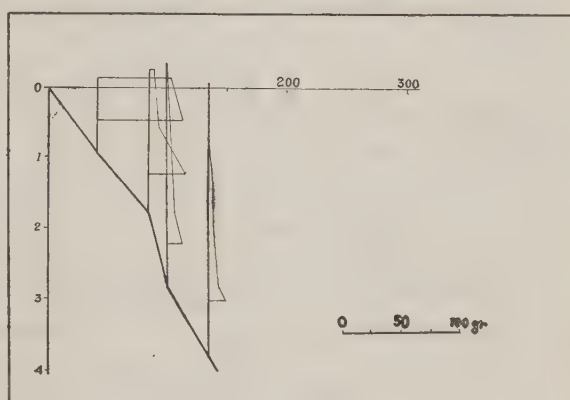


Fig. 19 Vertical distribution of suspended sediment for sampler B, Katase East.

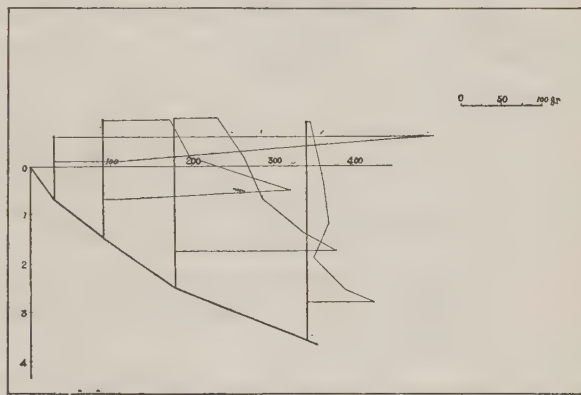


Fig. 20 Vertical distribution of suspended sediment for sampler B, Kamakura.

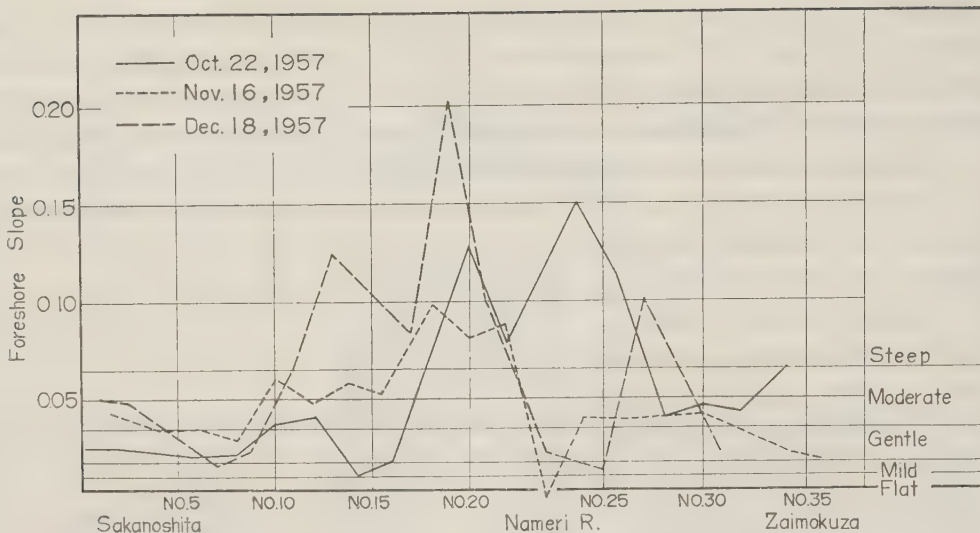


Fig. 21 Foreshore slope, Kamakura beach.

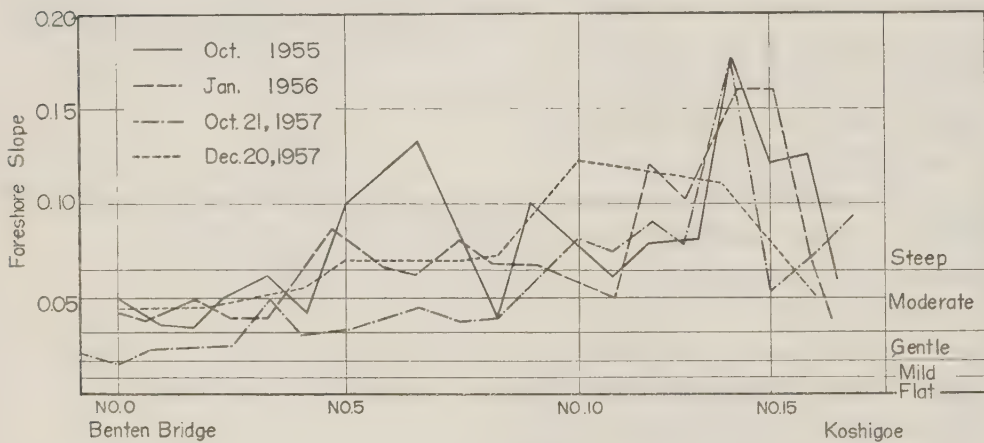


Fig. 22 Foreshore slope, Katase East beach.

tendency is distinguished in the vicinity of the outlet of the Katase gully. The foreshore slopes seem to have a close relation with the grain sizes, but they are primarily influenced by the intensity of waves.

(b) Beach cusp

At the middle part of the Kamakura beach the well-developed beach cusps are found frequently, but they are obscure in other locations. Fig. 23 shows the distribution of the beach cusps along the Kamakura beach. Generally speaking, a large wave seems to produce a large cusp. A large cusp constructed by extraordinary waves remains near the berm crest for a long time. The interspace, or pitch, is mostly uniform, but sometimes irregular due probably to local difference of wave intensities. The maximum beach cusp ever observed had a pitch of 30 m. Although some believe that the beach cusps are made only by waves approaching perpendicularly to the shoreline, remarkable cusps were observed even under the condition of wind waves which approached the shoreline from irregular directions. At any rate the active sorting beach deposits along the perpendicular direction to the shoreline seems to be the main reason for the formation of beach cusps.

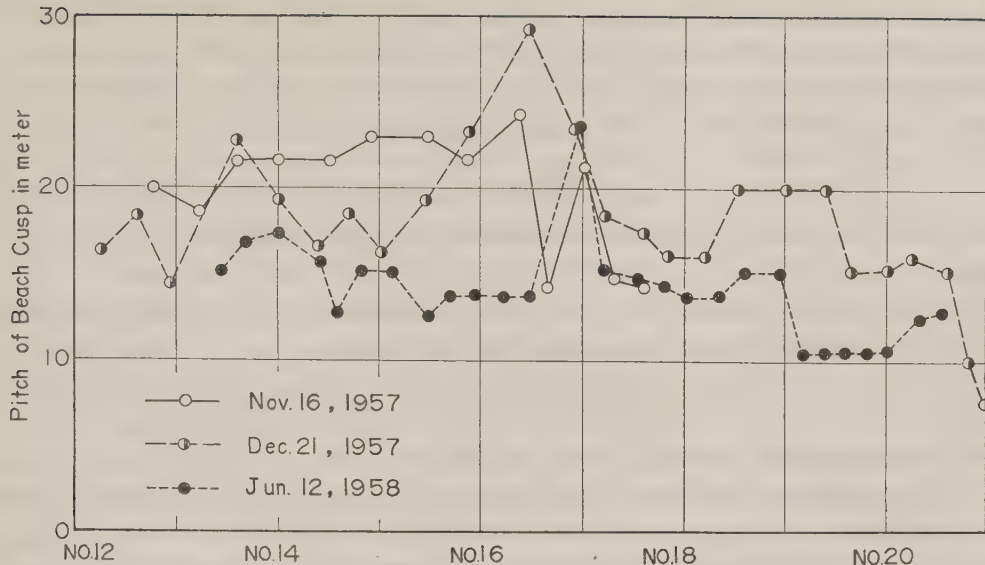


Fig. 23 Variation of beach cusp along Kamakura beach.

(c) Distribution of sediment size

The distribution of gravel was investigated along the north coast of the Sagami bay. Analysis was conducted by Mr. Aramaki on the assumption that quartz diorite and pyroxene andesite are representative rocks of the Sagami river and the Sakawa river, respectively. The result is shown in Fig. 24, where the plot gives the relative volume of a maximum

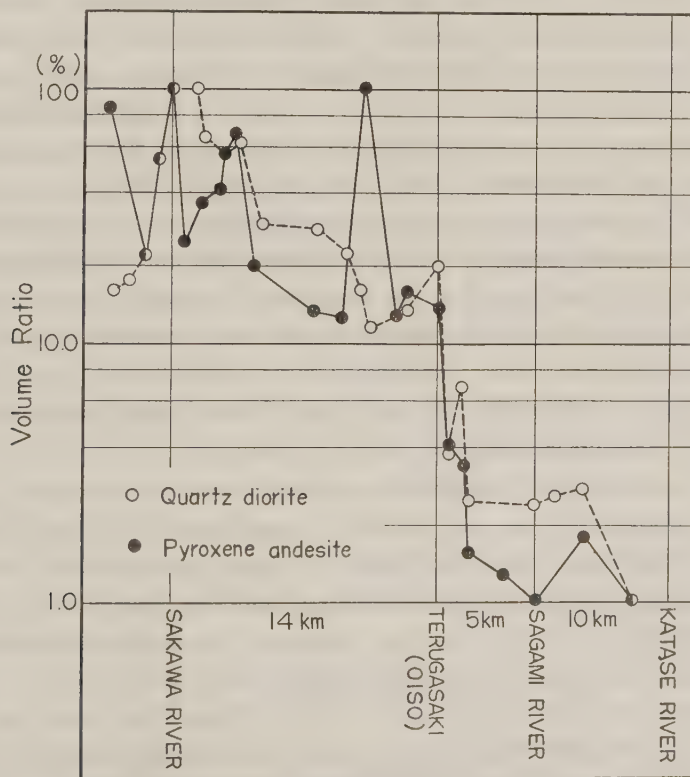


Fig. 24 Variation of volume ratios for each material along the northern coast of Sagami bay.

size found at each station in percent of that sampled at the mouth of the Sakawa river. According to this result the size of the gravels decreases smoothly with distance from the Sakawa river as far as Pt. Teruga-saki at Oiso, where it falls abruptly. Beyond the Katase gully no such gravel was found. The curves are roughly expressed by the following equation,

$$\frac{Q}{Q_0} = e^{-0.1L} \quad \dots \dots \dots \quad (4)$$

where Q_0 is the volume found at the Sakawa river and Q at a distance of L km from the Sakawa river.

The above relation is analogous to the Sternberg's equation for river gravels, provided that the slope of curves is obviously steeper than that for the rivers.

V. CONCLUSIONS AND RECOMMENDATIONS

The main conclusions reched as a result of this study are :

1. The regression of shoreline is in progress over the entire length of the north coast of the Sagami bay.

2. The earth level along the north coast of the Sagami bay was heaved by 1 to 2 m by the great Kanto earthquake in 1923, but the ensuing subsidence has reached about 1.2 m, i.e. about 10% of the total elevation, during the last 35 years. Therefore it seems inappropriate to attribute the beach erosion directly to the crustal movement. It is conceivable that the activities of the natural forces were rejuvenated as a result of the earth elevation. But this assumption does not account for the fact that the beach erosion progressed rapidly for the past several years.

3. The both beaches of Kamakura and Katase East are isolated from the adjacent area and do not have any source of beach materials. Hence, the mechanics of sand movement within the both basins are explained as follows; the sand eroded from the shore moves not to the adjacent area by the alongshore forces but mainly toward offshore and deposits there or dissipates around there. The beach of Kamakura seems to be isolated as a result of its geographical features, and the sand drifting along the shore or flowing out from the Nameri gully tends to fill the ancient underwater valley of this river. The Katase East beach seems to be completely separated from the Katase West beach due to artificial barriers, such as an embankment and a jetty constructed in the last decade. Therefore, the eastward side of this beach, near the Koyurugi promontory, is now in the worst condition since it is the remotest place from the Katase West beach. According to an ancient drawing showing this area, the Koyurugi promontory, marking the east end of the Katase East beach now, was once an island with a low tombolo behind it.

4. The main source of shore materials to the north coast of the Sagami bay is the Sagami river, which is estimated to have been supplying about 10,000,000 m³ of sediment. But the rate of supply to the beach decreased rapidly in recent years, because of the following reasons; 1) construction of dams for controlling flood discharge, and or developing the hydraulic power plants, and 2) tremendous increase of the volume of sand and gravel dug out from the bed of the river, amounting to 100,000,000 to 200,000,000 m³ annually. The relation between the regression of the shoreline at the Katase East beach and the shortage of sand supply from the Sagami river cannot be established unless an allout investigation is conducted concerning the sediment movement along the beach between the Sagami river and the Katase beach.

5. The coastal sand dunes and narrow beach zones are separated by a drive way. Such situation of the drive way is apt to give the impression that the beach width has been shortened after the drive way was constructed. The storm waves send swashes against the revetment of the drive way, scouring and washing away the beach materials. This negative function of the revetment may have probably accelerated the regression of the shoreline. However, the quantitative data accounting for such influence are not available.

6. The velocity of longshore current along the Kamakura and Katase East shores is generally very small, exceeding 1 knot only on rare occasions. At the Katase East beach the westward current seems to predominate between the middle and the east end of the beach when the waves are relatively high. At the Kamakura beach the longshore current seems to predominate in the eastward direction at the mouth of the Nameri gully and in the westward direction along the west part of this beach. Owing to the low velocity of the low velocity of the longshore current, the capability to transport the shore materials along the shoreline will be quite small. The longshore current has the same directions both in the surface and the bottom layers. Unfortunately the data concerning the longshore current induced by a rough sea are not available. A weak offshore-directed current occurred at the Koyurugi promontory, Katase East beach, and in the middle part of the Kamakura beach.

7. The movement of sediment is primarily directed toward onshore and offshore. Therefore the beach sand will be transported toward offshore by big waves, and returned onshore by gentle waves, alternately. At some parts of the beaches in the investigation area, the alongshore movement of beach sand is also observed mainly in the surf zone. Along the Katase East beach, the beach sand moves westward weakly at the middle region and toward offshore at the east end of the beach. Along the Kamakura beach, the beach sand moves eastward in the vicinity of the mouth of the Nameri gully and extends to the location where the rip current is recognized. But the capability of the rip current to transport the beach materials is quite doubtful.

Reviewing the results of our investigations, the causes of the beach erosion in this area seem to be related to various factors, notably alienation from the source of supply. In order to improve the analysis of the beach processes along the Sagami bay, it is recommended to continue the synthetic observations consisting of; 1) recording the wave and wind condition, 2) surveying the onshore and offshore profiles, 3) sampling the beach and bottom sand, and 4) collecting the data concerning the source of beach materials from the Sagami river and other tributaries.

In view of increasing demand for the health resorts along the coast, the strategic positions of the beaches of Katase and Kamakura are ideal because of the short distance from the Tokyo area. Especially the Katase beaches and the Enoshima island have taken flood-light recently as the site of a yacht harbor.

In this respect, it is recommended to carry on the artificial nourishment and at the same time construct a breakwater extending from the Enoshima east side in order to make a calm basin for yachts and the beach.

VI. ACKNOWLEDGEMENTS

The authors feel bound to express their grateful appreciation to : the engineers of the River and Harbor Section, Kanagawa Prefectural Government, and the Fujisawa Office, who rendered valuable assistance to the field operations during the investigation; Mr. M. Aramaki,

Tokyo Educational University, who gave valuable assistance concerning the gravel study along the Sagami bay coast; many other people who participated both in field works and analysis of data.

REFERENCES

- 1) Tayama, R. : A study on the topography and sediment distribution at the eastern coast of the Sagami bay, Bul. of Hydrographic Office, Japan, No. 17, April, 1950. (In Japanese)
- 2) Tayama, R. : A study on the topography and sediment near Eno-Shima, Bul. of Hydrographic Office, Japan, No. 20, Oct. 1950. (In Japanese)
- 3) Hanai, S. : A study on the characteristics of the beach ridge and the dune in Shonan, Geological Survey, 2, 1926. (In Japanese)
- 4) Imamura, G. : A study on the causes of the dune formation in Shonan, Geological Survey 2, 1926. (In Japanese)
- 4) Komukai, R. : A study on the topography and sediment distribution at the Sagami bay coast, May, 1957, A preliminary report on beach erosion at Eno-Shima and Kamakura, Japan. (In Japanese)
- 5) Fukushima, H. and Mizoguchi : A study on the sediment and its measurement, Coastal Engineering in Japan, Vol. 2 Nov. 1955.
- 6) Unoki, S. M. Nakano and Y. Kuga : On results of wave observations at Jogashima Island and its application to wave forecasting (1), Pap. Met. Geophys., 4 (3/4), Dec. 1953.
Unoki, S. and M. Nakano : On the Ocean waves at Hachijo Island, Pep. Met. Geophys., 6 (1). 1955.
- Unoki, S : General aspect of wind waves and swell in the vicinity of Japan, Pap. Met. Geophys., 6 (2), 1955.

ANNOUNCEMENT

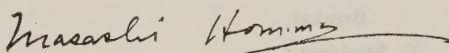
Dear Sirs :

Since 1954 the Committee on Coastal Engineering, the Japan Society of Civil Engineers, has been holding annual conferences on various key problems of coastal engineering. The results of numerous laboratory studies and field investigations thus accumulated, so far amounting to more than 150 articles, have been published in 7 consecutive volumes of "Proceedings of Coastal Engineering Conference in Japan" in Japanese language. In the mean time we have been convinced of a strong need to promote interchange of knowledge and experiences among the concerned engineers the world over. To meet this requirement we have established a plan to publish a series of English edition containing selected reports from the Japanese language Proceedings.

Three issues of the English edition, "COASTAL ENGINEERING IN JAPAN" Vols. 1, 2, and 3, each published in 1958, 1959, and 1960, respectively, are already on sale, and the subsequent issues will also be published periodically once a year.

Please survey the tables of contents shown below and mail your order to the Japan Society of Civil Engineers, 1-chome, Yotsuya, Shinjuku-ku, Tokyo, Japan. Any inquiry will be received at the same address.

Sincerely yours,



Masashi Hom-ma, Dr. Engg.

Chairman

Committee on Coastal Engineering, Japan

Japan Society of Civil Engineers

1-chome, Yotsuya Shinjuku-ku, Tokyo

Japan

